DIGITAL POLAR TRANSMITTER FOR MULTI-BAND OFDM ULTRA-WIDEBAND

LOKE WING FAI

A THESIS SUBMITTED

FOR THE DEGREE OF MASTER OF ENGINEERING

DEPARTMENT OF ELECTRICAL & COMPUTER ENGINEERING

NATIONAL UNIVERSITY OF SINGAPORE

2008

ABSTRACT

Multi-Band Orthogonal Frequency Division Modulation (MB-OFDM) Ultra-Wideband (UWB) suffers from a large peak-to-average ratio (PAR). Systems with large PAR require the linear power amplifier (PA) to back off from its maximum output power to ensure that the peak of the power is within the linear range of operation, hence, resulting in poor efficiency. Although the problem of low power efficiency and high PAR may be solved by polar modulation, the performance of polar transmitter is often degraded by non-ideal implementations.

This thesis studies the requirements for the envelope and phase signals in polar transmitter for UWB at system level. Results show that the bandwidth of the phase in the polar transmitter needs to be several times the bandwidth of in-phase (I) and quadrature phase (Q) in order to pass the Error Vector Magnitude (EVM) requirement in ECMA standard. On the other hand, the bandwidth of the amplitude does not need to have a bandwidth as large as the bandwidth of the phase – it needs to be only slightly larger than the bandwidth of I/Q.

To take advantage of the advancement of deep-submicron semiconductor technology which favors more digital circuitries, a new digital polar transmitter (DPT) for MB-OFDM UWB is proposed. It consists of a digital phase modulator (DPM) for generating the phase-modulated radio frequency (RF) signal and a digital power amplifier (DPA) for modulating the amplitude of the RF signal. The non-idealities in the amplitude and phase signals, like delay mismatch, mismatch in gain and error in phase, in this DPT are investigated in this thesis.

ACKNOWLEDGEMENTS

I would like to thank my supervisor, Dr. Michael Chia Yan-Wah, for providing me an opportunity to get exposure to the system level study of a UWB polar transmitter. The author would also like to thank him for his patience, guidance and help during the course of this project. Without his advice and guidance, this project will not be able to proceed as efficiently and smoothly.

Next, I would like to thank my colleagues at Institute for Infocomm Research, especially Mr. Chee Piew Yoong, Mr. Yin Jee Khoi and Mr. Seah Kwang Hwee for their valuable discussions and advice during the course of this project.

Last but not least, I would like to my parents and my wife, Ms. Wendy Woon, for their constant encouragement and support.

TABLE OF CONTENTS

LIST OF TABLES

LIST OF FIGURES

LIST OF ABBREVIATIONS

ADC	Analog-to-digital converter
AM	Amplitude modulation
BPF	Bandpass filter
CP	Charge pump
DAC	Digital-to-analog converter
DCM	Dual-carrier modulation
DDS	Direct digital synthesizer
DEM	Dynamic element matching
DLL	Delay-locked Loop
DPA	Digital power amplifier
DPM	Digital phase modulator
DPT	Digital polar transmitter
DSP	Digital signal processing
EER	Envelope elimination and restoration
EVM	Error vector magnitude
FCC	Federal Communications Commission
FFI	Fixed-frequency interleaving
FFT	Fast Fourier transform
FIR	Finite impulse response
I	In-phase
ICI	Intercarrier interference
ISI	Intersymbol interference
IDFT	Inverse discrete Fourier transform

IF	Intermediate frequency
IFFT	Inverse fast Fourier transform
LINC	Linear amplification with non-linear components
LO	Local oscillator
LSB	Least significant bit
MB	Multi-band
MSB	Most significant bit
OFDM	Orthogonal frequency division modulation
PA	Power amplifier
PAR	Peak-to-average ratio
PFD	Phase frequency detector
PLL	Phase-locked loop
PM	Phase modulation
PSD	Power spectral density
PSK	Phase shift keying
Q	Quadrature phase
QAM	Quadrature amplitude modulation
QPSK	Quadrature phase shift keying
RF	Radio Frequency
RMS	Root mean square
RX	Receiver
SNR	Signal-to-noise ratio
TDC	Time frequency code
TX	Transmitter
UWB	Ultra-wideband

VCO	Voltage-controlled oscillator

CHAPTER 1

INTRODUCTION

1.1 Motivation

In recent years, ultra-wideband (UWB) is fast emerging as the technology of choice which spurs wireless communications, networking, imaging, radar and positioning systems [1]. ECMA International has released two industrial standards (ECMA-368 [2] and ECMA-369 [3]) for UWB technology based on allocation of the bandwidth of 3.1-10.6 GHz at a transmit power below -41.3 dBm/MHz for UWB devices by Federal Communications Commission (FCC) in the United States [4]. These standards allow data rates of up to 480 Mb/s using MultiBand Orthogonal Frequency Division Modulation (MB-OFDM) scheme. However, MB-OFDM UWB suffers from a large peak-to-average ratio (PAR). Systems with large PAR require the linear power amplifier (PA) to back off from its maximum output power to ensure that the peak of the power is within the linear range of operation, resulting in poor efficiency. This can prove to be challenging for UWB transmitter.

The problem of low power efficiency and high PAR may be solved by polar modulation or envelope elimination and restoration (EER) [5]. Instead of transmitting complex data using in-phase (I) and quadrature (Q) or Cartesian representation, polar representation is used instead. The phase modulation in a polar transmitter can be upconverted and amplified by highly efficient, non-linear power amplifier which is controlled by the amplitude modulation. Although polar modulation alleviates the problem of low power efficiency and high PAR, the performance of polar transmitter

can be degraded by two major non-idealities: finite bandwidth of the amplitude and phase information, and time delay mismatch between the amplitude and phase signals [6]-[9].

As CMOS technology advances to deep-submicron and the prevalence of low-cost Digital Signal Processing (DSP), a digitally intensive approach to conventional RF functions is needed to allow high level of integration. Compared to older process technologies, the supply voltage becomes lower and the threshold voltage is relatively higher in deep-submicron process, resulting in smaller voltage headroom for analog circuits. Furthermore, the switching noise from surrounding digital circuits makes the analog circuits harder to resolve the signal in voltage domain. Hence, it becomes feasible to explore using digitally intensive approach to conventional RF circuits [10]. Digital polar transmitter (DPT) architecture has been reported in recent years and adopted for narrowband systems, like Bluetooth and GSM/EDGE [11][12].

Hence, the research in this thesis addresses the issues regarding the use of digital polar transmitter (DPT) for MB-OFDM UWB. Some practical considerations due to non-ideal effects in the proposed DPT are also studied to provide a better understanding. Some of these results are reported in [13] and [14].

1.2 Contributions

The contributions of this thesis are listed and discussed below:

- The non-idealities in the amplitude and phase signals of polar modulator for MB-OFDM are discussed. The results in EVM have been published in [13].

- A digital polar transmitter (DPT) architecture is proposed and has been accepted by IEEE Microwave Theory and Technique Society, International Microwave Symposium (IMS), June 2009 [14]. It consists of a digital phase modulator (DPM) generating the phase-modulated radio frequency (RF) signal and a digital power amplifier (DPA) which modulates the amplitude of the RF signal. The effects of the resolution of the DPM and DPA on error vector magnitude (EVM) for various data rates are studied.

- The mismatches in gain and errors in phase in the digital MB-OFDM UWB polar transmitter are discussed. The performances in EVM due to these non-idealities are presented.

1.3 Thesis Organization

Apart from this chapter, the rest of the thesis is divided into five chapters:

Chapter 2 discusses background of this thesis. UWB and various transmitter architectures reported in the various literatures are discussed.

Chapter 3 presents the system level design considerations in polar transmitter for MB-OFDM. Non-idealities like bandwidths of amplitude and phase, and time delay mismatch will be discussed.

Chapter 4 proposes a digital polar transmitter (DPT) architecture. The minimum resolutions of the digital power amplifier (DPA) and digital phase modulator (DPM) are determined for various data rates.

Chapter 5 presents the performance in EVM due to the mismatch in gain and error in phase in the proposed digital polar transmitter.

Chapter 6 summarizes the findings of this project and concludes the work done in this project. Future work and improvements are proposed.

CHAPTER 2

MB-OFDM UWB TRANSMITTER

In this chapter, MB-OFDM UWB and polar modulation are discussed. Various polar transmitters reported in literature are also discussed.

2.1 Orthogonal Frequency Division Multiplexing (OFDM)

OFDM is a special case of multicarrier transmission where the high-rate data stream is split into a number of lower rate streams that are transmitted simultaneously over a number of sub-carriers [15]. It can be seen as either a modulation technique or a multiplexing technique. In normal frequency-division multiplex system, many carriers are spaced apart in such a way that the signals can be received using conventional filters and demodulators as shown in Figure 2-1. However, in OFDM, the carriers are arranged in such a way that the sidebands of the individual carriers overlap as shown in Figure 2-1 and the signals can still be received without any adjacent carrier interference. Hence, orthogonal multicarrier modulation technique results in increased spectrum efficiency [15].

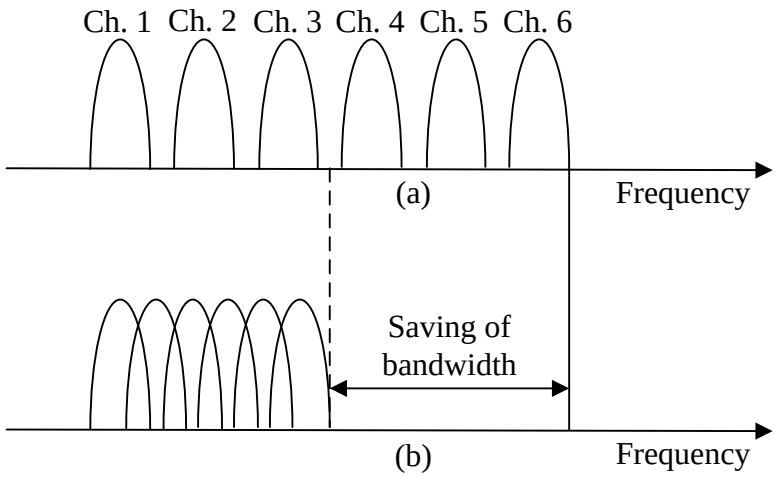

Figure 2-1: (a) Conventional multicarrier technique, and (b) OFDM technique.

OFDM provides the following advantages over single-carrier modulation:

- OFDM is an efficient way to deal with multipath.
- It is possible to enhance the capacity significantly by adapting the data rate per subcarrier according to the signal-to-noise ratio (SNR) of that particular subcarrier in relatively slow time-varying channels.
- OFDM is robust against narrowband interference as only a small percentage of the subcarriers will be affected by such interferences.
- OFDM makes single-frequency networks possible.

However, it also has the following drawbacks:

- OFDM is more sensitive to frequency offset and phase noise.
- OFDM has a relatively large peak-to-average ratio (PAR), which reduces the power efficiency of the RF amplifier.

2.1.1 Generation of Subcarriers

OFDM signal consists of a sum of subcarriers that are modulated by using schemes like phase shift keying (PSK) or quadrature amplitude modulation (QAM). The complex baseband notation of an OFDM symbol starting at $t = t_s$ is written as

$$s(t) = \begin{cases} \sum_{i=-\frac{N_s}{2}}^{\frac{N_s}{2}-1} d_{i+\frac{N_s}{2}} e^{j2\pi \frac{i}{T}(t-t_s)} & , \quad t_s \le t \le t_s + T \\ 0 & , \quad otherwise \end{cases} \tag{2.1}$$

where d_i are the complex symbols, N_s is the number of subcarriers, and T is the symbol duration.

In (2.1), the real and imaginary parts corresponds to the in-phase (I) and quadrature (Q) parts of the OFDM signal, which need to be multiplied by a cosine and sine of the desired carrier frequency to produced the final OFDM signal. The operation of the OFDM modulator in a block diagram is shown in Figure 2-2.

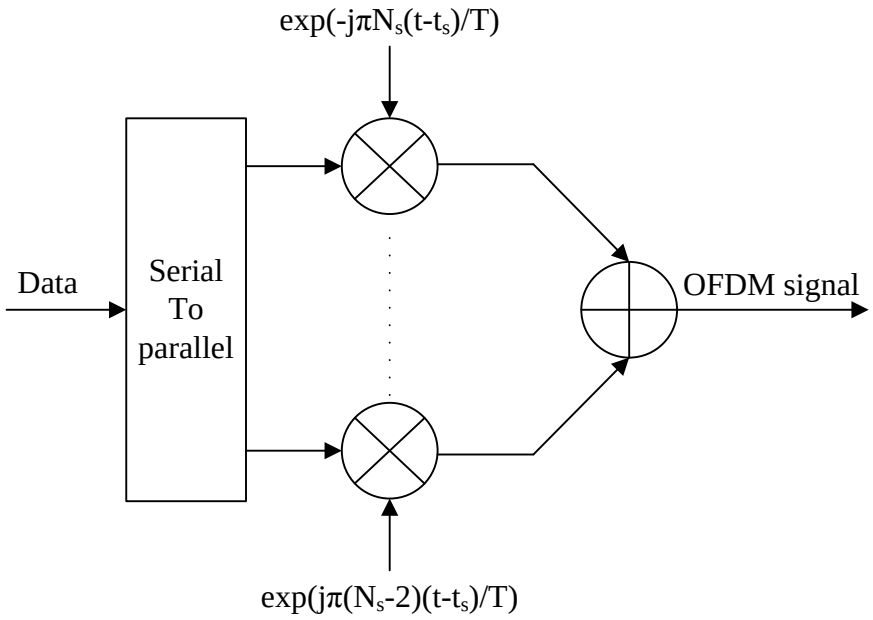

Figure 2-2: OFDM modulator.

Each subcarrier has exactly an integer number of cycles in the interval T, and the number of cycles between adjacent subcarriers differs by exactly one. This property accounts for the orthogonality between the subcarriers. If the jth subcarrier (2.1) is demodulated by downconverting the signal with a frequency of j/T and then integrating it over time T, the result becomes (2.2). The integration over the demodulated signal gives the desired output $d_{j+N/2}$ (multiplied by a constant factor T), which is the complex symbol value for the jth carrier. The integration for all other subcarriers is zero as the frequency difference $(i-j)/T$ produces an integer number of cycles within the integration interval T, such that the integration result is always zero.

$$\begin{aligned}\int_{t_s}^{t_s+T} e^{-j2\pi\frac{i}{T}(t-t_s)} s(t)\,dt &= \int_{t_s}^{t_s+T} e^{-j2\pi\frac{i}{T}(t-t_s)} \sum_{i=-\frac{N_s}{2}}^{\frac{N_s}{2}-1} d_{i+\frac{N_s}{2}} e^{j2\pi\frac{i}{T}(t-t_s)}\,dt \\ &= \sum_{i=-\frac{N_s}{2}}^{\frac{N_s}{2}-1} d_{i+\frac{N_s}{2}} \int_{t_s}^{t_s+T} e^{j2\pi\frac{i}{T}(t-t_s)}\,dt \\ &= d_{i+N_s/2}T\end{aligned} \tag{2.2}$$

The orthogonality of the subcarrier can also be explained in another way. Each OFDM symbol contains subcarriers that are nonzero over an interval T, so the spectrum of each symbol is a convolution of a group of Dirac pulses located at the subcarrier frequencies with the spectrum of a square pulse that is one for a period of T and zero otherwise. The amplitude spectrum of the square pulse is $\mathrm{sinc}(\pi fT)$, which has zeros for all frequencies f that are an integer multiple of $1/T$. Figure 2-3

shows the overlapping sinc spectra of individual subcarriers. At the maximum of each subcarrier spectrum, the spectra of the rest of the subcarriers are zero. An OFDM receiver calculates the spectrum values at those points that correspond to the maxima of individual subcarriers, it can demodulate each subcarrier without any interference from other subcarriers. As a result, intercarrier interference (ICI), which is crosstalk between different subcarriers, is avoided.

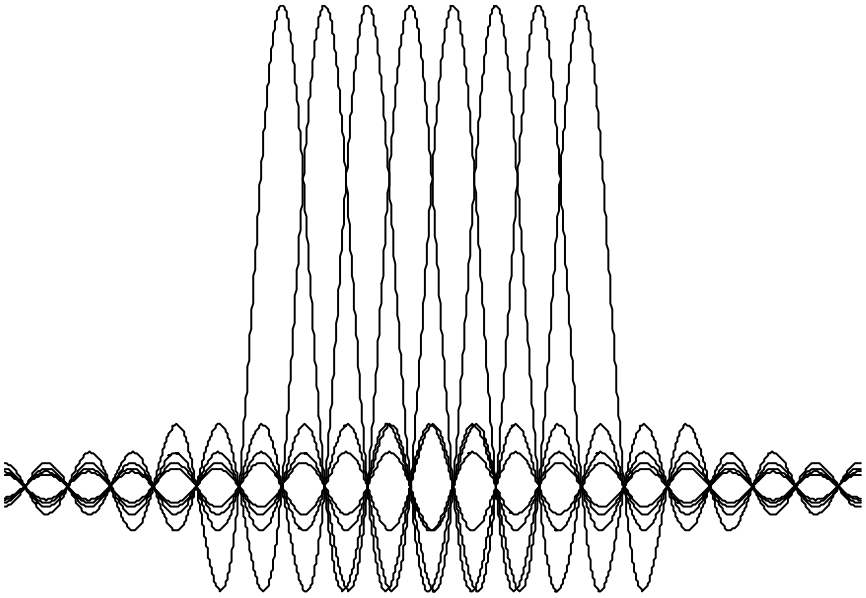

Figure 2-3: Spectra of subcarriers.

The complex baseband OFDM signal defined in (2.1) is actually the inverse Fourier transform of N_s input symbols. The time discrete equivalent is the inverse discrete Fourier transform (IDFT), which is given by (2.3). In practice, this transform can be implemented using inverse fast Fourier transform (IFFT).

$$s(n) = \sum_{i=0}^{N_s-1} d_i e^{j2\pi\frac{in}{N}} \tag{2.3}$$

2.1.2 Guard Time and Cyclic Extension

When the input datastream is divided in N_s subcarriers, the symbol duration becomes N_s times smaller. This also reduces the relative multipath delay spread, relative to the symbol time by N_s times. A guard time is needed for each OFDM symbol to eliminate the intersymbol interference (ISI) almost completely. The guard time is chosen to be larger than the expected delay spread, such that the multipath components from one symbol do not interfere with the next symbol. The guard time could consist of no signal at all. However, in that case, the problem of ICI would occur as the subcarriers are no longer orthogonal as illustrated in Figure 2-4.

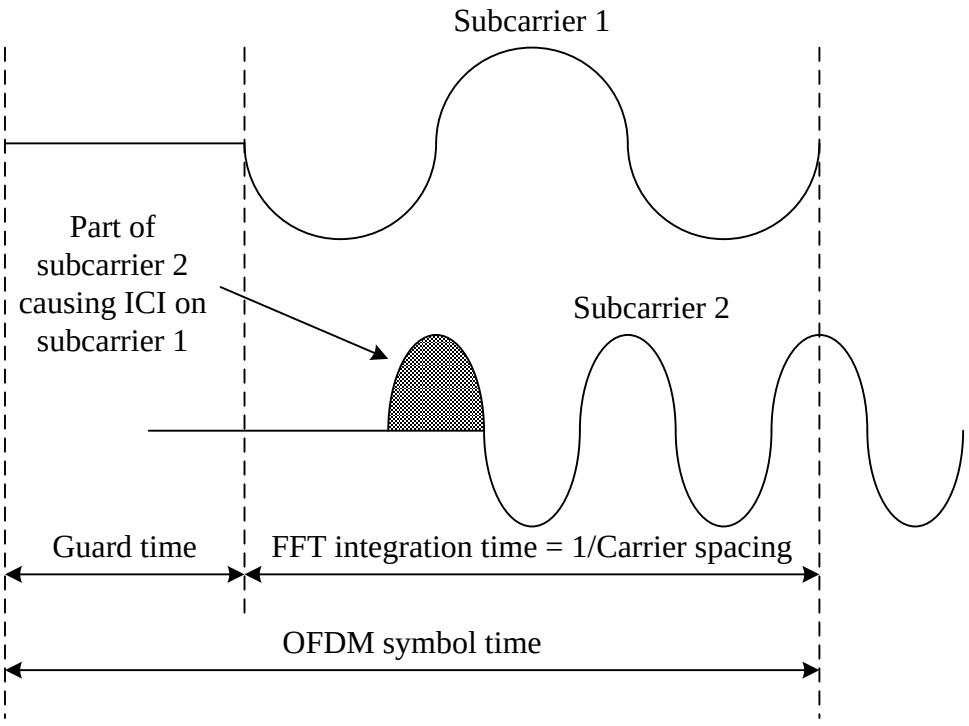

Figure 2-4: Effect of multipath on subcarriers with no signal in the guard time.

To eliminate this effect, the OFDM symbol is cyclically extended in the guard time, as shown in Figure 2-5. This ensures that, as long as the delay is smaller than the

guard time, delay replicas of the OFDM symbol always have an integer number of cycles within the fast Fourier transform (FFT) interval. Hence, multipath signals with delays smaller than the guard time will not cause ICI.

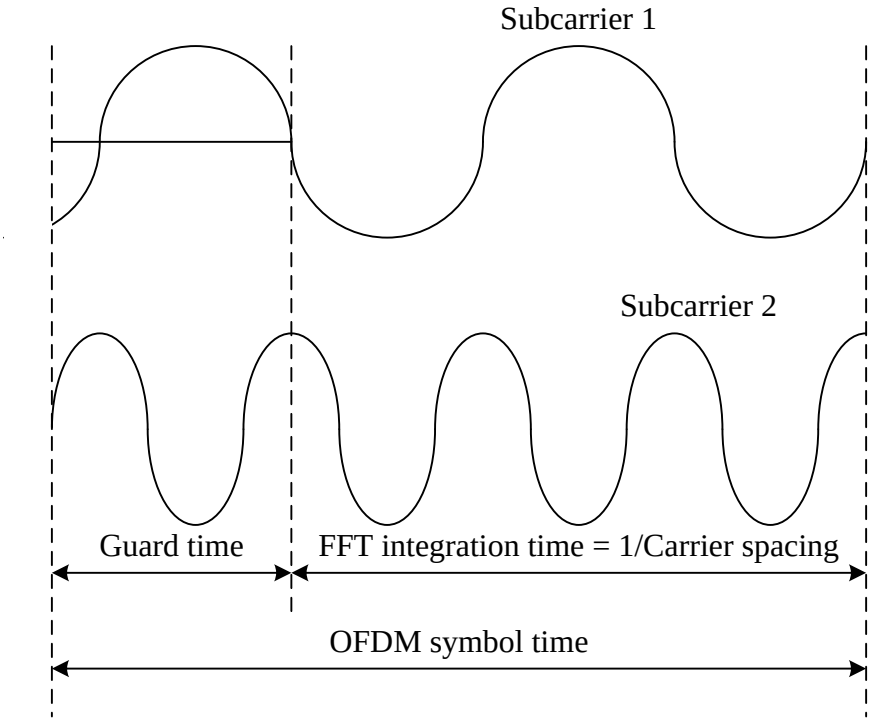

Figure 2-5: OFDM symbol with cyclic extension.

2.1.3 Windowing

For an OFDM signal consisting of unfiltered subcarriers, sharp phase transistion caused by modulation can be seen at the symbol boundaries. As a result, the out-of-band spectrum decreases rather slowly. For larger number of subcarriers, the spectrum goes down more rapidly in the beginning as the sidelobes are closer together. To make the spectrum go down more rapidly, windowing is applied to individual OFDM symbols. Windowing an OFDM symbol makes the amplitude go smoothly to zero at

the symbol boundaries. A commonly used window type is the raised cosine window, defined as

$$w(t)=\begin{cases}0.5+0.5\cos\left(\pi+\dfrac{t\pi}{\beta T_s}\right) & , \quad 0\le t\le \beta T_s \\ 1.0 & , \quad \beta T_s \le t \le T_s \\ 0.5+0.5\cos\left(\dfrac{(t-T_s)\pi}{\beta T_s}\right) & , \quad T_s \le t \le (1+\beta)T\end{cases} \tag{2.4}$$

where T_s is symbol interval and β is the roll-off factor.

T_s is shorter than the total symbol duration as adjacent symbols are allowed to partially overlap in the roll-off region. The time structure of the OFDM signal is shown in Figure 2-6, where T_s is the symbol time, T is the FFT interval, T_G is the guard time, T_{prefix} is the preguard time interval, $T_{postfix}$ is the postguard time interval and β is the roll-off factor.

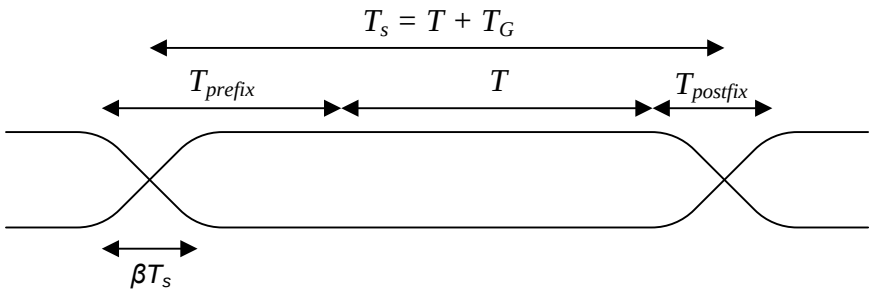

Figure 2-6: OFDM cyclic extension and windowing.

2.1.4 OFDM Transceiver

Figure 2-7 shows the block diagram of an OFDM transceiver. The upper path is the transmitter chain while the lower path is the receiver chain. In the center of the transmitter chain is the IFFT block, which modulates the input QAM values onto the subcarriers. The subcarriers are demodulated by the FFT in the receiver chain. FFT is the reverse operation of an IFFT but an interesting feature about FFT/IFFT is that the FFT is almost identical to the IFFT. IFFT can be made using an FFT by conjugating input and output of the FFT and dividing the output by the FFT size. This allows the use of the same hardware for both the transmitter and receiver, thus reducing the complexity of the transceiver.

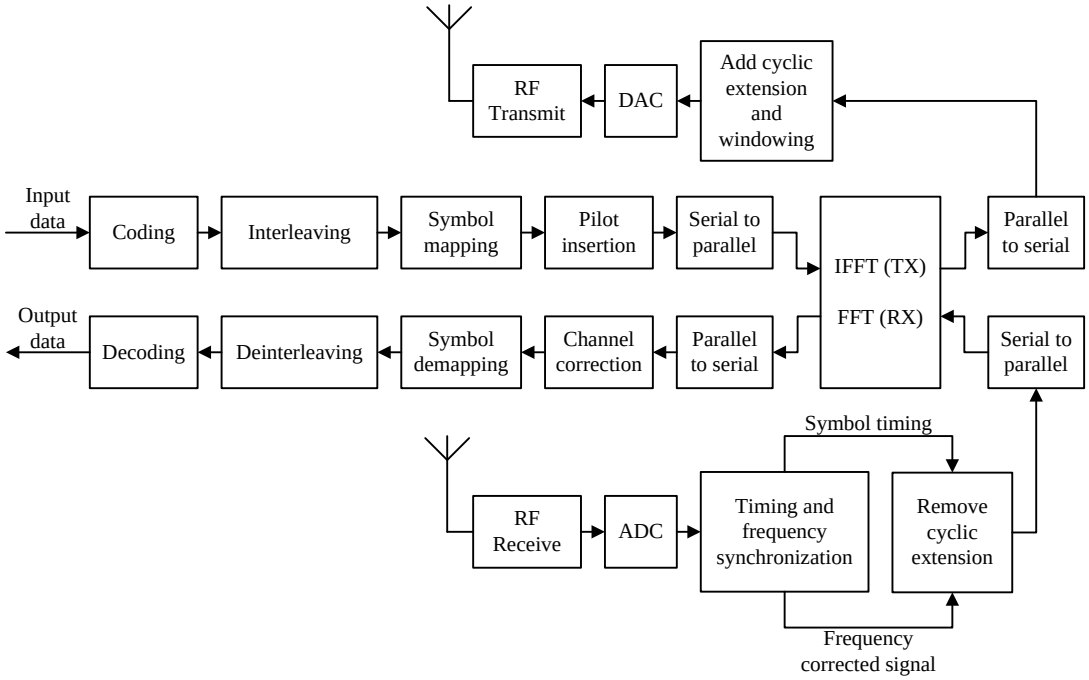

Figure 2-7: Block diagram of an OFDM transceiver.

2.2 Ultra Wideband (UWB)

2.2.1 History

In February 2002, the Federal Communications Commission (FCC) in the United States defined a UWB device as any device emitting signals with a fractional bandwidth greater than 0.2 or a bandwidth of at least 500 MHz at all times of transmission. The fractional bandwidth is defined by $2(f_H - f_L)/(f_H + f_L)$, where f_H is the upper frequency and f_L the lower frequency at the -10 dB emission point. The center frequency of the signal spectrum emitted by such a system is defined as the average of the upper and lower -10 dB points (i.e. $f_C = (f_H + f_L)/2$). FCC allocated a large bandwidth of 3.6-10.1 GHz at a transmit power below -41.3 dBm/MHz for UWB devices [4][16]. The spectrum mask for indoor situation is shown in Figure 2-8.

The extremely large bandwidth occupied by UWB allows very high potential capacity, giving very high data rates. This is shown in Shannon's capacity equation [17]:

$$C = B\log\left(1+\frac{S}{N}\right) \tag{2.5}$$

where C is the maximum channel capacity, B is the signal bandwidth, S is the signal power and N is the noise power. (2.5) shows that the channel capacity can be improved by increasing the signal bandwidth or power. Furthermore, it shows that increasing channel capacity requires linear increases in bandwidth while similar increases in channel capacity would require exponential increases in power [18].

Hence, from (2.5), it can be observed that UWB system has a great potential for high-speed wireless communications.

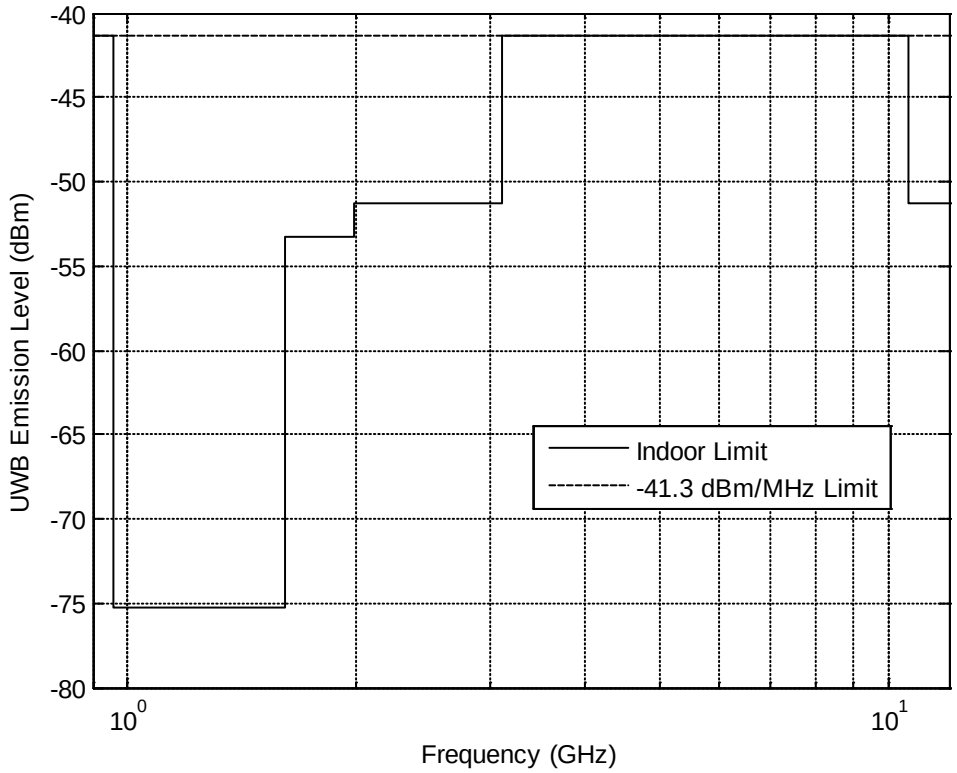

Figure 2-8: UWB spectral mask in indoor situations.

UWB has several advantages that make it attractive for consumer communications applications [18][19]:

- Potential for high data rates.
- Potentially low complexity and low cost.
- Noise-like signal.
- Resistant to severe multipath and jamming.
- Very good time domain resolution allowing for location and tracking applications.

2.2.2 Different Transmission Schemes

Although FCC has regulated the spectrum and transmitter power levels for UWB, there is no standard for a UWB transmission scheme. Traditional approach for UWB communication system uses narrow time-domain pulses which occupy a very large spectrum. The main disadvantages for this approach is the difficulties faced in building RF and analog circuits with large bandwidths, high speed analog-to-digital converters (ADCs) to process the signal and the digital complexity needed to capture the multi-path energy in dense multi-path environments [20].

Another approach based on pulsed multi-band [21] solves the need to process the signal over the large bandwidth. This reduces the complexity of the design, power consumption and overall solution cost [20]. However, this approach poses difficulty in collecting significant multi-path energy when using a single RF chain and requires a very stringent band-switching timing [20]. Furthermore, the system performance is sensitive to the group delay variations introduced by the analog front-end components when the number of RAKE fingers used is small [20].

The use of orthogonal frequency division multiplexing (OFDM) with multi-banding to manage the allocated UWB spectrum allows the strengths of the pulsed multi-band system to be retained while addressing the issue of multi-path energy capture. This system proposed by WiMedia Alliance which consists of a number of major players in consumer electronics, personal computing and mobile phone industry like Hewlett-Packard Company, Intel Corporation, Nokia Corporation, Philips, Sony Corporation, STMicroelectronics and Texas Instruments, Inc., is known as Multi-Band OFDM (MB-OFDM) [22]-[24].

Some advantages of MB-OFDM include [23]:

- Good coexistence with narrowband systems.
- Robust multipath tolerance.
- Low cost.
- High data rate.
- Low Power consumption.
- Adaptation to different regulatory environments.
- Future scalability and backward compatibility.

2.2.3 MultiBand OFDM (MB-OFDM) Ultra Wideband (UWB)

In the MB-OFDM approach [2][23], the available 7.5 GHz allocated by FCC is divided into fourteen bands as shown in Figure 2-9 and Table 2-1. The relationship between the centre frequency, f_c, and the Band ID, n_b, is given by

$$f_c(n_b) = 2.904 + 0.528 \times n_b \text{ (in GHz).} \tag{2.6}$$

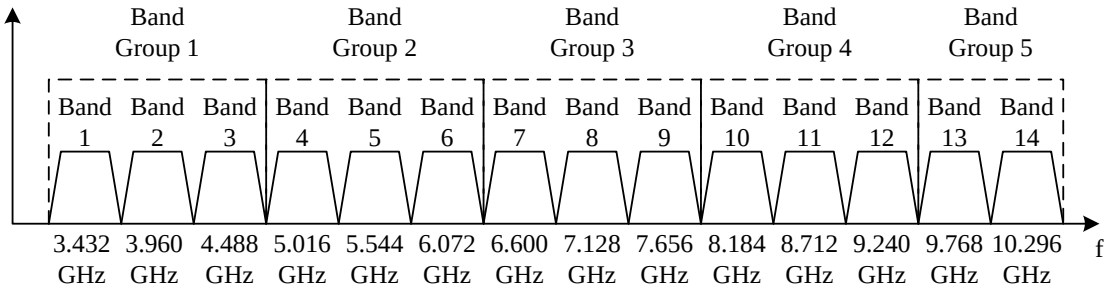

Figure 2-9: Diagram of band group allocation in MB-OFDM UWB.

Table 2-1: Band group allocation in MB-OFDM UWB.

Band Group	Band ID (n_b)	Lower Frequency (GHz)	Centre Frequency (GHz)	Upper Frequency (GHz)
1	1	3.186	3.432	3.696
	2	3.696	3.960	4.224
	3	4.224	4.488	4.752
2	4	4.752	5.016	5.280
	5	5.280	5.544	5.808
	6	5.808	6.072	6.336
3	7	6.336	6.600	6.864
	8	6.864	7.128	7.392
	9	7.392	7.656	7.920
4	10	7.920	8.184	8.448
	11	8.448	8.712	8.976
	12	8.976	9.240	9.504
5	13	9.504	9.768	10.032
	14	10.032	10.296	10.560

Each band has a bandwidth of 528 MHz. Within each band, OFDM modulation is used to transmit the information over 128 subcarriers. Of the 128 subcarriers, 100 are allocated for data, 10 are guard subcarriers (5 on each edge of the occupied frequency band) and 12 are pilot subcarriers for coherent detection and robustness against frequency offset and phase noise. The rest of the 6 subcarriers (62 to 66 and DC) are set to zero. The subcarriers falling at DC is not used to avoid difficulties in DAC and ADC offsets and carrier feedthrough in the RF chain. Unique logical channels are defined by using up to seven different Time Frequency Codes (TFCs) for each band group. The TFCs and the associated base sequences (and corresponding preambles) for band group 1 are defined in Table 2-2 as a function of Band ID (n_b). The TFCs and the associated base sequences (and corresponding preambles) for other band groups can be found in [2].

Table 2-2: Time-Frequency Code (TFC) and Preamble Patterns for Band Group 1

TFC Number	Base Sequence / Preamble	Band ID (n_b) for TFC					
1	1	1	2	3	1	2	3
2	2	1	3	2	1	3	2
3	3	1	1	2	2	3	3
4	4	1	1	3	3	2	2
5	5	1	1	1	1	1	1
6	6	2	2	2	2	2	2
7	7	3	3	3	3	3	3

The transmitted spectral mask will have the following break points: an emissions level of 0 dBr (dB relative to the maximum spectral density of the signal) from -260 MHz to 260 MHz around the centre frequency, -12 dBr at 285 MHz frequency offset, and -20 dBr at 330 MHz frequency offset and above [2]. The transmitted spectral mask is shown in Figure 2-10.

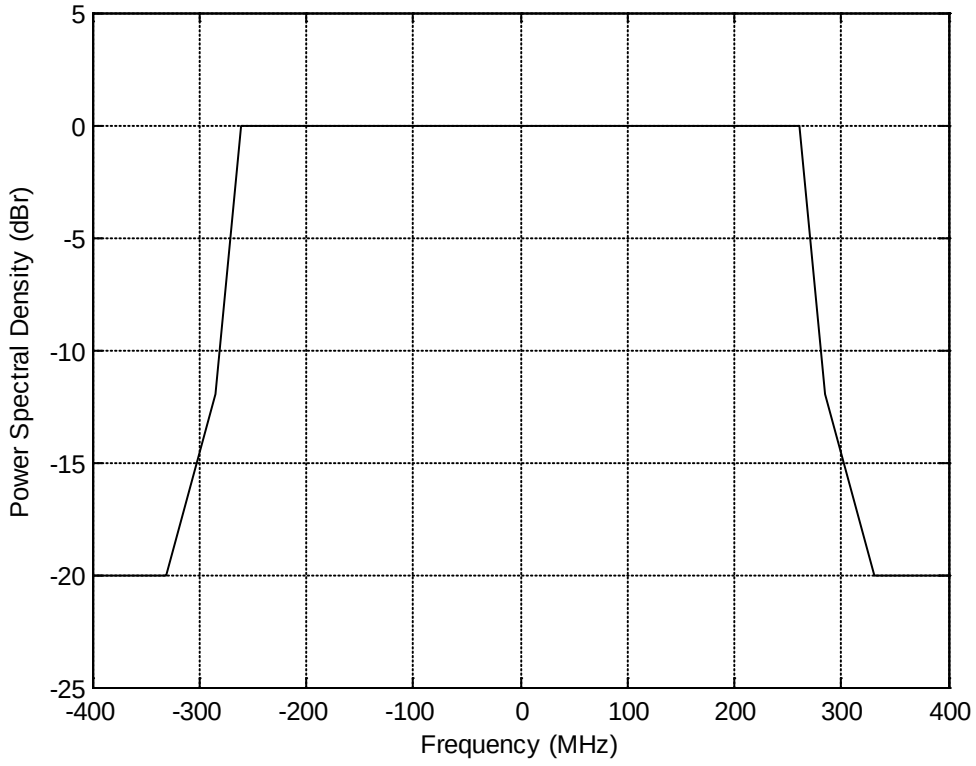

Figure 2-10: Transmit power spectral mask.

2.3 Transmitter Architectures

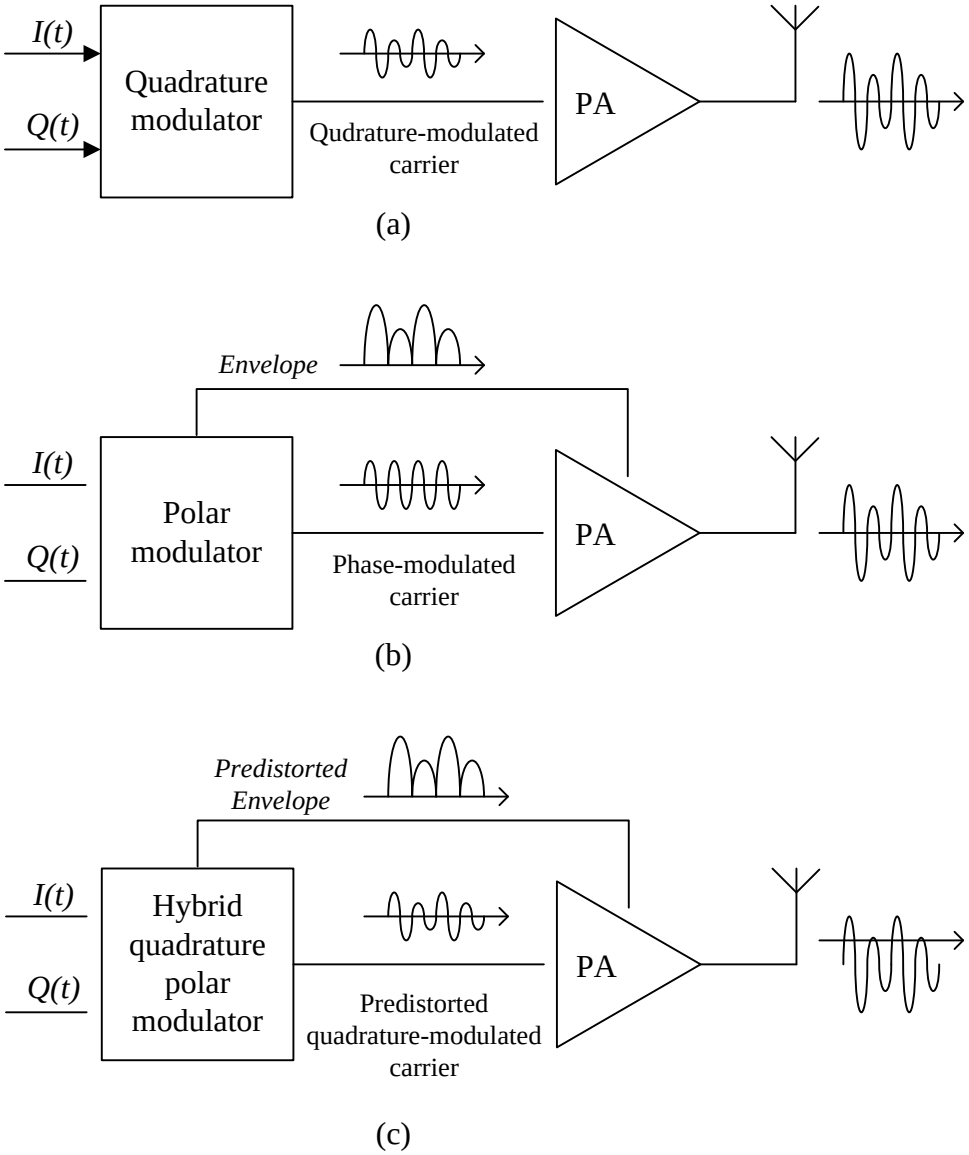

Figure 2-11: Comparison of RF carrier modulation techniques for (a) quadrature modulation, (b) polar modulation and (c) hybrid quadrature polar modulation

A RF transmitter modulates and upconverts the baseband signal to RF signal which is then amplified by the power amplifier (PA) before transmission. The transmit power has to be large to overcome the rapid attenuation of electromagnetic waves over distance. In addition, the transmitted signals should not interfere with other parts of

the spectrum. Transmitter architectures can be classified according to the modulator implementation – quadrature architecture and polar architecture. In quadrature architecture (Figure 2-11(a)), I/Q components of the signal are modulated and then combined before being amplified by the PA. On the other hand, in polar architecture (Figure 2-11(b)), the magnitude and phase are modulated and then combined. Besides the two architectures, it is also possible to combine both architectures to form a hybrid quadrature polar architecture [25] as shown in Figure 2-11(c).

2.3.1 Quadrature Architecture

In quadrature architecture [26][27], I/Q signals is fed to the I/Q modulator, as shown in Figure 2-12, and the output of the I/Q modulator is a complex transmit signal. The complex transmit signal, $S(t)$, is related to the I/Q signals by

$$S(t) = I(t)\cos(\omega_c t) - Q(t)\sin(\omega_c t) \tag{2.7}$$

where $I(t)$ is the in-phase signal, $Q(t)$ is the quadrature signal and ω_c is the carrier frequency.

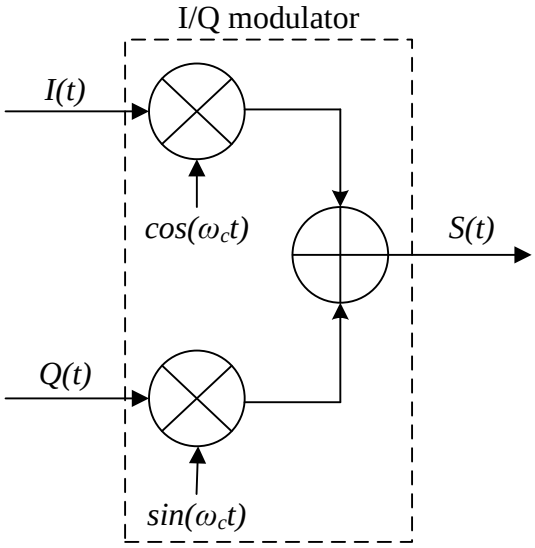

Figure 2-12: Relationship between *S(t)* and I/Q signals.

2.3.1.1 Direct-Conversion (Homodyne) Transmitter

In the direct-conversion transmitter [28] shown in Figure 2-13, the I/Q modulator operates at local oscillator (LO) frequency. As modulation and upconversion occur in the same circuit, this architecture offers the advantages of simplicity with minimum amount of circuitry and ease of high level integration.

However, this architecture suffers from an important drawback, where disturbance of LO by the PA occurs through a mechanism called “injection pulling” or “injection locking” [26]. This problem will worsen if the PA is turned on and off periodically to save power. Furthermore, the I/Q modulator also suffers from various circuit and device mismatches. Each mixer produces an output equal to the product of the input signal and the LO signal. Any dc level or offset at the mixer inputs feeds a portion of the unmodulated LO frequency to its output, resulting in carrier leakage. Any amplitude or phase mismatch between the two mixers degrades the orthogonality and causes the inputs to spill into each other. This effect is known as I/Q leakage. In addition, this architecture requires a PA with good linearity.

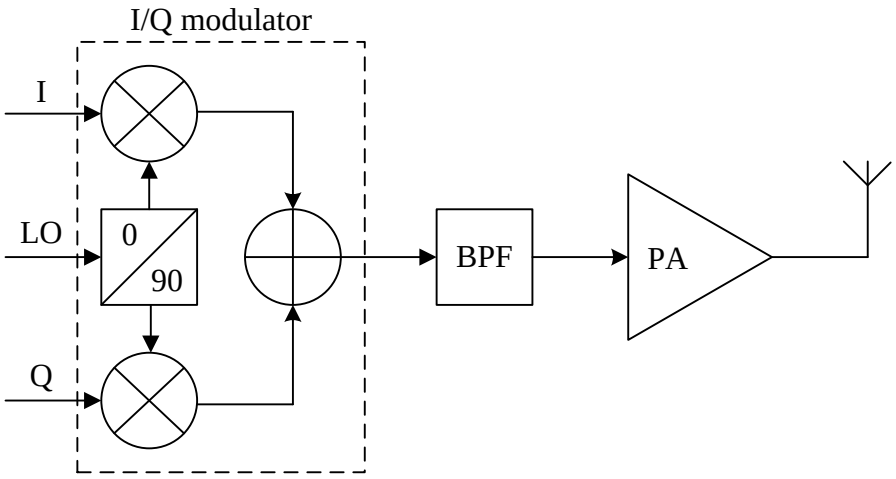

Figure 2-13: Direct-conversion (homodyne) transmitter.

2.3.1.2 Two-Step Conversion (Super-heterodyne) Transmitter

The problem of LO pulling in direct-conversion is alleviated if the PA output spectrum is sufficiently higher or lower than the LO frequency. This can be accomplished by upconverting the baseband signal in two (or more) steps so that the PA output spectrum is far from the LO frequency [26].

In the two-step transmitter shown in Figure 2-14, the I/Q modulator operates at an intermediate frequency (IF) or LO_1 and the IF signal is subsequently upconverted to the RF frequency or LO_2. An IF bandpass filter (BPF) is required to eliminate the LO_1 harmonics after the modulation. Another BPF is required following the second upconversion to reject the unwanted sideband. Two-step transmitter offers the advantages of having the PA output spectrum far away from the LO frequencies and having I/Q modulation performed at lower frequency (i.e. at immediate frequency). However, this architecture needs a significant amount of circuitry and, hence, allows low integration level. Furthermore, multi-mode implementation using this architecture is difficult. Similar to the direct-conversion transmitter, this architecture requires a PA with good linearity.

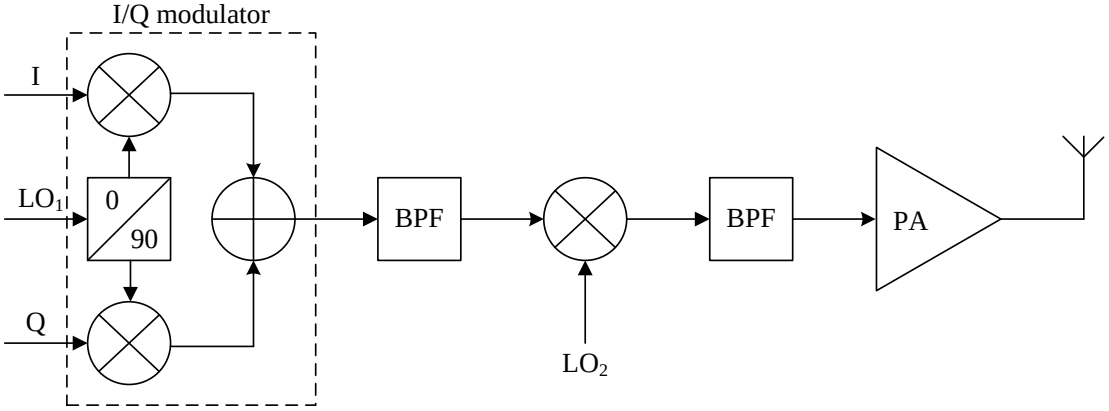

Figure 2-14: Two-step (super-heterodyne) transmitter.

2.3.2 Linearization

The output of the I/Q modulator is a complex transmit signal and the amplifier following it needs to preserve the amplitude variation or the modulation will spill into nearby frequency channels. This effect is known as spectral regrowth [29]. To minimize spectral regrowth, linear PA is required. Furthermore, amplifiers that simultaneously process many channels may need to be linear enough to avoid cross modulation. Unfortunately, linear PA does not have high power efficiency. To achieve higher efficiency, a non-linear PA is used by applying some linearization techniques. Common methods of linearization techniques are back-off, predistortion, feedforward, feedback, linear amplification with non-linear components (LINC), and envelope elimination and restoration (EER) [26][27][30].

2.3.2.1 Back-off

As the output power of a PA approaches the 1-dB compression point, the output signal is distorted. Hence, in order to improve the linearity of the PA, its output power is limited to a level below the 1-dB compression point. In other words, the output power of the PA is said to be backed off from the compression point, as shown in Figure 2-15. The amount of back-off required is often a function of the modulation scheme as well as AM-to-AM and AM-to-PM distortions in the PA [30]. In some instances, additional back-off is needed to avoid phase distortion, which can be served as the output power increases [30].

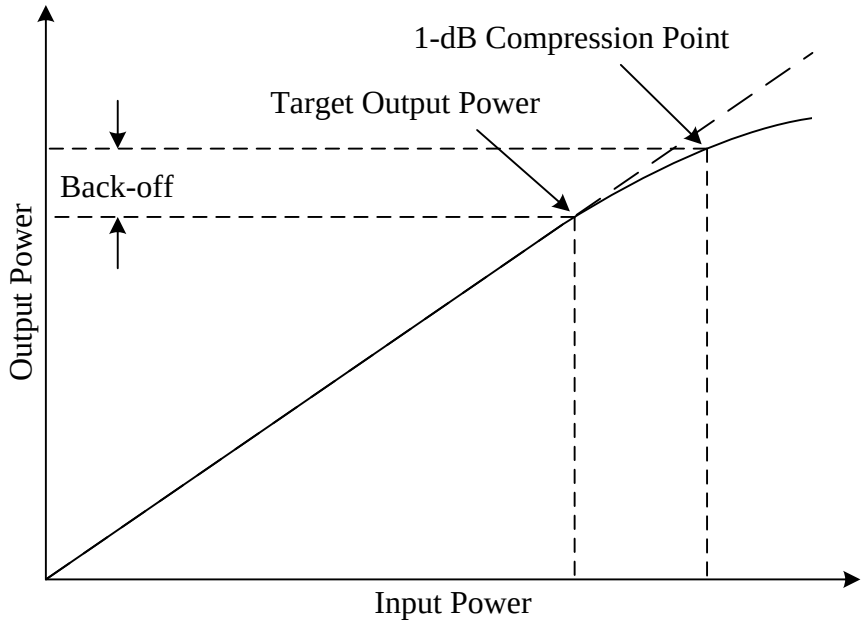

Figure 2-15: Power amplifier compression curve and the 1-dB compression point.

Although back-off is the simplest means of linearization, it does have its drawback. To ensure that the backed-off PA is in linear operation, the maximum output power is over-designed by a certain margin. This results in the efficiency at the maximum output power being greatly reduced.

2.3.2.2 Predistortion

Non-linearity in the input-output transfer characteristic of a PA can be corrected for at its input by predistorting the signal delivered to it [30]. The input predistortion is designed to cancel the distortion introduced by the PA, providing a linear overall transfer function, as shown in Figure 2-16.

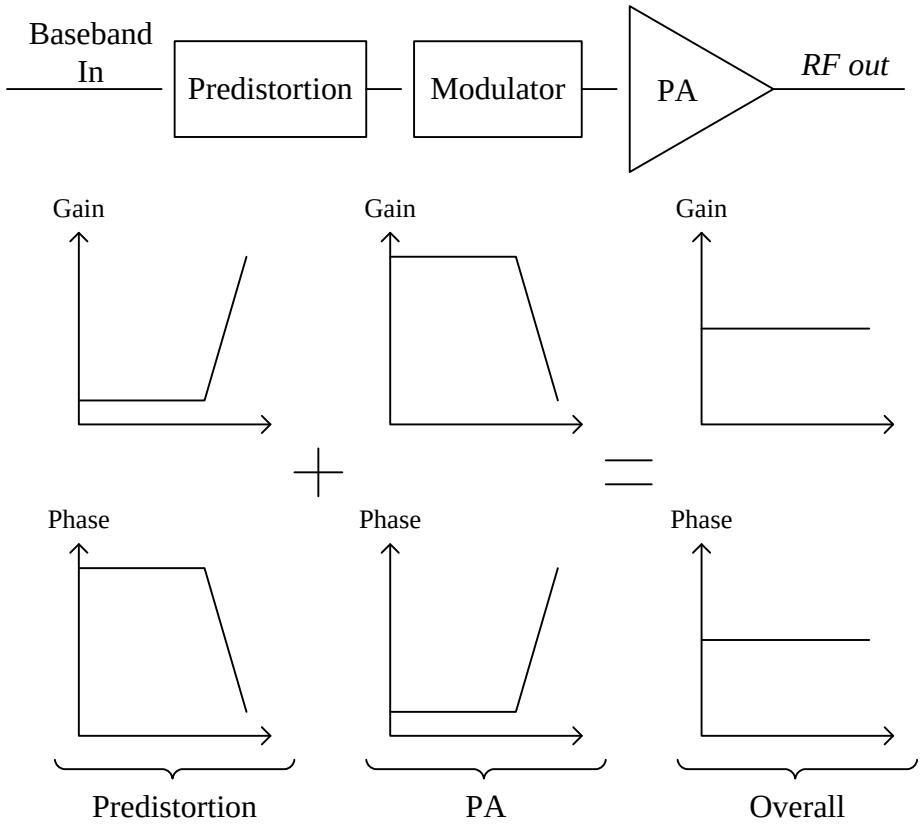

Figure 2-16: Predistortion.

If the magnitude and the phase of the PA transfer are known, deviation from the constant gain and phase can be corrected for at the input [30].Correction can be done on the baseband signal before it modulates the RF carrier. If the PA introduces gain and phase distortions at higher levels of output power, the baseband signal can be preamplified and phase shifted to compensate for the PA distortion.

Although predistortion seems quite straightforward, practical problems arise in implementing it. The PA must be characterized in order to determine its transfer function. However, the gain and phase responses of the PA changes with factors like temperature, bias conditions, supply voltage and process variation. All these factors will result in less than perfect compensation of the PA linearity using predistortion.

2.3.2.3 Feedforward

A non-linear PA generates a waveform that can be viewed as the sum of the linear replica of the input waveform and an error signal [26]. A feedforward topology computes the error signal and, with proper scaling, subtracts it from the output waveform. As shown in Figure 2-17, the output of the main PA, $V_m = A_v V_{in} + V_e$, is scaled by $1/A_v$, generating $V_N = V_{in} + V_e / A_v$, V_e is the error signal. The input, V_{in}, is subtracted from V_N, and the result is scaled by A_v and subtracted from V_M. Hence, $V_{out} = A_v V_{in}$.

The advantage of feedforward topologies over feedback methods is inherent stability even when each building block has finite bandwidth and substantial phase shift [26]. This is important for RF and microwave circuits as poles and resonances at frequencies near the band of interest will make it difficult to achieve stable feedback.

However, feedforward topologies suffer from some drawbacks [26]. First, the two amplifiers (PA and error amplifier), shown in Figure 2-17, exhibit substantial phase shift at high frequencies, mandating the need of delay elements (Δ_1 and Δ_2) to compensate for their phase shift. The implementation of the delay elements requires passive devices, such as microstrip lines, resulting in loss of power along the paths. Second, the output subtractor must be realized using a low-loss component, such as a high-frequency transformer. Third, the amount of linearization depends on the gain and phase matching of the signals sensed by each subtractor.

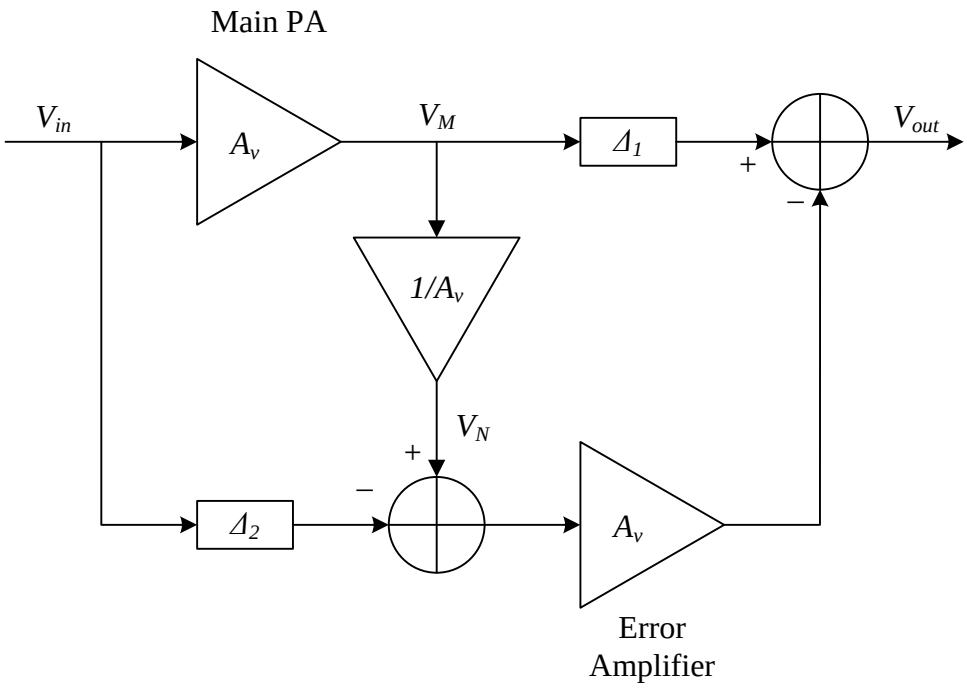

Figure 2-17: Feedforward topology to improve PA linearity.

2.3.2.4 Feedback

Feedback technique to improve the linearity of the PA is shown in Figure 2-18. Feedback techniques cannot be easily applied to RF PA at high frequencies. This is because, for a heavily non-linear PA, a high loop gain must be achieved and it is a difficult task at high frequencies [26]. Hence, in order to alleviate this problem, most of the loop gain is obtained at low frequencies. A transmitted signal from the output of the PA originates from upconverting a baseband or IF signals. Hence, if the output of the PA is downconverted and compared with the original low-frequency signal in a negative feedback loop, the distortion in the PA can be removed.

For transmitters incorporating upconversion of both I and Q signals, the output of the PA must be downconverted back into quadrature phases before it can be compared with the inputs. This technique is called Cartesian feedback [31] and is shown in

Figure 2-19. Cartesian feedback has its drawbacks. First, the added complexity resulting from the feedback demodulator and error amplifiers increases power consumption. Second, the two feedback loops must maintain strict orthogonality or they will not act independently [27]. The amount by which the two feedback loops are not orthogonal may vary with time, temperature, supply voltage and RF carrier.

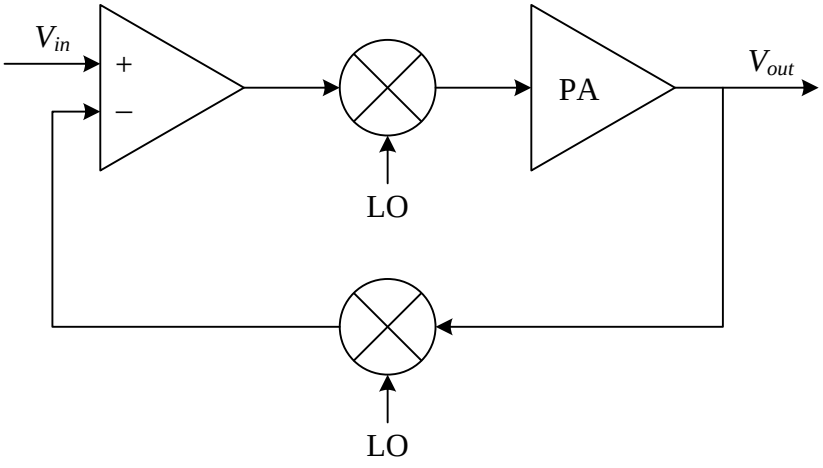

Figure 2-18: Negative feedback to improve PA linearity.

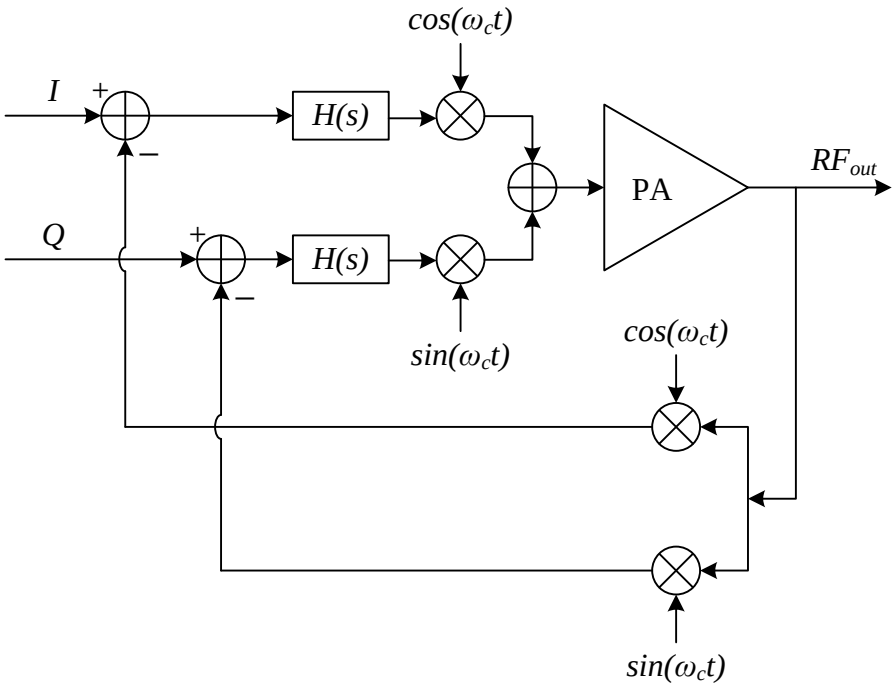

Figure 2-19: Cartesian feedback.

2.3.2.5 Linear Amplification with Non-linear Components (LINC)

Non-linear amplification of constant-amplitude signals offers higher efficiency. In order to improve efficiency, variable-amplitude signals can be separated into two constant-amplitude signal components, encoding the information carried in the amplitude of the variable-amplitude signals into phase difference between the two constant-amplitude signal components. This allows each constant-amplitude signal component to be amplified using a highly efficient non-linear PA, with the outputs combined to reconstruct an amplified version of the variable-amplitude signals, as illustrated in Figure 2-20. This technique is known as linear amplification using non-linear components (LINC) [32].

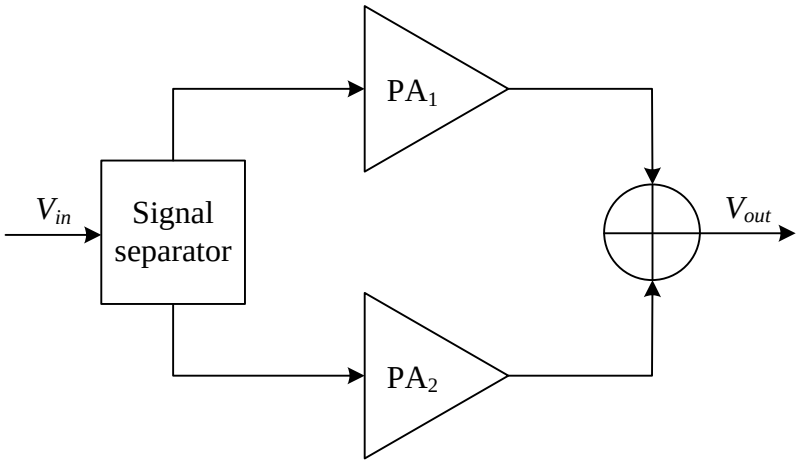

Figure 2-20: Linear amplification using non-linear components (LINC).

Although LINC is simple in theory, the implementation of such a system poses serious challenges. First, gain and phase mismatch between the two signal paths will result in residual distortion [26]. Second, the implementation of signal separator at high frequencies is extremely challenging. Last but not least, the output adder introduces significant loss because it must achieve high isolation between the two PAs [26].

2.3.2.6 Envelope Elimination and Restoration (EER)

Any bandpass RF signal, $S(t) = A(t)\cos\left(\omega_c t + \phi(t)\right)$, can be represented by its envelope component, $A(t)$, and phase component, $\phi(t)$. Hence, it is possible to decompose $S(t)$ into a envelope signal, $A(t)$, and a phase-modulated signal, $\cos\left(\omega_c t + \phi(t)\right)$, amplifying each separating, and combining the results at the end. This concept is called envelope elimination and restoration (EER) [5] and is shown in Figure 2-21. The input signal drives both an envelope detector and a limiter, producing the envelope signal and the phase-modulated signal. A non-linear switching PA is used to amplify the phase-modulated signal and the envelope can be combined with the output of this PA by modulating the power supply of the PA.

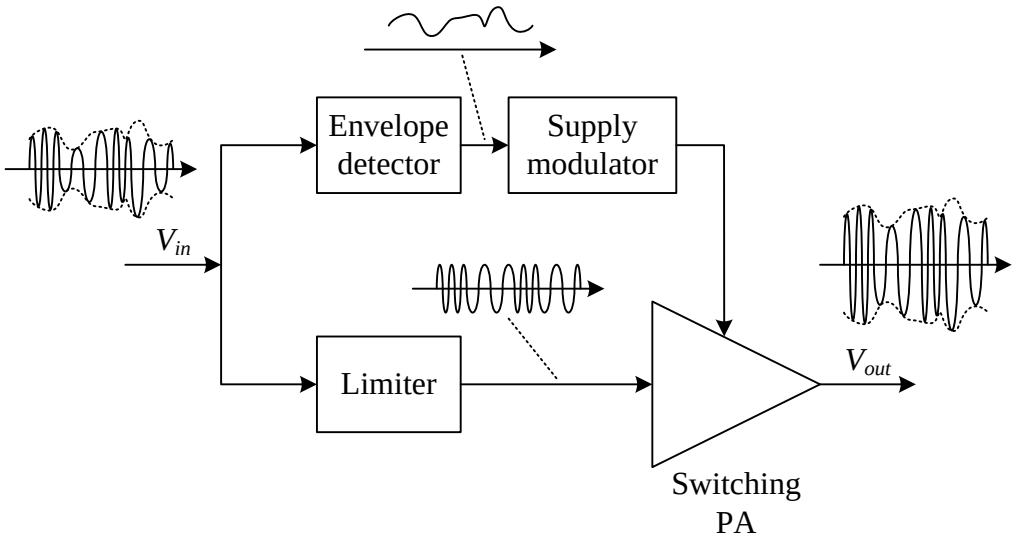

Figure 2-21: Envelope elimination and restoration (EER).

The main advantage of EER is that it requires no linearity in the PA, allowing the output stage to be designed for maximum efficiency. However, it suffers from other drawbacks. First, substantial power could be dissipated in the circuitry modulating supply of the PA since it must provide all the current drawn by the PA. Second, the

mismatch between the envelope and the phase signals must be maintained below an acceptable level. This is a difficult task as the two signals employ different type of circuits operating at different frequencies. Furthermore, it is difficult to have equal delays in both signals that track process and temperature variations.

2.3.3 Polar Architecture

In quadrature architecture, the I/Q modulator uses rectangular or Cartesian modulation to form the complex transmit signal. On the other hand, polar modulator in the polar transmitter uses amplitude and phase to form the complex transmit signal, as shown in Figure 2-22. This concept is similar on the EER mentioned in Section 2.3.2.6, where the complex transmit signal, $S(t)$, can be represented by $S(t) = A(t)\cos(\omega_c t + \phi(t))$ where $A(t)$ is the amplitude signal, $\phi(t)$ is the phase signal and ω_c is the carrier frequency.

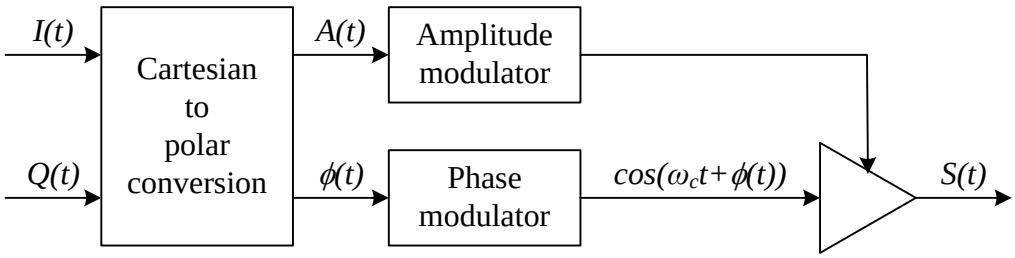

Figure 2-22: Polar architecture.

For the complex transmit signal, $S(t)$,

$$\begin{aligned} S(t) &= A(t)\cos\left(\omega_c t + \phi(t)\right) \\ &= I(t)\cos\left(\omega_c t\right) - Q(t)\sin\left(\omega_c t\right) \end{aligned} \tag{2.8}$$

where $I(t)$ is the in-phase signal and $Q(t)$ is the quadrature signal.

From (2.8),

$$I(t) = A(t)\cos\left(\phi(t)\right) \tag{2.9}$$

and

$$Q(t) = A(t)\sin\left(\phi(t)\right) \tag{2.10}$$

Summing the square of (2.9) and (2.10) will give

$$I(t)^2 + Q(t)^2 = A(t)^2 \tag{2.11}$$

Dividing (2.10) by (2.9) will give

$$\frac{Q(t)}{I(t)} = \tan\left(\phi(t)\right) \tag{2.12}$$

Hence, from (2.11) and (2.12), it can be observed that $A(t)$ and $\phi(t)$ are related to $I(t)$ and $Q(t)$ by

$$A(t) = \sqrt{I(t)^2 + Q(t)^2} \tag{2.13}$$

and

$$\phi(t) = \tan^{-1}\left(\frac{Q(t)}{I(t)}\right) \tag{2.14}$$

This relation is also illustrated in Figure 2-23.

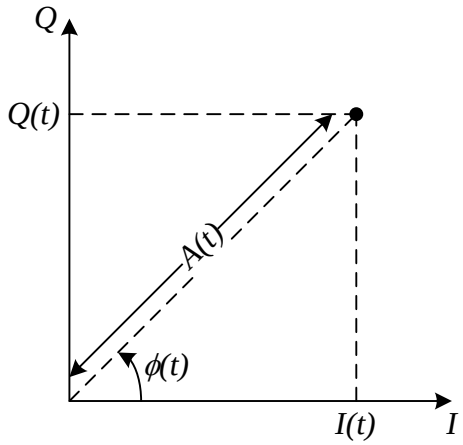

Figure 2-23: Relation between Cartesian representation and polar representation.

2.3.3.1 Polar Lite Transmitter

In the polar lite transmitter [12] shown in Figure 2-24, the I/Q signals are converted into amplitude and phase signals. The phase signal controls the phase modulator to generate a phase-modulated RF signal while the amplitude signal controls the amplitude modulator which modulates the amplitude on the phase-modulated RF signal. The final RF signal is passed through a linear PA before transmission.

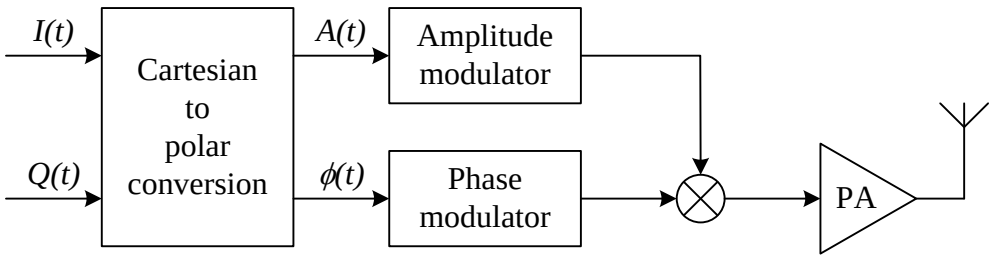

Figure 2-24: Polar lite transmitter.

This architecture provides a lower wideband noise floor than what is available from a linear design using an I/Q modulator. This is because the wideband noise floor from a

well-designed polar modulator is equal to the VCO phase noise [33]. Another advantage is that since the envelope and phase signals are all at a lower frequencies, it is possible to use digital techniques to realize both the phase and amplitude modulators, allowing much of the transmitter circuitry to be brought into the digital domain. Hence, this allows improved integration with digital baseband devices compared to an I/Q modulator. The obvious disadvantage from this architecture is the use of a linear PA. Transmitter efficiency will not improve with this architecture. Furthermore, the amplitude and phase signals need to be time aligned to reduce any delay mismatch.

2.3.3.2 Direct Polar Transmitter

Similar to the polar lite transmitter discussed in Section 2.3.3.2, the I/Q signals are converted into amplitude and phase signals and the phase signal controls the phase modulator to generate a phase-modulated RF signal. Instead of modulating the amplitude on the phase-modulated RF signal before the linear PA like the polar lite transmitter, the amplitude modulator in the direct polar transmitter applies the modulation directly to the PA, as illustrated in Figure 2-25. Several examples of the direct polar transmitter architecture can be found in [34]-[36].

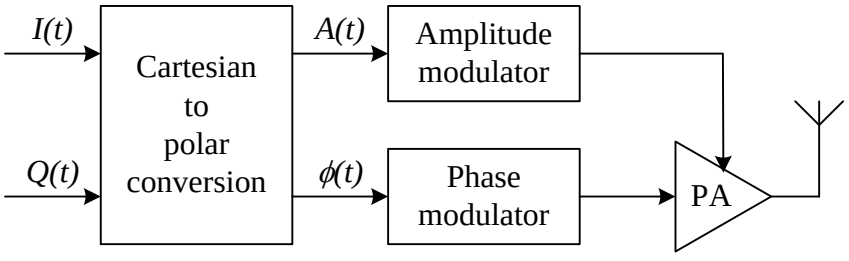

Figure 2-25: Direct polar transmitter.

This architecture allows a high efficient, non-linear PA to be used, generating very high energy efficiency for the transmitter. Furthermore, RF circuit linearity is not required [33]. Despite these advantages, direct polar transmitter does have its drawbacks. First, the non-linear PA needs to be characterized in compressed operation. Second, it requires accurate time alignment of the amplitude and phase signals. Last but not least, it suffers from AM-AM and AM-PM distortion effects which will require predistortions to correct these effects. The applied predistortions will need to take into account any temperature and supply voltage variations.

2.3.3.3 Polar Loop Transmitter

The polar loop transmitter [37], as shown in Figure 2-26, is similar to the direct polar transmitter discussed in Section 2.3.3.2. The difference is that the polar loop transmitter uses feedback control to correct the output signal into its desired form. By using closed-loop feedback control for both amplitude and phase of the output signal, some limitations of the direct polar transmitter can be overcome. The need for characterization and predistortion of the PA can be overcome.

Despite the advantages offered by polar loop transmitter, it does have its drawbacks. Having a receiver in the feedback loop will lead to increased complexity and higher power consumption. Furthermore, there is a need to take care of loop stability, which will vary with output power. Zero output power will pose a huge problem to the feedback loop [33].

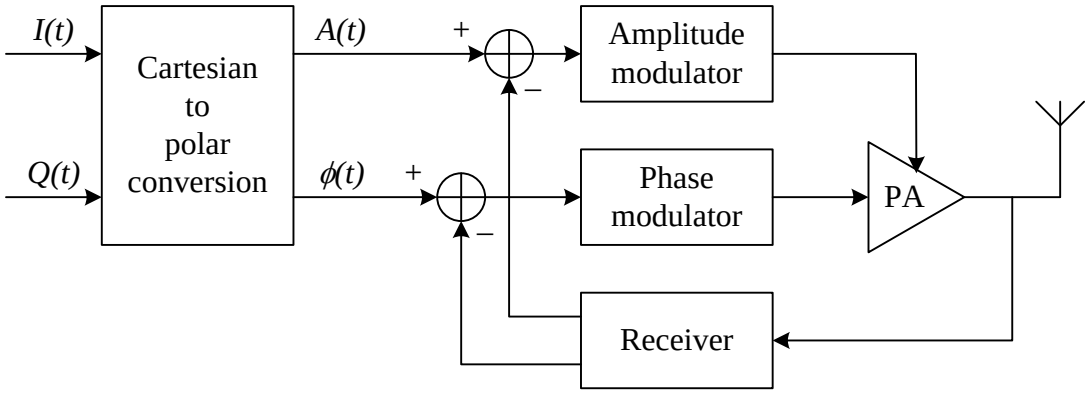

Figure 2-26: Polar loop transmitter.

2.4 Polar Transmitter Implementations

As mentioned in Section 2.3.3, polar modulator in the polar transmitter consists of the phase modulator that generates the phase-modulated RF signal and the amplitude modulator that modulates the amplitude information onto the phase-modulated RF signal to form the complex transmit signal. This section will discuss various architectures for phase and amplitude modulators reported in literature.

2.4.1 Phase Modulator

The role of the phase modulator is to generate a phase-modulated signal, $\cos\left(\omega_c t + \phi(t)\right)$. A common architecture is to use a phase-locked loop (PLL) and apply phase modulation directly to the synthesized RF carrier [38][39]. A PLL, as shown in Figure 2-27, consist of phase frequency detector, charge pump, loop filter, voltage-controlled oscillator (VCO) and frequency divider. The phase frequency detector and the charge pump generate either positive or negative charge pulses depending on whether the divided VCO signal leads or lag the reference signal. With

a constant division of *N*, the loop forces the VCO frequency, f_{VCO}, to be *N* times the reference frequency, f_{ref}.

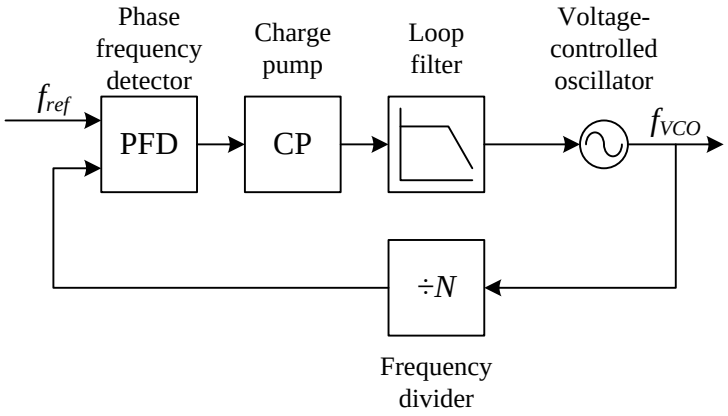

Figure 2-27: Phase-locked loop (PLL).

Since phase, ϕ, is related to frequency, ω, by

$$\omega = \frac{d\phi}{dt}, \tag{2.15}$$

it is possible to use the PLL as a phase modulator by causing the VCO to adjust its output frequency. In other words, the PLL performs frequency modulation in order to act as a phase modulator.

The frequency modulation in PLL can be controlled by three ways:

1. Shifting the phase of the reference signal (see Figure 2-28(a)).
2. Changing the frequency division (see Figure 2-28(b)).
3. Direct control of the VCO (see Figure 2-28(c)).

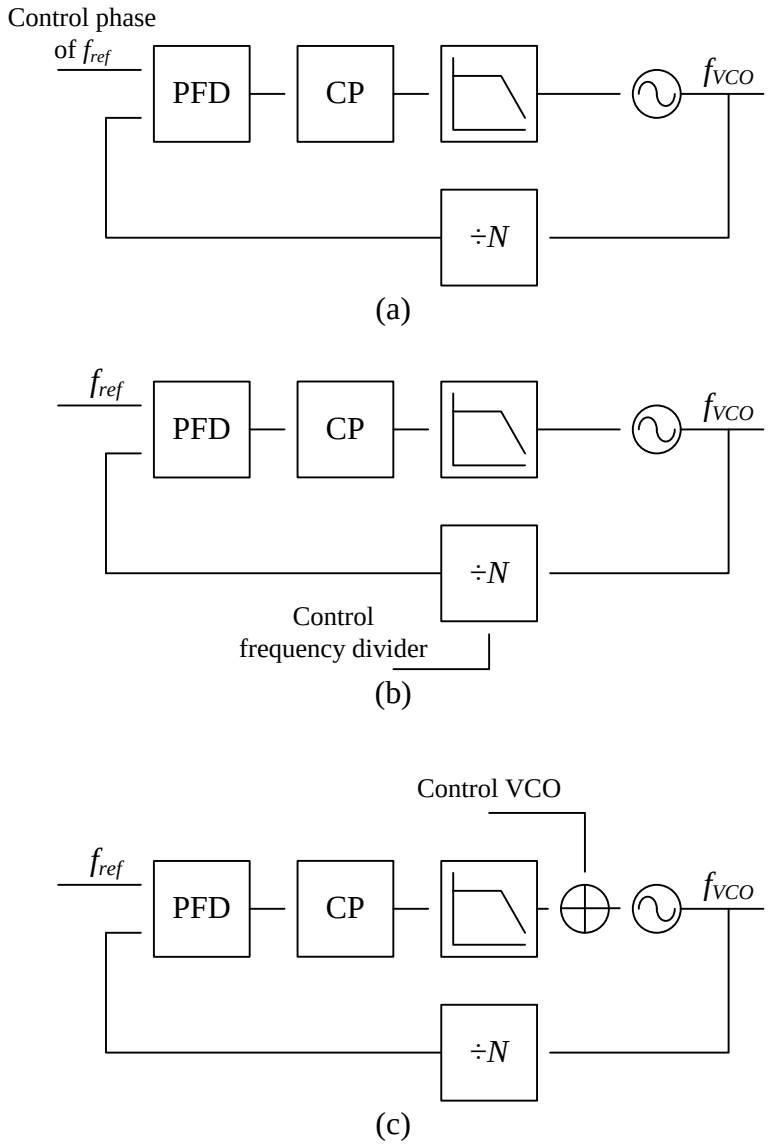

Figure 2-28: Different ways to modulate frequency in PLL: (a) controlling phase of reference signal, (b) controlling the frequency divider, and (c) controlling the VCO.

Another method of implementing the phase modulator is to use a direct digital synthesizer (DDS) [40][41]. Unlike PLL technique which is analog in nature, DDS technique is digital in nature. In PLL, the basic signal generator is the analog VCO. However, in DDS, the signal is generated and manipulated digitally, and after all the digital manipulations are completed, it is converted to analog signal using a digital-to-analog convertor (DAC) [42]. The DDS operation is illustrated in Figure 2-29.

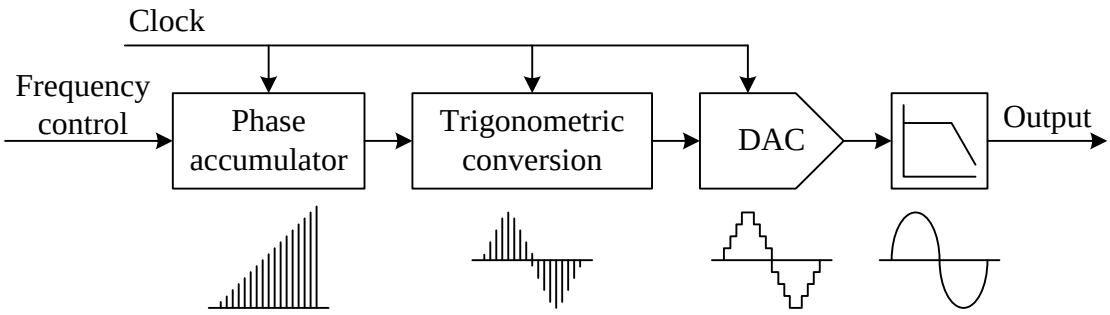

Figure 2-29: Direct digital synthesis (DDS).

By inserting phase information, $\phi(n)$, between the phase accumulator and the trigonometric conversion block, the DDS can be modified to become a phase modulator. This is illustrated in Figure 2-30.

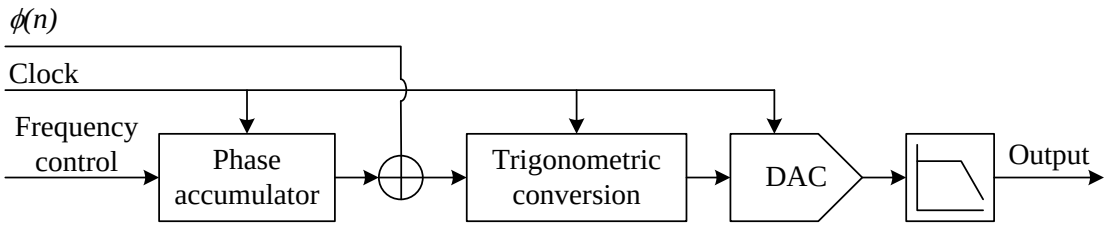

Figure 2-30: DDS as phase modulator.

2.4.2 Amplitude Modulator

The amplitude modulator in a polar modulator modulates amplitude onto the phase-modulated signal generated by the phase modulator. One way is to modulate the power supply of the PA as shown in Figure 2-31. By changing the power supply of the PA, the amplitude of the phase-modulated signal can be modulated to produce the RF signal for transmission. An example of such methods is found in [43].

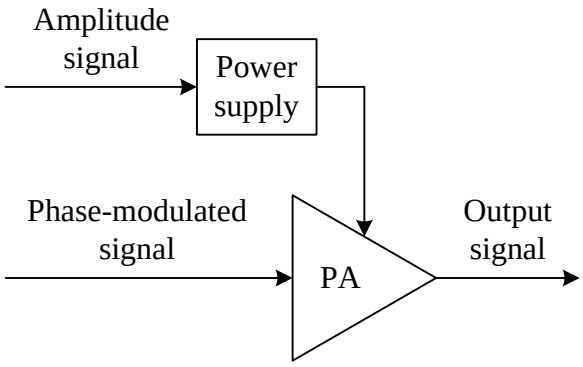

Figure 2-31: Amplitude modulation using power supply.

Another method is to use a digitally-controlled PA reported in [12]. The digitally-controlled PA shown in Figure 2-32 consists of unit-weighted multiple transistor switches. By regulating the number of active transistor switches, digital amplitude modulation can be achieved.

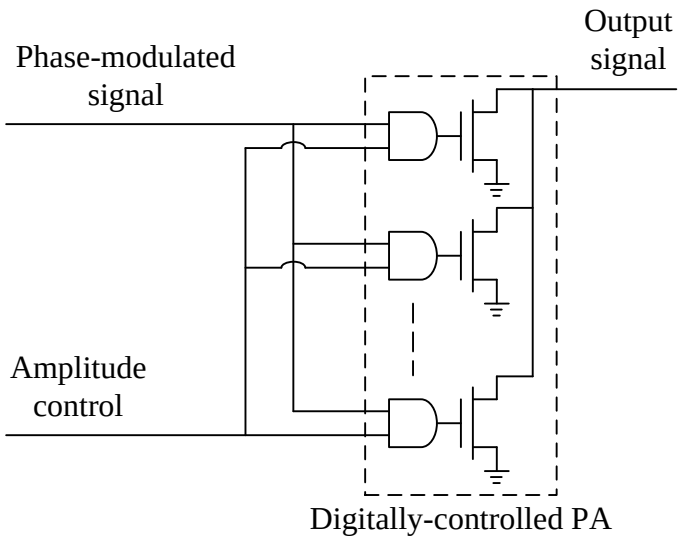

Figure 2-32: Digitally-controlled PA.

2.5 Performance Measure

There is a need to measure the performance of the transmitter. A common way is to use error vector magnitude (EVM). An information signal sent by an ideal transmitter is represented by a set of constellation points. However, imperfections in the transmitter cause these to deviate from the ideal locations. EVM is a measure of this deviation. As shown in Figure 2-33, EVM is the scalar distance between the ideal and the measured points, i.e. it is a magnitude of the difference vector. EVM can be defined as [44]

$$EVM = \sqrt{\frac{\frac{1}{N}\sum_{i=1}^{N}\left|\vec{e}_i\right|^2}{S_{\max}^2}} \tag{2.16}$$

where $\vec{e}_i$ is the error vector, N is the number of points in the measurement and $S_{\max}$ is the maximum amplitude of the constellation points that define the ideal signal.

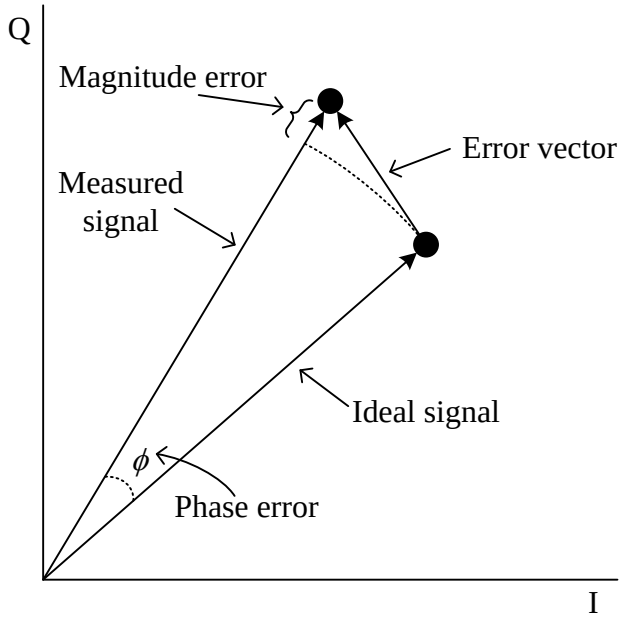

Figure 2-33: Error vector magnitude (EVM) and related quantities.

The permissible EVM for MB-OFDM UWB defined in [2] is shown in Table 2-3.

Table 2-3: Permissible EVM for various data rates in MB-OFDM UWB.

Data Rate (Mb/s)	Error Vector Magnitude (dB)
53.5, 80, 106.7, 160, 200	-17.0
320, 400, 480	-19.5

CHAPTER 3

POLAR TRANSMITTER FOR MB-OFDM

MB-OFDM UWB provides many advantages in various applications like wireless communications and networking. However, it suffers from a large peak-to-average ratio (PAR). Systems with large PAR require that the linear power amplifier (PA) be backed off from its maximum output power to ensure that the peak of the amplitude is within the linear range of operation, resulting in poor efficiency. This can prove challenging for UWB transmitter.

The problem of low power efficiency and high PAR can be solved by using the polar transmitter architecture. Instead of transmitting using Cartesian representation, polar representation is used instead. The phase modulation in a polar transmitter can be generated digitally, upconverted and amplified by highly efficient, but non-linear power amplifier which is controlled by the amplitude modulation.

Although polar modulation alleviates the problem of low power efficiency and high PAR, the performance of polar transmitter can be degraded by non-idealities along the amplitude and phase signals. This chapter explores the various non-idealities along the amplitude and phase signals in a UWB polar transmitter. This work has been published in [13].

3.1 Challenges for MB-OFDM Polar Transmitter

The linearity of the MB-OFDM UWB polar transmitter system is achieved by accurate recombination of the amplitude and phase information. Non-idealities like finite bandwidth of the amplitude and phase information, and time delay mismatch between amplitude and phase information will affect the linearity of the transmission [6]-[9].

3.1.1 Finite Bandwidth

In order to transmit signal using polar modulation, there is a need to perform Cartesian to polar conversion. However, the bandwidths of the amplitude and phase in polar format are significantly different from those in I and Q. This is due to the non-linear relationship between the Cartesian and Polar components given in (2.11) and (2.12).

The spectra of Cartesian I and Q, and polar amplitude and phase signals for MB-OFDM UWB are shown in Figure 3-1. It can be observed that the spectra of amplitude and phase signals are higher than the spectra of I and Q signals at higher frequencies. The spectrum of the amplitude signal is higher than spectra of the I/Q signals at frequencies between 0.3 GHz and 0.5 GHz. However, the spectrum of the phase signal is higher than the spectra of the I/Q signal for frequencies above 0.25 GHz. Both the spectra of the amplitude and phase signals also exceed the transmit spectral mask defined in [2], as shown in Figure 3-2.

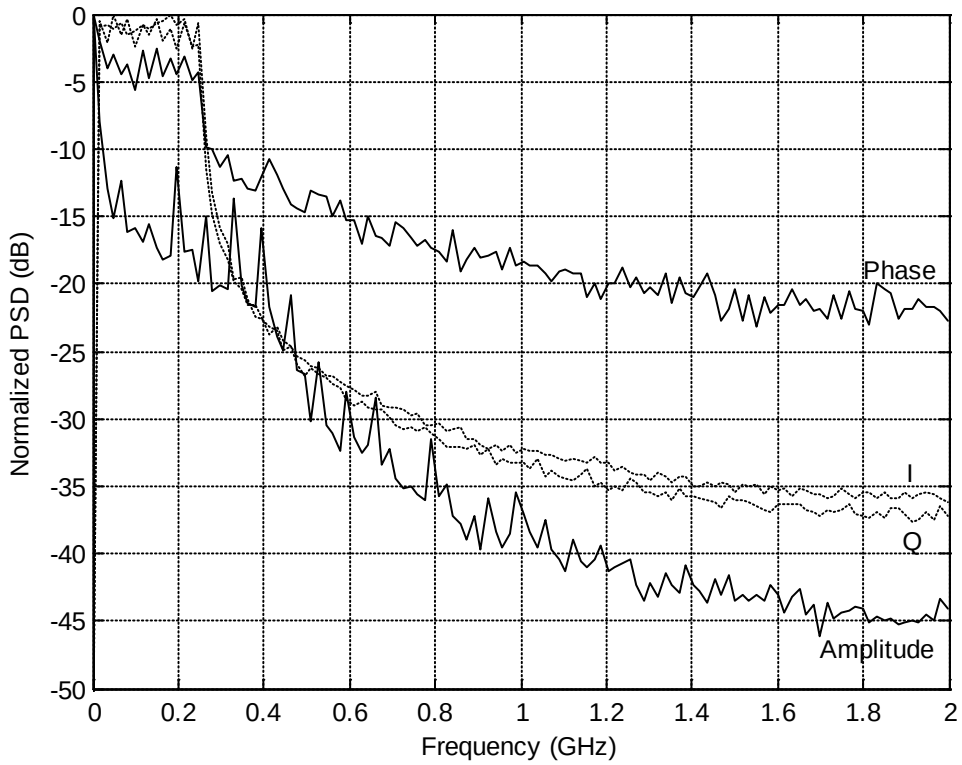

Figure 3-1: Normalized spectra of in-phase, quadrature, amplitude and phase signals.

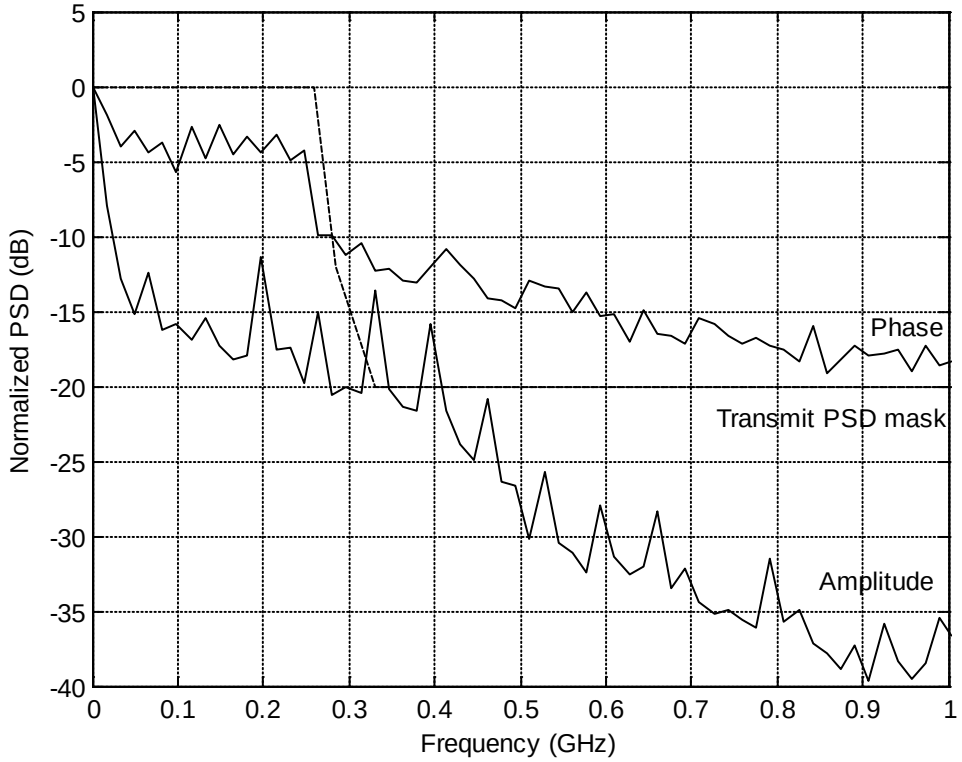

Figure 3-2: Normalized spectra of amplitude and phase signals with transmit spectral mask.

As the bandwidths of the amplitude and phase are wider, the polar circuitry needs to be able to accommodate wider bandwidth or the composite RF signal will be distorted. This complicates the design of the amplitude and phase modulators. Hence, the effects of finite bandwidths of the amplitude and phase on the performance on an MB-OFDM UWB polar transmitter will need to be studied.

3.1.2 Time Delay Mismatch

A time delay mismatch between the amplitude and phase signals will result in the wrong restoration of the amplitude signal to the phase signal, causing linearity degradation in the polar transmitter. To restore the correct amplitude signal onto the phase-modulated signal, the delay of the amplitude and phase signals have to be matched. However, in practice, the amplitude and phase modulators contain different circuitries. Hence, they have very different frequency responses, resulting in different group delays. This increases the complexity of having matched delays. The amount of time delay mismatch the MB-OFDM UWB polar modulator can tolerate will need to be studied.

3.2 Simulation Setup

Computer simulations using Agilent Advanced Design System (ADS) Ptolemy [45] are performed to evaluate the effect of bandwidth on the UWB amplitude and phase signals and the time delay mismatch. Figure 3-3 shows the simulation setup. The I and Q signals are generated from a MB-OFDM UWB signal source centered at 3.960 GHz (Band 2) and conforms to the Fixed-Frequency Interleaving (FFI) scheme – Time-

Frequency Code 6 under Band Group 1 [2]. An ideal Cartesian-to-polar converter converts the I and Q signals from the UWB signal source to amplitude and phase signals. The amplitude and phase signals are then combined to form the transmitting signal. The power of the UWB signal source is adjusted to ensure that the output power density of the transmitting signal, assuming a 0-dBi gain antenna, does not exceed the power spectral density (PSD) limit of -41.3 dBm/MHz defined by FCC [4]. Blocks A and B in Figure 3-3 will be replaced for different type of simulations. Error Vector Magnitude (EVM) will evaluated at different data rates – 53.3 Mb/s, 106.7 Mb/s, 200 Mb/s and 480 Mb/s. Time step of $1/(528\ \text{MHz} \times 2^3) \approx 0.237$ ns is used for the simulations.

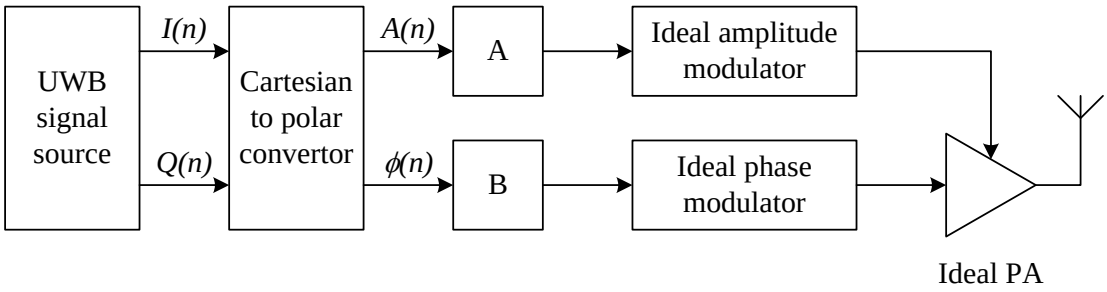

Figure 3-3: Simulation setup.

3.2.1 Design of Digital Filter

To study the effect of the bandwidths of the amplitude and phase on the performance of polar transmitter, finite impulse response (FIR) filter is used to limit the amplitude and phase signals. FIR filter is chosen as it is linear-phase and does not introduce any phase or delay distortion to the signals.

The FIR filters are designed using Agilent ADS Digital Filter Designer [46]. As time step of $1/(528\ \text{MHz} \times 2^3)) \approx 0.237$ ns is used for the simulations, a sampling frequency of $528\ \text{MHz} \times 2^3 = 4224$ MHz is used for the design of the FIR filters. Table 3-1 shows the specifications for various FIR filter designed and Figure 3-4 shows the frequency response for FIR filter with cut-off frequency of 1056 MHz. The frequency responses of other FIR filters can be found in Appendix A.

Table 3-1: Specifications of the FIR filters designed.

FIR Filter	Cut-off Frequency (MHz)	Order of Filter	Group Delay (ns)
1	264	397	46.94
2	528	396	46.87
3	792	396	46.82
4	1056	396	46.91
5	1320	396	46.83
6	1584	396	46.88
7	1848	396	46.92
8	1948	396	46.90
9	2064	396	46.88

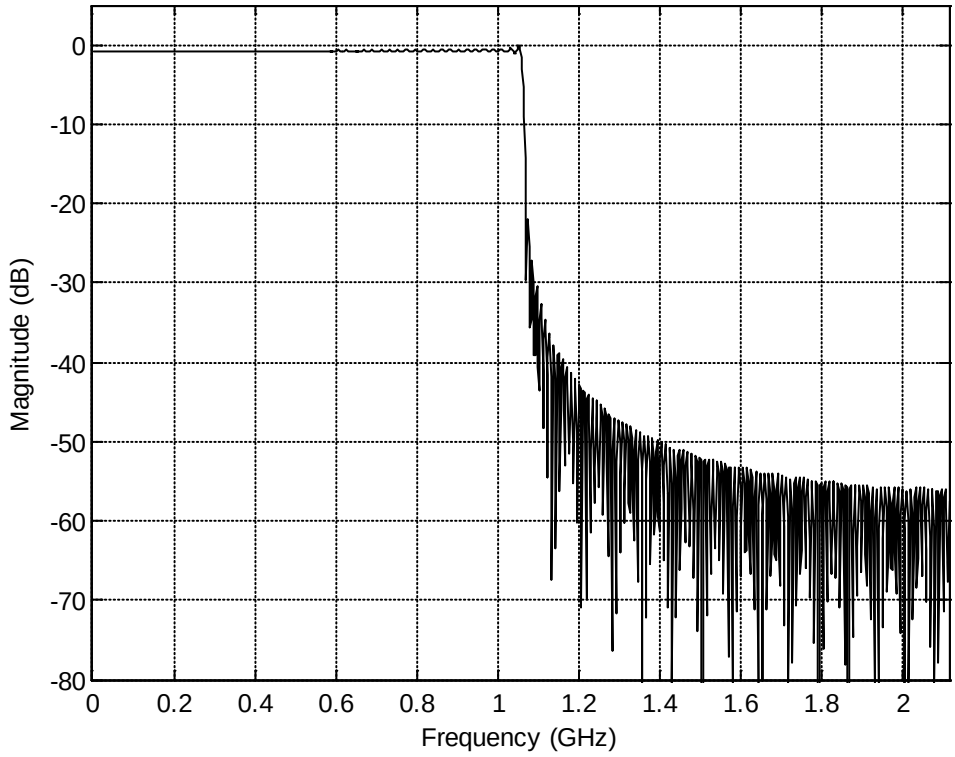

Figure 3-4: Frequency response of FIR filter with cut-off frequency at 1056 MHz.

3.3 Bandwidth of Amplitude

The effect of the bandwidth of the amplitude on the performance of polar transmitter is simulated by sweeping the bandwidth. FIR filter designed in Section 3.2.1 replaces block A in Figure 3-3 to limit the bandwidth of the amplitude. To prevent any delay mismatch between the amplitude and phase signals, block B is replaced by a delay block with the same delay as the group delay generated by the FIR filter. The simulation setup is shown in Figure 3-5. In order to investigate the effect of the bandwidth of the amplitude on EVM, the bandwidth of the amplitude is set to multiples of (i.e. *m* times) the bandwidth of the I/Q signals (264 MHz) by using FIR filters with different cut-off frequencies. The spectra of the amplitude signal before

and after the FIR filter with cut-off frequency of 1056 MHz for data rate of 53.3 Mb/s are shown in Figure 3-6.

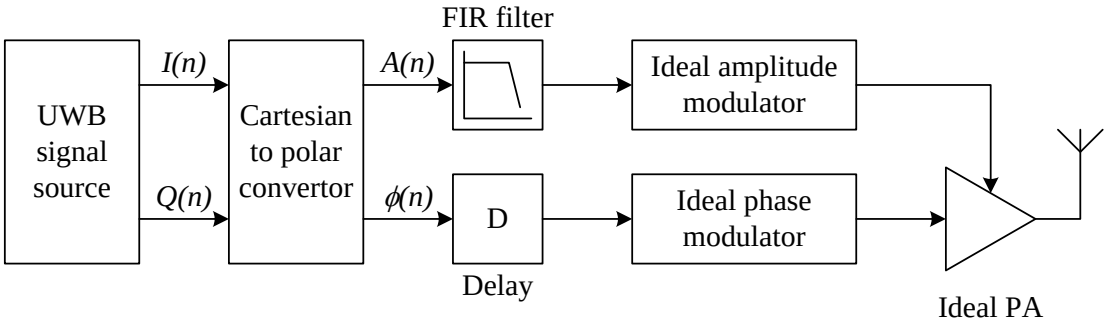

Figure 3-5: Simulation setup to evaluate effect of bandwidth of amplitude.

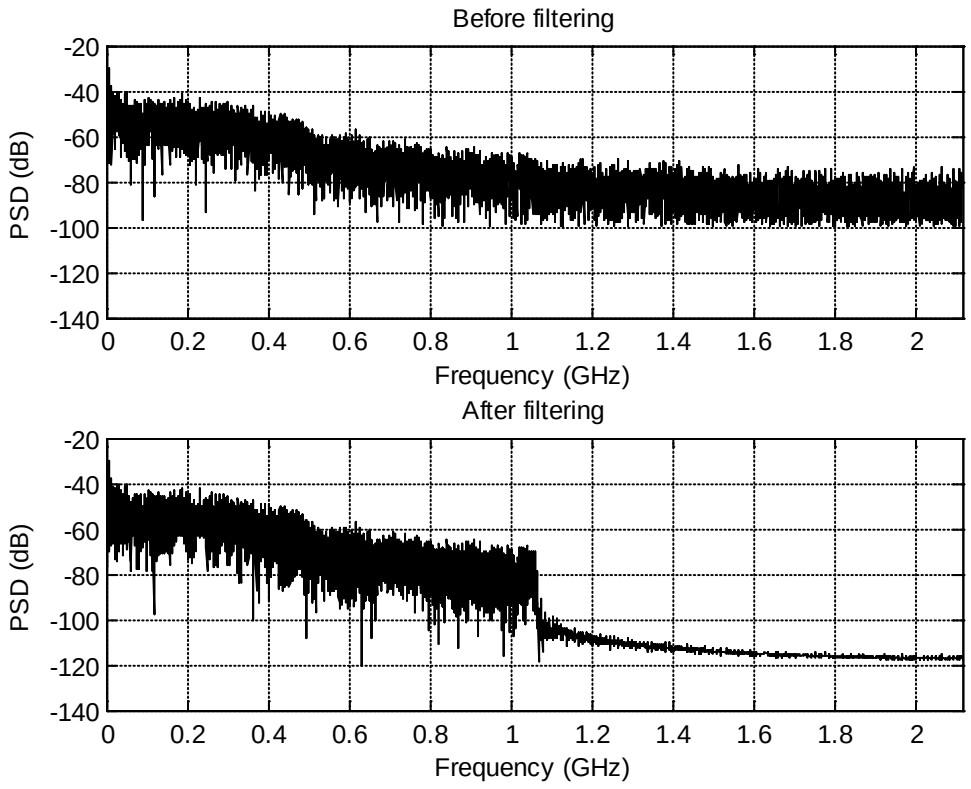

Figure 3-6: PSD of amplitude signal before filtering and after filtering with FIR filter (cut-off frequency at 1056 MHz) for data rate of 53.3 Mb/s.

3.3.1 Results

The results are shown in Figure 3-7 and Figure 3-8 for different data rates. Several observations can be made. First, EVM is observed to improve as the bandwidth of the amplitude increases for all data rates. Next, different data rates do not have significant impact on the EVM. Finally, the bandwidth of the amplitude needs to be approximately 1.1 times wider than that of the I/Q signals or 290.4 MHz to meet the EVM requirement of -17.0 dB for data rates of 53.3 Mb/s, 106.7 Mb/s and 200 Mb/s. For data rate of 480 Mb/s, the bandwidth of the amplitude needs to be approximately 1.2 times wider than that of the I/Q signals or 316.8 MHz to meet the EVM requirement of -19.5 dB. The results are summarized in Table 3-2.

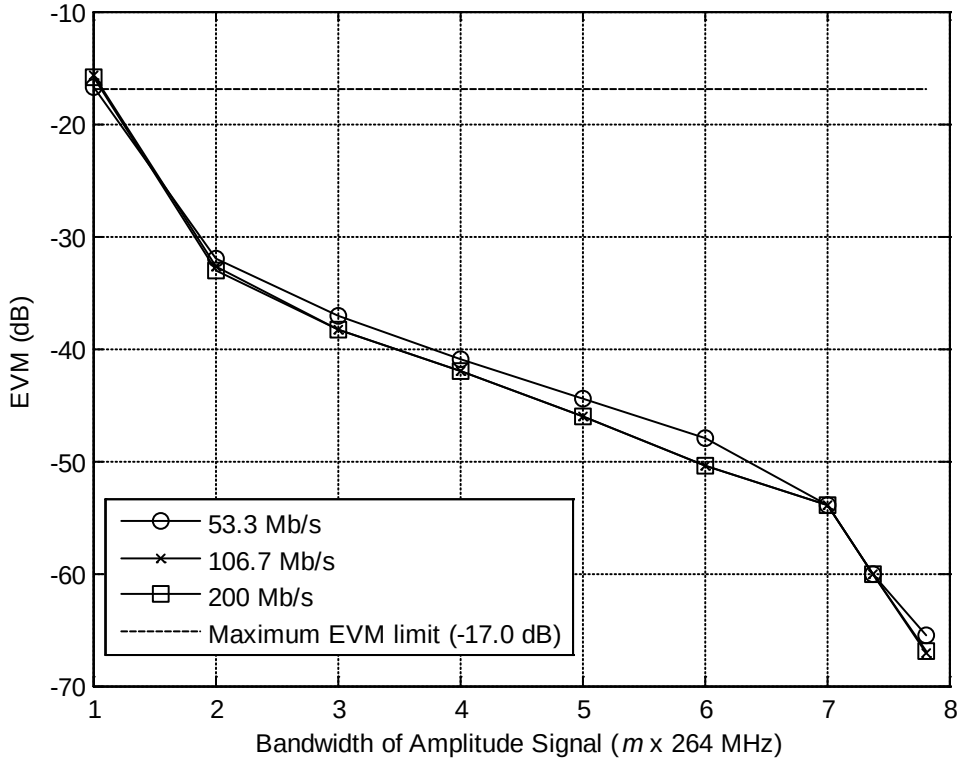

Figure 3-7: Performance in EVM with bandwidth of amplitude for 53.3 Mb/s, 106.7 Mb/s and 200 Mb/s.

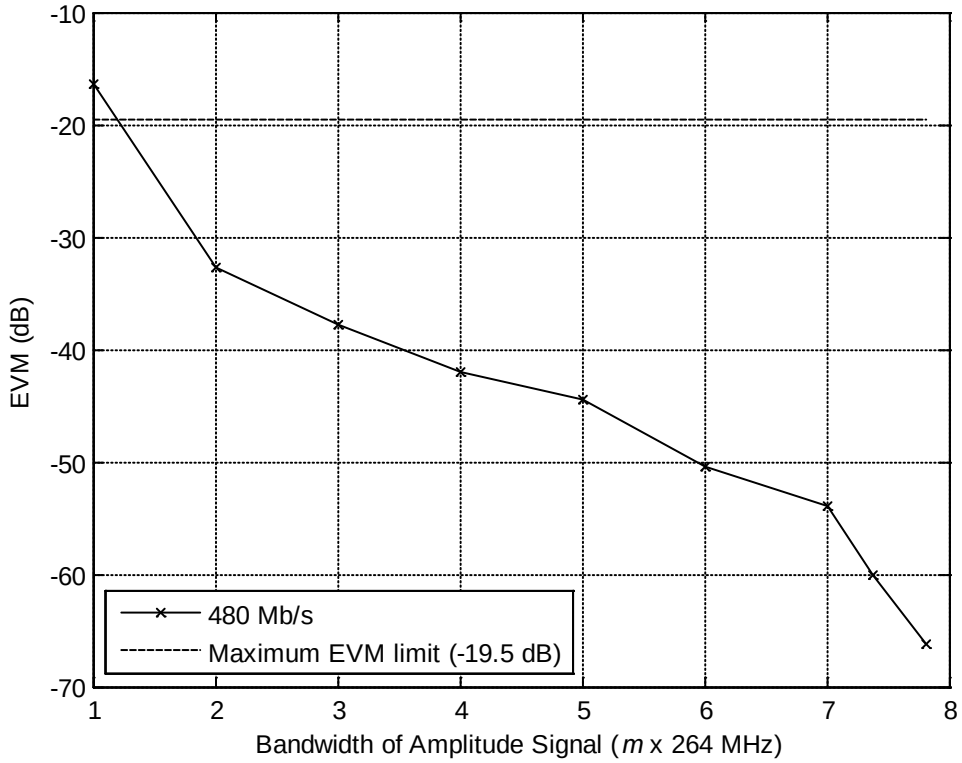

Figure 3-8: Performance in EVM with bandwidth of amplitude for 480 Mb/s.

Table 3-2: Summary of minimum bandwidth of amplitude for various data rates.

Data Rate (Mb/s)	Maximum EVM Limit (dB)	Minimum Bandwidth of Amplitude Required	
		m × Bandwidth of I/Q	MHz
53.3	-17.0	1.1	290.4
106.7	-17.0	1.1	290.4
200	-17.0	1.1	290.4
480	-19.5	1.2	316.8

3.4 Bandwidth of Phase

The effect of the bandwidth of the phase on the performance of polar transmitter is simulated by sweeping the bandwidth. FIR filter designed in Section 3.2.1 replaces block B in Figure 3-3 to limit the bandwidth of the phase. To prevent any delay

mismatch between the amplitude and phase signals, block A is replaced by a delay block with the same delay as the group delay generated by the FIR filter. The simulation setup is shown in Figure 3-9. In order to investigate the effect of the bandwidth of the phase on EVM, the bandwidth of the phase is set to multiples of (i.e. *m* times) the bandwidth of the I/Q signals (264 MHz) by using FIR filters with different cut-off frequencies. The spectrum of the phase signal before and after the FIR filter with cut-off frequency of 1056 MHz is shown in Figure 3-10.

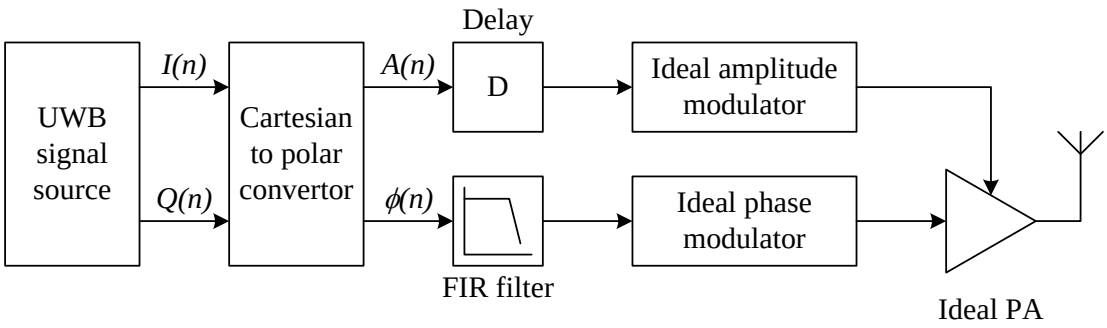

Figure 3-9: Simulation setup to evaluate effect of the bandwidth of phase.

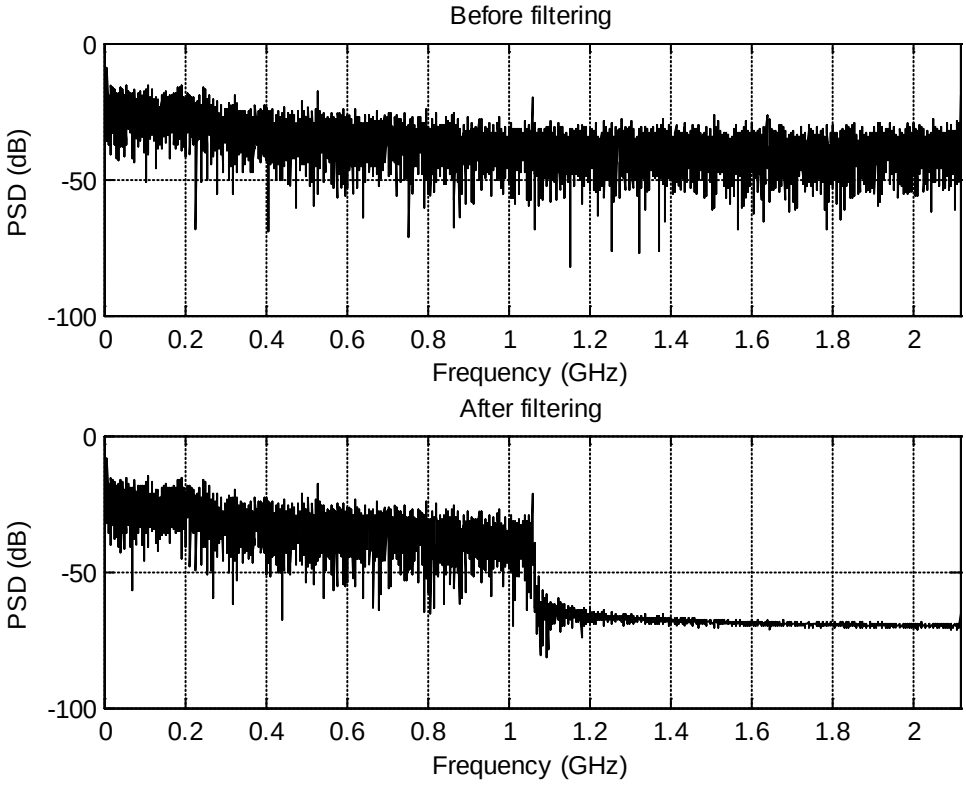

Figure 3-10: PSD of phase signal before filtering and after filtering with FIR filter (cut-off frequency at 1056 MHz) for data rate of 53.3 Mb/s.

3.4.1 Results

The results are shown in Figure 3-11 and Figure 3-12 for different data rates. Several observations can be made. First, EVM is observed to improve as the bandwidth of the phase increases for all data rates. Next, different data rates do not have significant impact on the EVM. Finally, it can be observed the bandwidth of the phase needs to be at least 7.1, 5.9 and 6.4 times wider than that of the I/Q signals (or 1874.4 MHz, 1557.6 MHz and 1689.6 MHz) to meet the EVM requirement of -17.0 dB for data rates of 53.3 Mb/s, 106.7 Mb/s and 200 Mb/s. For data rate of 480 Mb/s, the bandwidth of the phase needs to be approximately 7.1 times wider than that of the I/Q signals or 1874.4 MHz to meet the EVM requirement of -19.5 dB. The wider requirement in the bandwidth of the phase compared to that of the amplitude is

expected as the spectrum of the phase signal shows a wider spread than that of the amplitude signal as shown in Figure 3-1 and Figure 3-2. The results are summarized in Table 3-3.

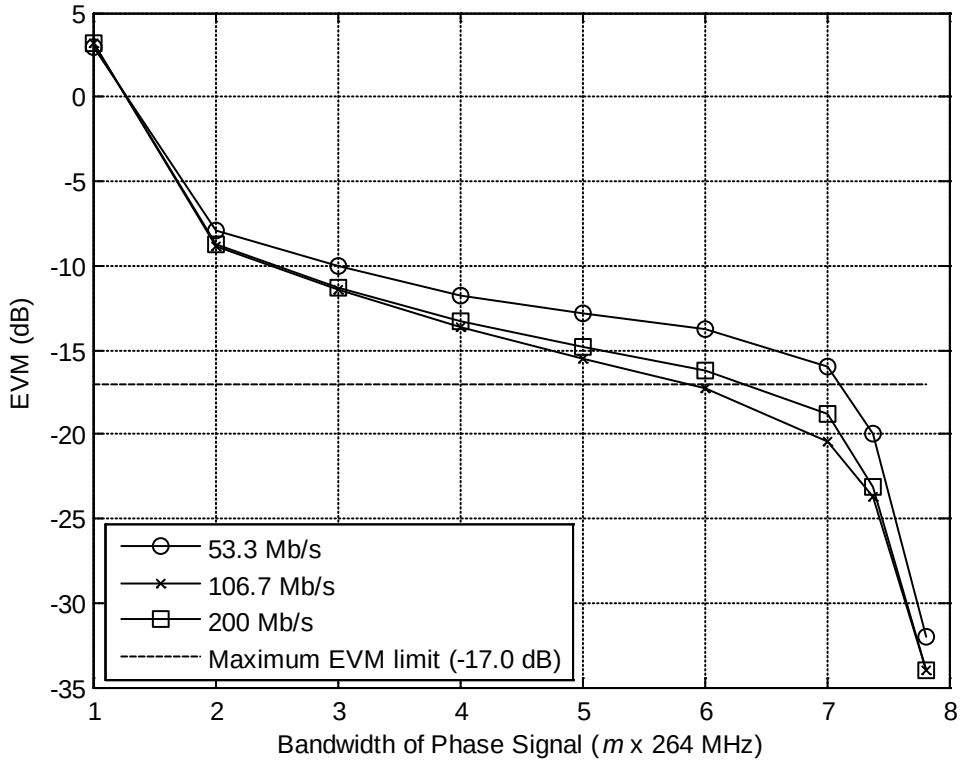

Figure 3-11: Performance in EVM with bandwidth of phase for 53.3 Mb/s, 106.7 Mb/s and 200 Mb/s.

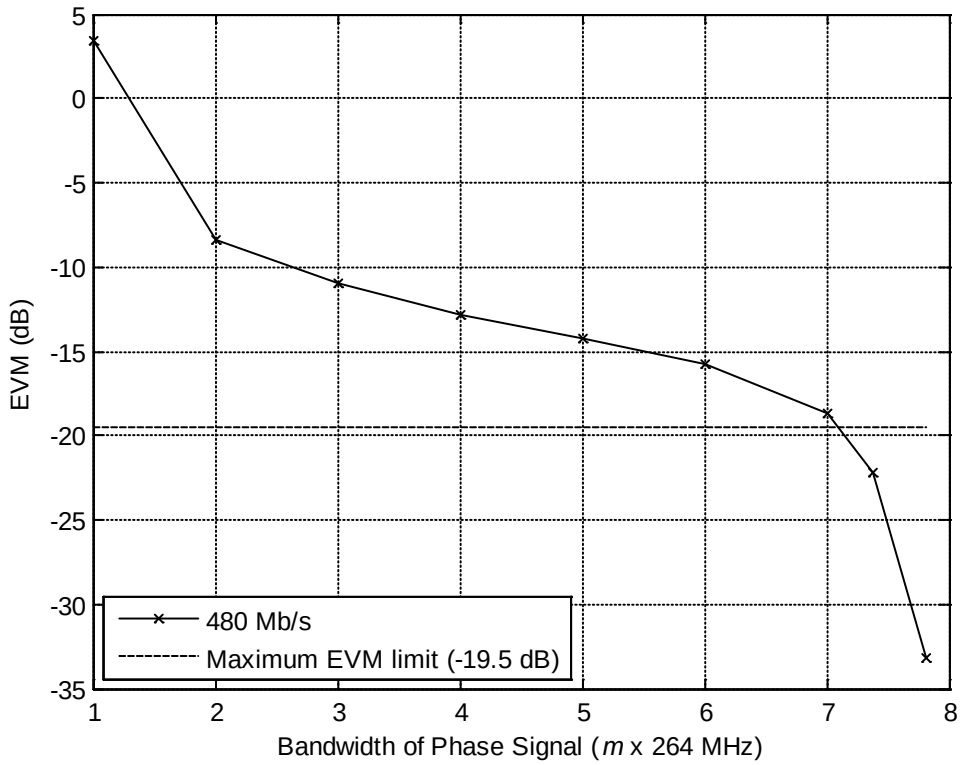

Figure 3-12: Performance in EVM with bandwidth of phase for 480 Mb/s.

Table 3-3: Summary of minimum bandwidth of phase for various data rates.

Data Rate (Mb/s)	Maximum EVM Limit (dB)	Minimum Bandwidth of Phase Required	
		$m \times$ Bandwidth of I/Q	MHz
53.3	-17.0	7.1	1874.4
106.7	-17.0	5.9	1557.6
200	-17.0	6.4	1689.6
480	-19.5	7.1	1874.4

3.5 Time Delay Mismatch

The simulation setup in Figure 3-3 can also be used to evaluate the effect of the delay mismatch on the performance of polar transmitter. Blocks A and B are replaced with delay blocks, D_1 and D_2, respectively as shown in Figure 3-13. The differential time

delay is defined as $D_2 - D_1$. The delays are set to multiple, *n*, of the Time Step (Time Step = 1/(528 MHz × 2^3)). A differential delay of less than 0, i.e. $D_2 - D_1 < 0$, means that the amplitude signal contribute more delay than the phase signal while a differential delay of more than 0, i.e. $D_2 - D_1 > 0$, means that the phase signal contributes more delay than the amplitude signal. Simulations are performed by sweeping the differential time delay.

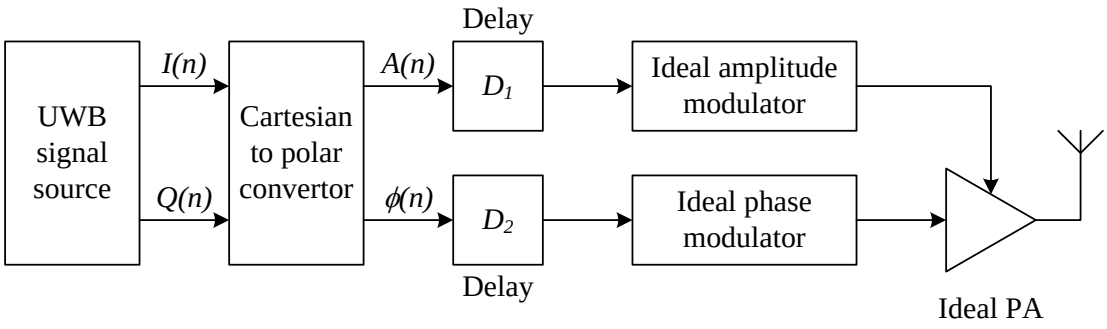

Figure 3-13: Simulation setup to evaluate effect of differential time delay.

3.5.1 Results

The results are shown in Figure 3-14, Figure 3-16, Figure 3-15 and Figure 3-17. It can be observed that the trend is the same for different data rates. The results are summarized in Table 3-4. For data rate of 53.3 Mb/s, a time delay mismatch of less than 0.65 ns can be tolerated. On the other hand, the time delay mismatch requirement is more stringent for other data rates as a time delay mismatch of more than 0.40 ns would cause the system to fail the EVM requirement.

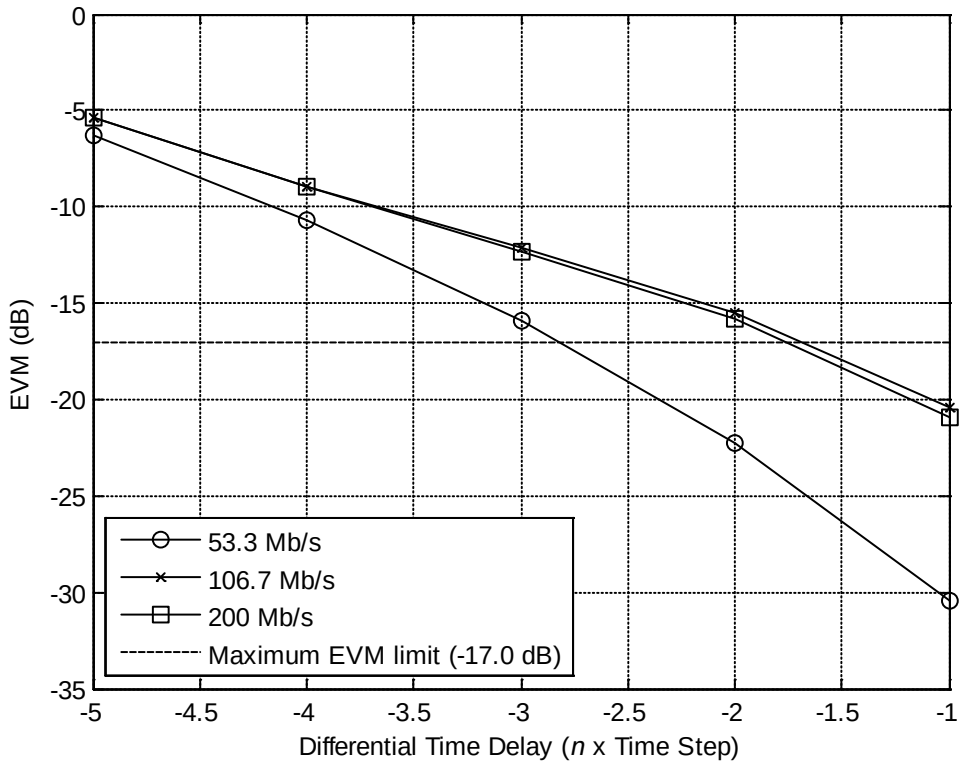

Figure 3-14: Performance in EVM with amplitude delay for 53.3 Mb/s, 106.7 Mb/s and 200 Mb/s.

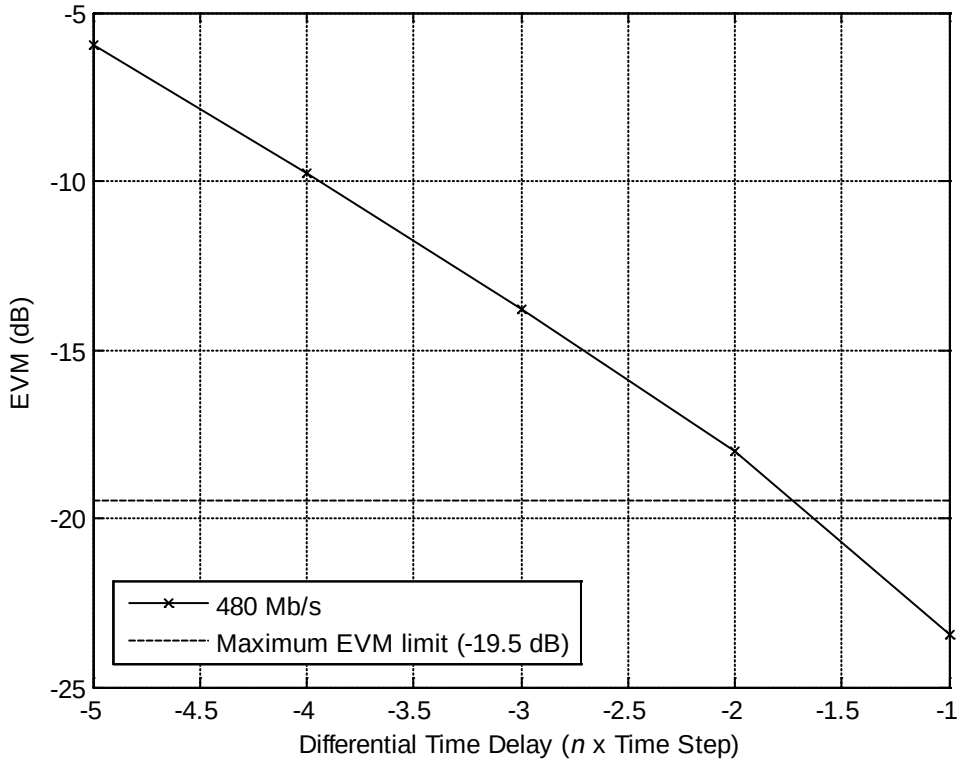

Figure 3-15: Performance in EVM with amplitude delay for 480 Mb/s.

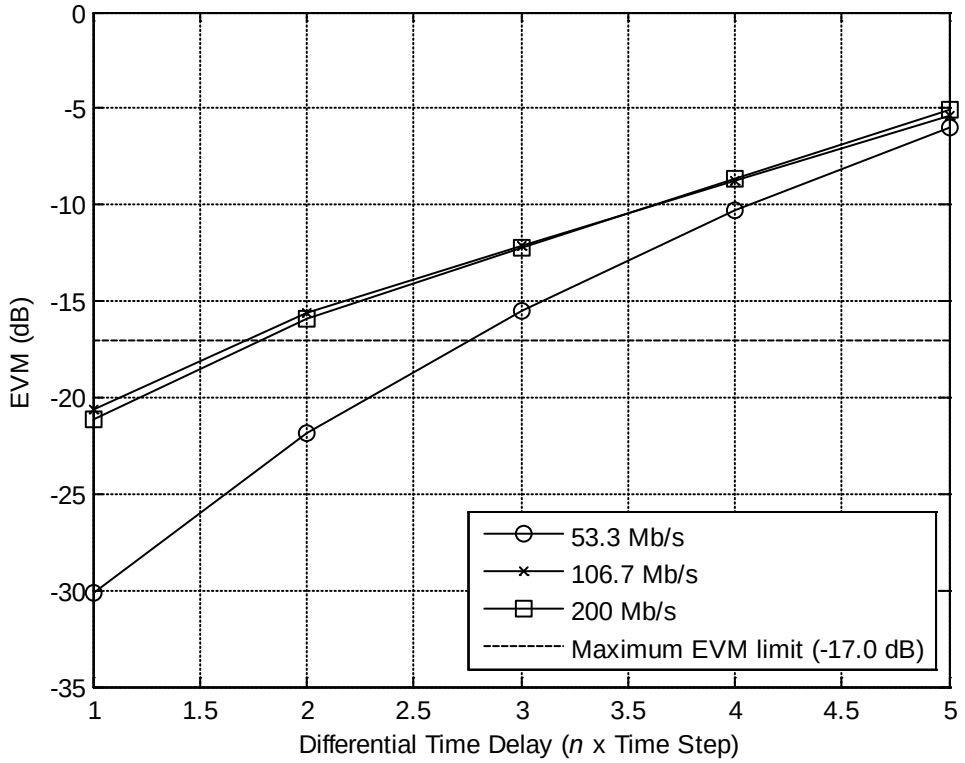

Figure 3-16: Performance in EVM with phase delay for 53.3 Mb/s, 106.7 Mb/s and 200 Mb/s.

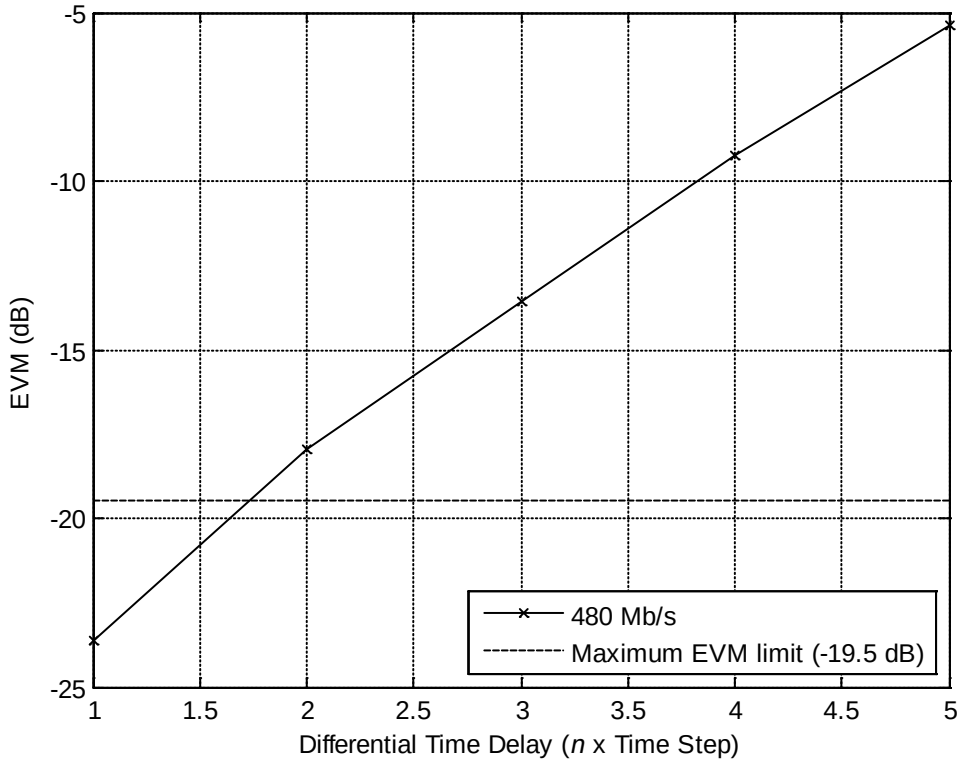

Figure 3-17: Performance in EVM with phase delay for 480 Mb/s.

Table 3-4: Summary of differential time delay for various data rates.

Data Rate (Mb/s)	Maximum EVM Limit (dB)	$D_2 - D_1 < 0$ (Amplitude Delay)		$D_2 - D_1 > 0$ (Phase Delay)	
		n × Time Step	ns	n × Time Step	ns
53.3	-17.0	-2.80	-0.66	2.75	0.65
106.7	-17.0	-1.65	-0.39	1.70	0.40
200	-17.0	-1.75	-0.41	1.75	0.41
480	-19.5	-1.70	-0.40	1.70	0.40

3.6 Design Considerations

Although it has been suggested that the frequency responses of the amplitude and phase signals should have the same bandwidth to avoid differences in group delay [8][9], it can be observed that the bandwidth of the phase needs to be several times wider than that of the amplitude signal. Furthermore, both the amplitude and phase signals require different circuitries. Even if both the bandwidths of the amplitude and phase are same, it is difficult to guarantee that both signals will have the same delay. Hence, the bandwidth of the amplitude can be relaxed as compared to that of the phase provided that the time delays for the two signals are matched.

Simulation verifies this: both the bandwidths of the amplitude and phase are limited by FIR filters. The bandwidth of the amplitude is limited to 528 MHz (2 times the bandwidth of I/Q) while the bandwidth of the phase is limited to 1948 MHz (7.38 times the bandwidth of I/Q). Figure 3-18 and Figure 3-19 show the results in EVM for bandwidth-limited polar transmitter and Table 3-5 summarizes the results. It can be observed that having different bandwidths for both signals are possible if the differential time delay is less than 0.52 ns for data rate of 53.3 Mb/s and less than 0.37

ns for data rates of 106.7 Mb/s and 200 Mb/s. For data rate of 480 Mb/s, a differential time delay of less than 0.26 ns will be required instead. However, it is crucial to note that linear-phase FIR filters are used in the simulations. In practice, the frequency responses of both signals are not necessarily linear-phase and this might create distortion in the delay in each signal. If this happens, delay equalization would be needed to reduce this distortion.

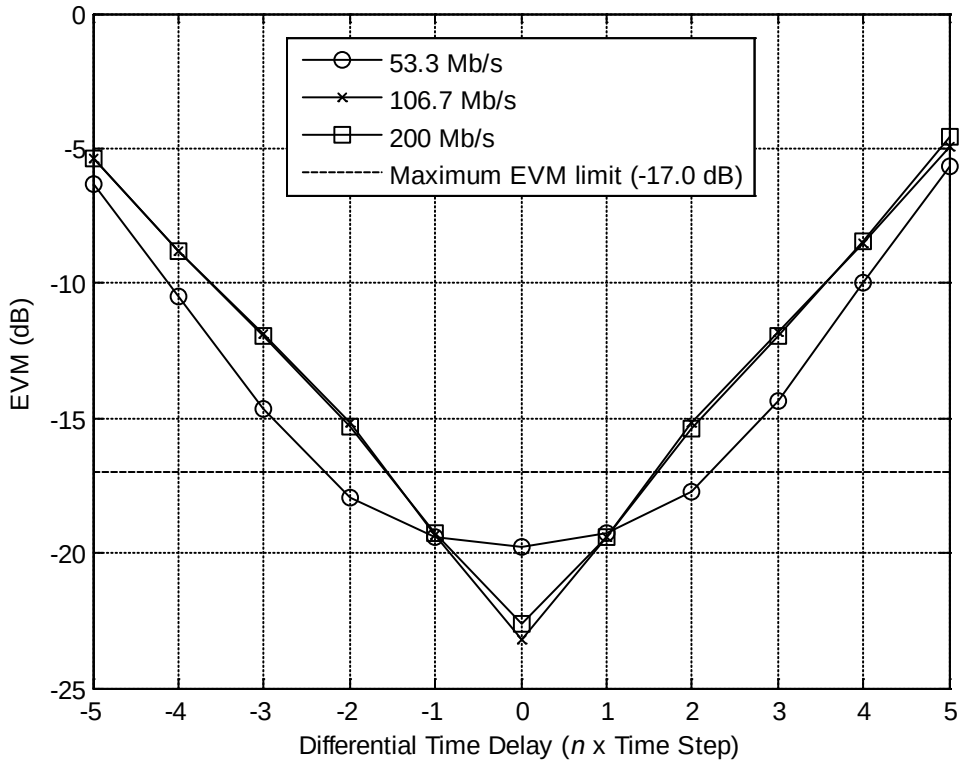

Figure 3-18: Performance in EVM for bandwidth-limited polar modulator with differential time delay for 53.3 Mb/s, 106.7 Mb/s and 200 Mb/s.

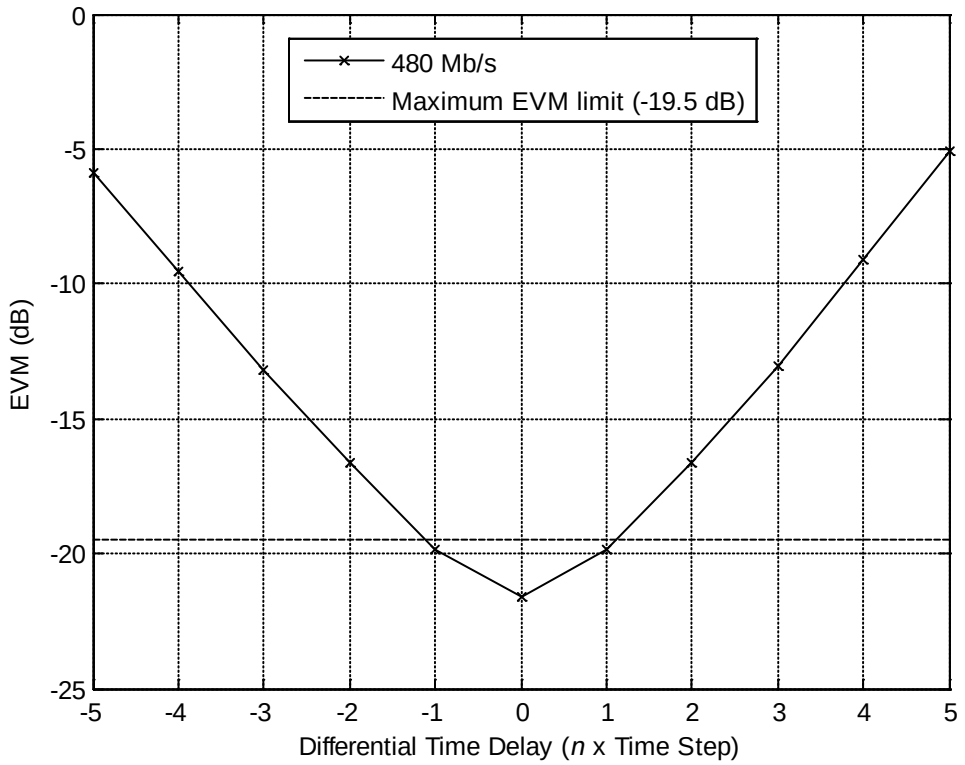

Figure 3-19: Performance in EVM for bandwidth-limited polar modulator with differential time delay for 480 Mb/s.

Table 3-5: Summary of differential time delay in bandwith-limited polar transmitter for various data rates.

Data Rate (Mb/s)	Maximum EVM Limit (dB)	$D_2 - D_1 < 0$ (Amplitude Delay)		$D_2 - D_1 > 0$ (Phase Delay)	
		n × Time Step	ns	n × Time Step	ns
53.3	-17.0	-2.25	-0.53	2.20	0.52
106.7	-17.0	-1.55	-0.37	1.55	0.37
200	-17.0	-1.55	-0.37	1.60	0.38
480	-19.5	-1.10	-0.26	1.10	0.26

3.7 Summary

In this chapter, the system considerations for the amplitude and phase signals in the MB-OFDM UWB polar transmitter are studied. By limiting the bandwidth using FIR filter in one signal and compensating the other signal with the same group delay generated by that FIR filter, it has been found the bandwidth of the phase needs to be several times wider than that of the amplitude signal. The frequency responses of the amplitude and phase signals may not necessarily have the same bandwidth. The bandwidth of the amplitude can be relaxed in comparison to that of the phase provided that the frequency responses of the signals are linear-phase and the time delays between the amplitude and phase signals are matched. In the case where frequency responses are not linear-phase, delay equalization has to be employed.

CHAPTER 4

DIGITAL POLAR TRANSMITTER FOR UWB

Although polar modulation alleviates the problem of low power efficiency and high PAR in MB-OFDM UWB systems, most of the prior works have investigated digital polar transmitter (DPT) architecture for narrowband wireless systems like GSM/EDGE system [11][12]. This chapter had extended the studies to MB-OFDM UWB where a DPT will be proposed for MB-OFDM UWB. This work has been accepted by IEEE Microwave Theory and Technique Society, International Microwave Symposium (IMS), June 2009 [14].

4.1 Digital Polar Transmitter (DPT)

Figure 4-1 shows our proposed DPT for Multi-band OFDM UWB. The amplitude and phase signals, A and ϕ, are generated from the I/Q signals using Cartesian to polar conversion. The amplitude signal, A, is mapped to the amplitude control, represented in m binary bits $\{a_{m-1},\ldots,a_1,a_0\}$, which will control the digital power amplifier (DPA). The phase signal, ϕ, is mapped to the phase control, represented in n binary bits $\{p_{n-1},\ldots,p_1,p_0\}$, which will control the digital phase modulator (DPM).

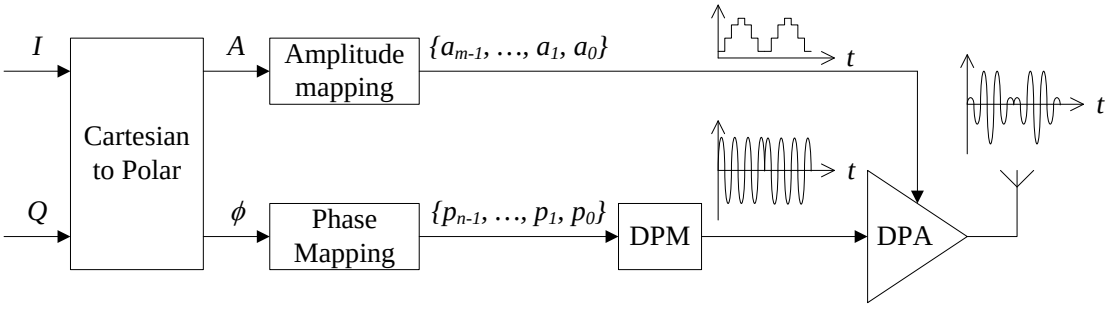

Figure 4-1: Proposed digital polar transmitter (DPT).

4.1.1 Mapping of Amplitude Control

The quantization and mapping of the amplitude signal, A, is similar to the function of an analog-to-digital converter (ADC) using rounding-based quantization as shown in Figure 4-2(a). A_{ref} is defined as the reference amplitude signal and the input amplitude signal is encoded to one in 2^m different levels between 0 and A_{ref} such that the least significant bit (LSB) change of the control bits for amplitude is

$$A_{LSB} = \frac{A_{ref}}{2^m}. \tag{4.1}$$

Any value between 0 and $0.5A_{LSB}$ is mapped to $\{a_{m-1},\ldots,a_1,a_0\} = \{0,\ldots,0,0\}$ while any value of A above $A_{ref}\left(1-2^{-m}\right)$ is mapped to $\{a_{m-1},\ldots,a_1,a_0\} = \{1,\ldots,1,1\}$, resulting in amplitude signal clipping.

The quantization error of the amplitude signal, A_e, is defined as the difference between the actual input amplitude signal and the value of the quantized output amplitude signal that the control bits for amplitude will control. The quantization error contributed by the amplitude mapping is shown in Figure 4-2(b). At best, the

mapping to the control bits for amplitude will have quantization error of $\pm 0.5A_{LSB}$ if the maximum value of amplitude signal does not exceed $A_{ref}\left(1-2^{-m}\right)+0.5A_{LSB}$.

The root mean square (RMS) of the amplitude quantization error, A_e, is given by

$$A_{e,RMS}=\sqrt{\frac{1}{A_{LSB}}\int_{-0.5A_{LSB}}^{0.5A_{LSB}}\left(A_{LSB}\right)^2 dA_{LSB}}=\frac{A_{LSB}}{\sqrt{12}}=\frac{A_{ref}}{2^m\sqrt{12}}. \tag{4.2}$$

(4.2) implies that $A_{e,RMS}$ is dependent on the reference amplitude signal, A_{ref}, and the number of control bits for amplitude, m.

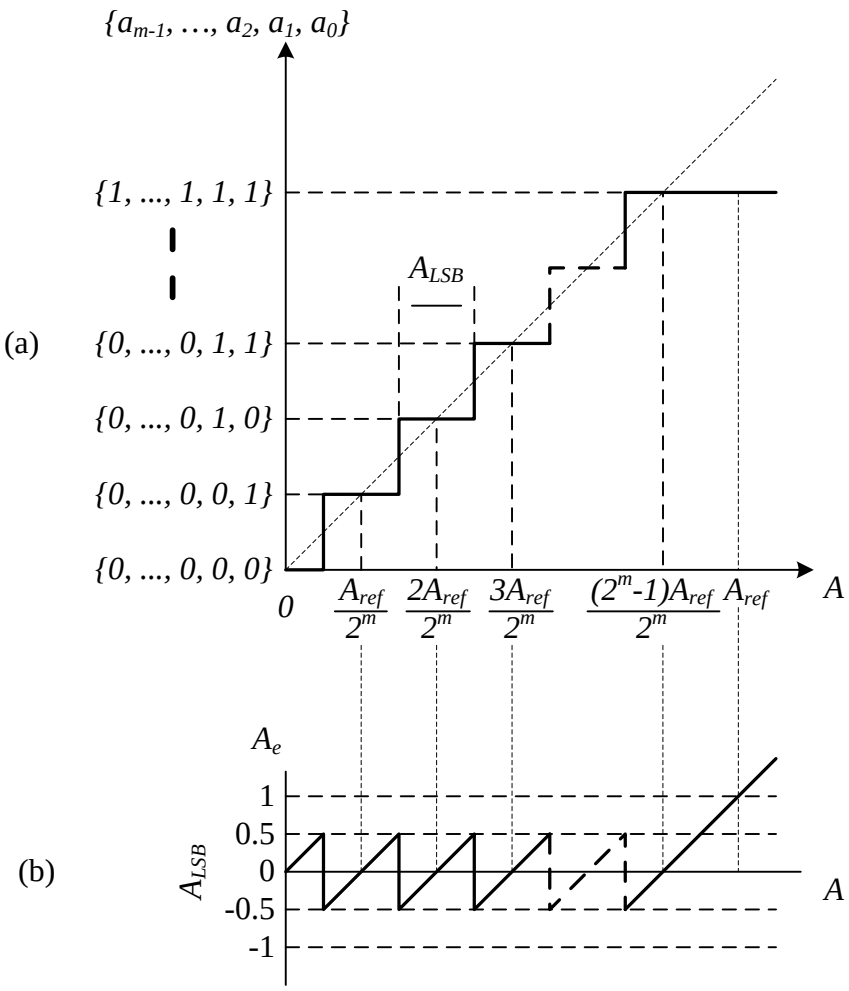

Figure 4-2: (a) Transfer curve for mapping of amplitude signal to amplitude control with (b) its quantization error.

4.1.2 Mapping of Phase Control

The quantization and mapping of the phase signal, ϕ, to the phase control bits is slightly different. Unlike the amplitude signal, the phase signal does not lose information due to clipping. This is because any phase signal above 2π can be wrapped back to values between 0 and 2π, i.e. $\phi = \phi + 2l\pi$, $l \in \mathbb{Z}$, as illustrated in Figure 4-3 and Figure 4-4(a). During the quantization and mapping process, the input signal is encoded to one in 2^n different levels between 0 and 2π such that the least significant bit (LSB) change of the control bits for phase is

$$\phi_{LSB} = \frac{2\pi}{2^n}. \tag{4.3}$$

As $\phi = \phi + 2l\pi$, $l \in \mathbb{Z}$, $0 \le \phi < 0.5\phi_{LSB}$ and $\left(2\pi - 0.5\phi_{LSB}\right) \le \phi < 2\pi$ are mapped to $\left\{p_{n-1}, \ldots, p_1, p_0\right\} = \left\{0, \ldots, 0, 0\right\}$.

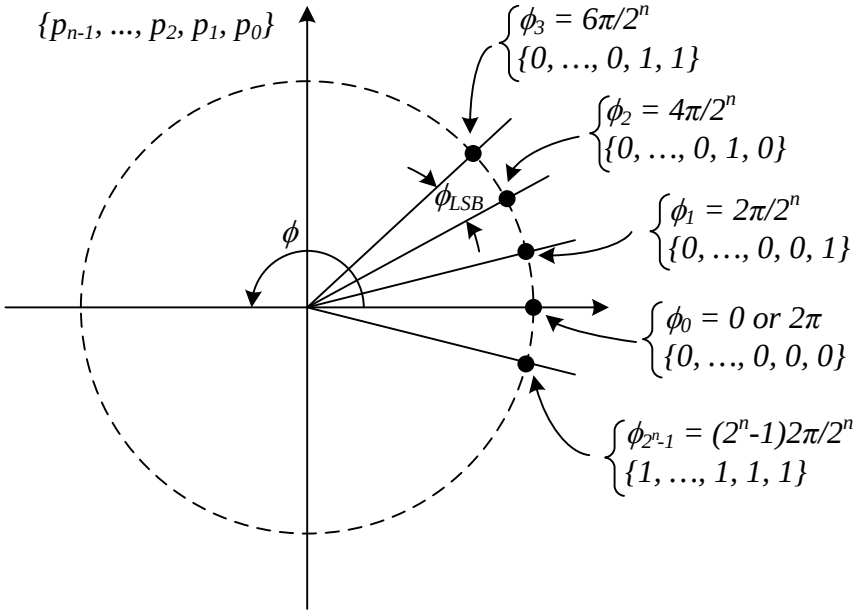

Figure 4-3: Mapping of phase signal to phase control.

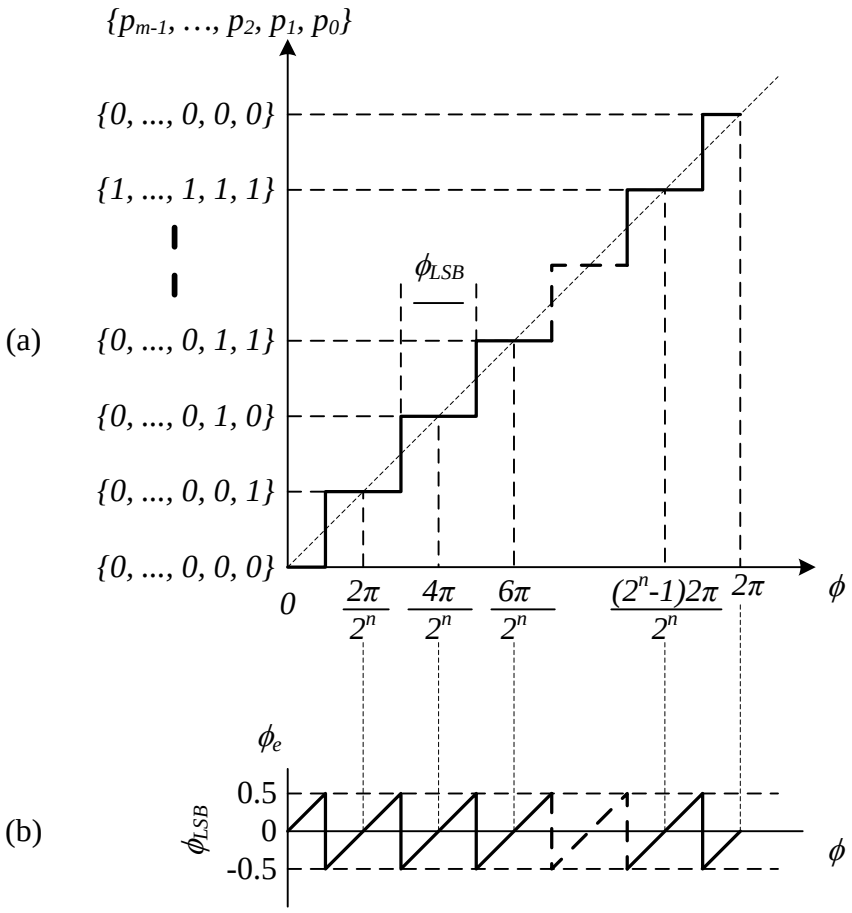

Figure 4-4: (a) Transfer curve for mapping of phase signal to phase control with (b) its quantization error.

Similarly, the quantization error of the phase signal, ϕ_e, is defined as the difference between the actual input phase signal and the value of the quantized output phase signal that the control bits for phase will control. The quantization error contributed by the phase mapping is shown in Figure 4-4(b). At best, the mapping to the control bits for phase will have quantization error of $\pm 0.5\phi_{LSB}$ and the RMS of the phase quantization error, ϕ_e, is given by

$$\phi_{e,RMS} = \frac{\phi_{LSB}}{\sqrt{12}} = \frac{2\pi}{2^n\sqrt{12}}. \tag{4.4}$$

(4.2) implies that $\phi_{e,RMS}$ is only dependent the number of control bits for phase, n.

4.1.3 Digital Phase Modulator (DPM)

Due to the expansion of the bandwidth of the phase in Chapter 3, a close-looped digital phase modulator proposed by Staszewski [10], may not be sufficient for UWB signals. As such, an open-looped DPM with phase wrapping is proposed for DPT as shown in Figure 4-5.

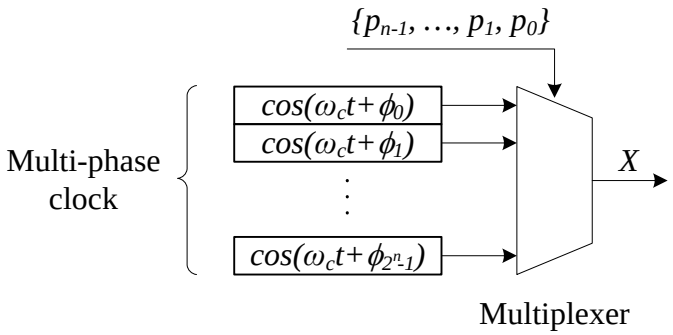

Figure 4-5: Digital phase modulator (DPM).

Here, the DPM consists of a multi-phase clock generating 2^n different phases, $\left\{\phi_{2^n-1},\ldots,\phi_1,\phi_0\right\}$, of the carrier frequency (ω_c) signal and a multiplexer. The selection of the phase-modulated RF signal, X, is determined by the control bits for phase, $\left\{p_{n-1},..., p_1, p_0\right\}$. Based on the assumption that the multi-phase clock generates signals of unity amplitude, the phase-modulated RF signal, X, generated by DPM is given by

$$X = \cos\left(\omega_c t + \phi_k\right) \tag{4.5}$$

$\left\{p_{n-1},..., p_1, p_0\right\}$ select the ϕ_k-phase carrier frequency signal based on the following relationship

$$k = \sum_{i=0}^{n-1} 2^i\, p_i\ . \tag{4.6}$$

For example, for a resolution of 8 phases (or n = 3) as shown in Figure 4-6, $\{p_2, p_1, p_0\} = \{0,0,0\}$ will select the carrier frequency signal with $\phi_0 = 0$ or 2π phase and $\{p_2, p_1, p_0\} = \{0,1,1\}$ will select the carrier frequency signal with $\phi_3 = 3\pi/4$ phase.

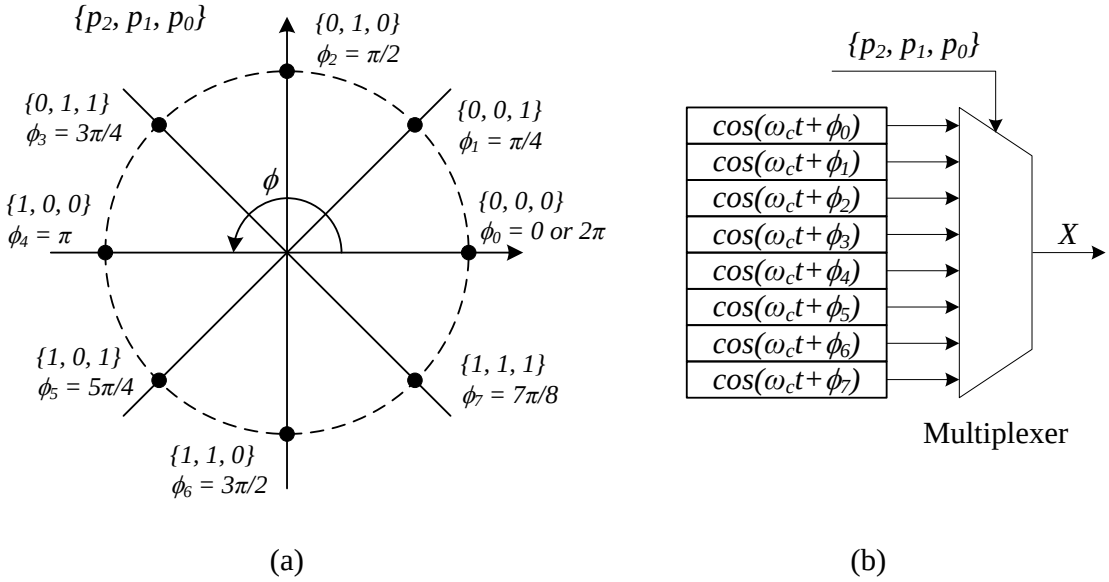

Figure 4-6: (a) Mapping of phase signal and (b) digital phase modulator (DPM) for *n*=3.

4.1.4 Digital Power Amplifier (DPA)

The phase-modulated RF signal, X, is then applied at the input of the digital power amplifier (DPA). The DPA, based on the DPT reported in [47], consists of an array of parallel amplifiers of equal amplification, G, as shown in Figure 4-7. The control bits for amplitude, $\{a_{m-1},\ldots,a_1,a_0\}$, is used to switch on/off the amplifiers. Each a_i bit will control a group of 2^i parallel amplifiers, where $i = 0,1,\ldots,m-1$. Hence, there will be a total of $(2^{m-1}+\ldots+2^1+2^0 = 2^m-1)$ parallel amplifiers. For example, for a resolution of 3 bits (or 7 amplifiers) as shown in Figure 4-8, $\{a_2, a_1, a_0\} = \{0,0,0\}$ will

switch off all the amplifiers, $\{a_2, a_1, a_0\} = \{0,1,1\}$ will switch on a total of 3 amplifiers and $\{a_2, a_1, a_0\} = \{1,1,1\}$ will switch on all the 7 amplifiers.

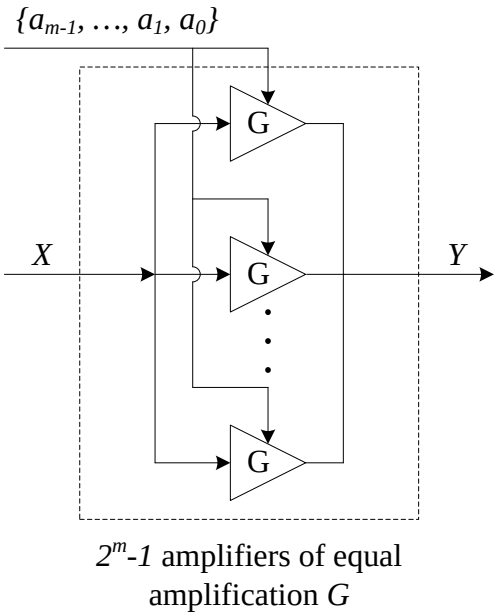

Figure 4-7: Digital power amplifier (DPA).

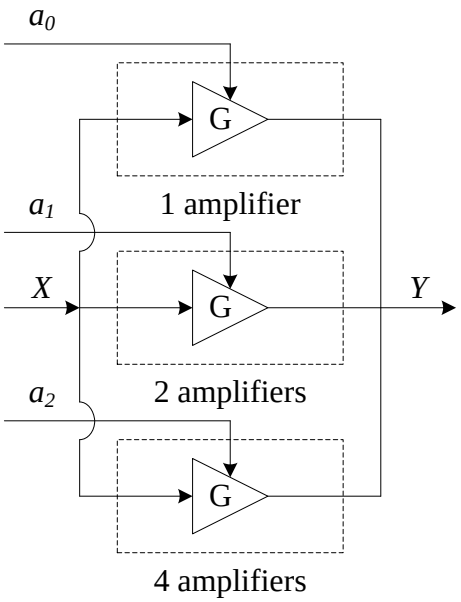

Figure 4-8: Digital power amplifier (DPA) for *m*=3.

By using $\{a_{m-1},\ldots,a_1,a_0\}$ to switch on/off the amplifiers, the amplitude signal can be modulated onto the phase-modulated RF signal, X, to produce the amplitude-modulated phase-modulated RF signal, Y, to be transmitted via the antenna. The envelope-modulated phase-modulated RF signal, Y, is given by

$$Y = \left(\sum_{j=0}^{m-1} a_j 2^j G\right) X = \left(\sum_{j=0}^{m-1} a_j 2^j G\right) \cos\left(\omega_c t + \phi_k\right) \tag{4.7}$$

where $k = \sum_{i=0}^{n-1} 2^i p_i$.

4.2 Simulation Setup

The proposed DPT, shown in Figure 4-1, is modelled in Agilent Advanced Design System (ADS) Ptolemy [48] and error vector magnitude (EVM) is evaluated at various data rates – 53.3 Mb/s, 106.7 Mb/s, 200 Mb/s and 480 Mb/s. A MB-OFDM UWB signal source, using quadrature phase shift keying (QPSK) for 53.3 Mb/s, 106.7 Mb/s and 200 Mb/s while using dual-carrier modulation (DCM) [48] for 480 Mb/s according to ECMA standards [2], generates the baseband I/Q signals. The baseband I/Q signals from the UWB signal source are converted to amplitude and phase representations using an ideal Cartesian-to-Polar converter. The amplification, G, of each amplifier in the DPA is adjusted to ensure that the output power density of the transmitting signal, assuming a 0-dBi gain antenna, does not exceed the power spectral density (PSD) limit of -41.3 dBm/MHz defined by regulatories such as FCC [4].

4.3 Digital Power Amplifier (DPA) Simulation

The DPA is simulated with different resolutions to determine the minimum resolution, m, required to meet the EVM requirement in [2]. A_{ref} of 0.5V is used and the phase signal is kept ideal (i.e. the DPM is not used) as shown in Figure 4-9.

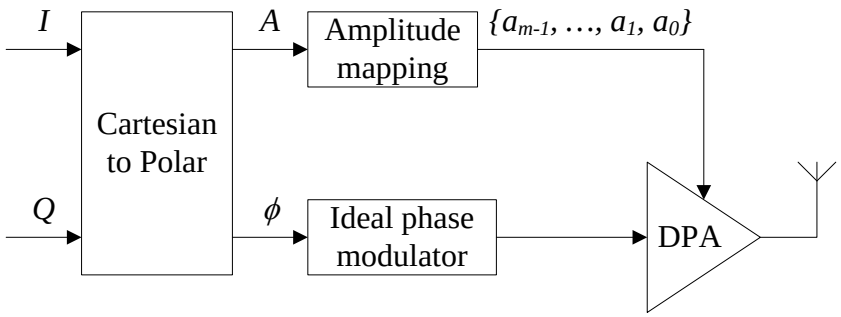

Figure 4-9: Simulation setup to determine the resolution of DPA.

4.3.1 Results

The DPA is simulated with from $m=1$ to $m=10$. As shown in Figure 4-10 and Figure 4-11, it can be observed that the trend is the same for different data rates. EVM improves as the resolution of the DPA, m, increases for the various data rates. The results are summarized in Table 4-1. For data rate of 53.3 Mb/s, a minimum resolution of $m=2$ is required to meet the EVM requirement of -17.0 dB. For data rate of 106.7 Mb/s and 200 Mb/s, a minimum resolution of $m=3$ is required to meet the EVM requirement of -17.0 dB. For data rate of 480 Mb/s, a minimum resolution of $m=3$ is required to meet the EVM requirement of -19.5 dB.

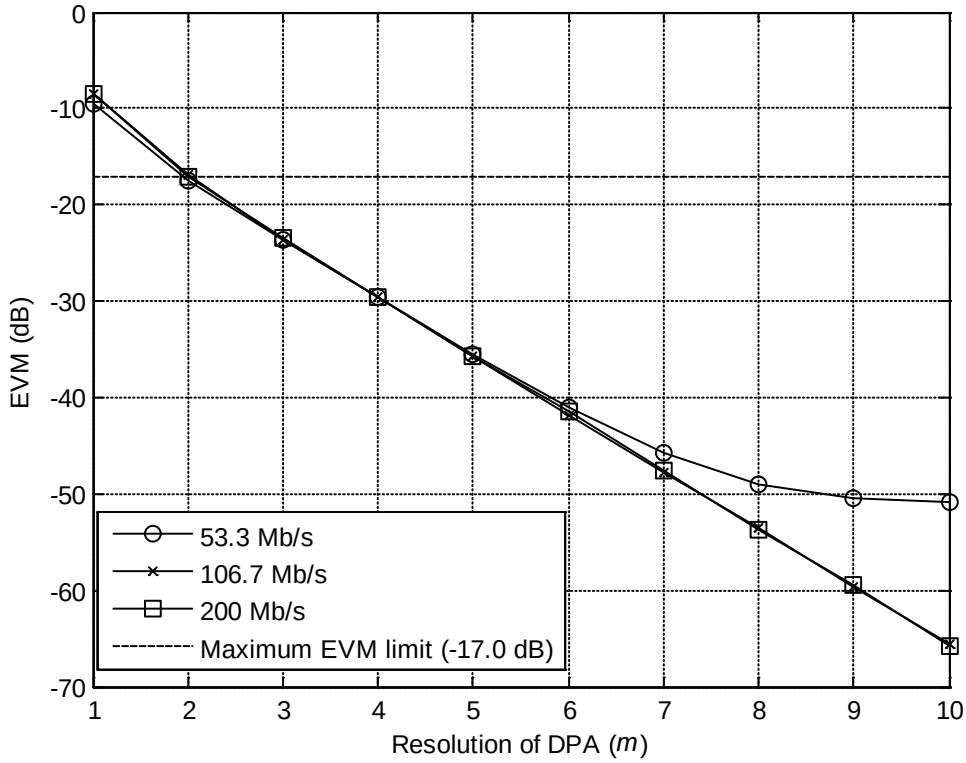

Figure 4-10: Performance in EVM with resolution *m* for 53.3 Mb/s, 106.7 Mb/s and 200 Mb/s.

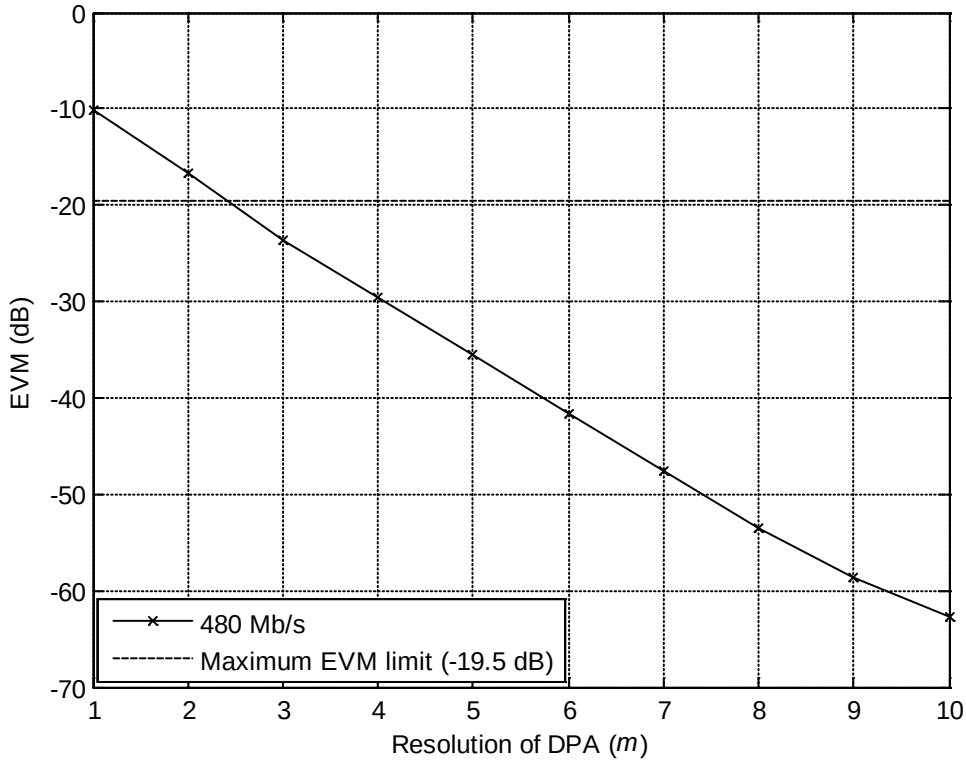

Figure 4-11: Performance in EVM with resolution *m* for 480 Mb/s.

Table 4-1: Summary of minimum resolution *m* for various data rates.

Data Rate (Mb/s)	Maximum EVM Limit (dB)	Minimum Resolution of DPA (*m*)
53.3	-17.0	2
106.7	-17.0	3
200	-17.0	3
480	-19.5	3

4.4 Digital Phase Modulator (DPM) Simulation

The result is simulated for DPM with different *n* bits resolution to determine the minimum resolution to meet the maximum EVM limit [2] when the amplitude signal kept ideal (i.e. the DPA is replaced by an ideal PA) as shown in Figure 4-12. The ideal PA is adjusted to ensure that the output power density of the transmitting signal, assuming a 0-dBi gain antenna, does not exceed the power spectral density (PSD) limit of -41.3 dBm/MHz defined by regulatories such as FCC [4].

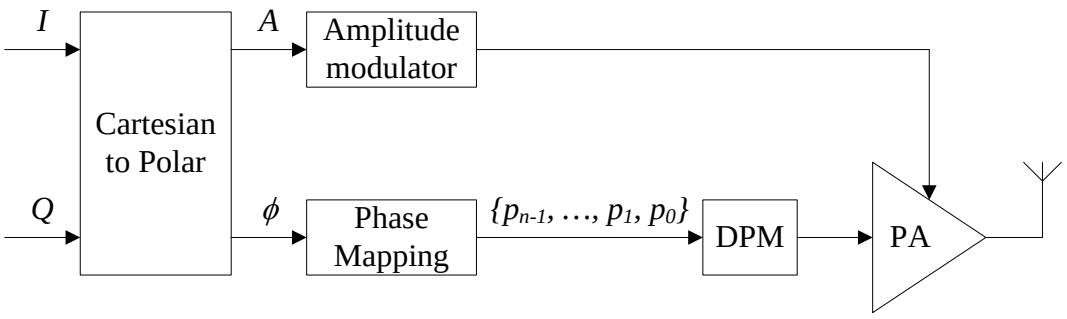

Figure 4-12: Simulation setup to determine the resolution of DPM.

4.4.1 Results

The DPA is simulated with from $n=1$ to $n=10$. As shown in Figure 4-13 and Figure 4-14, it can be observed that the trend is the same for different data rates – 106.7 Mb/s, 200 Mb/s and 480 Mb/s. The result for data rate of 53.3 Mb/s is not plotted as a consistent EVM value of -132.47 dB across different n bits. This is because the phase signal for data rate of 53.3 Mb/s fluctuates between only two phase values (0 and π) and hence, there is no loss of phase information during the phase mapping. EVM improves as the resolution of the DPM, n, increases for the rest of the data rates (106.7 Mb/s, 200 Mb/s and 480 Mb/s). For data rates of 53.3 Mb/s, since different n bits do not results in degradation of the EVM, $n=1$ will be enough to pass the EVM requirement of -17.0 dB. For data rates of 106.7 Mb/s and 200 Mb/s, a minimum of $n=3$ is required to pass the EVM requirement of -17.0 dB. For data rate of 480 Mb/s, a minimum of $n=4$ is required to pass the EVM requirement of -19.5 dB. The results are summarized in Table 4-2.

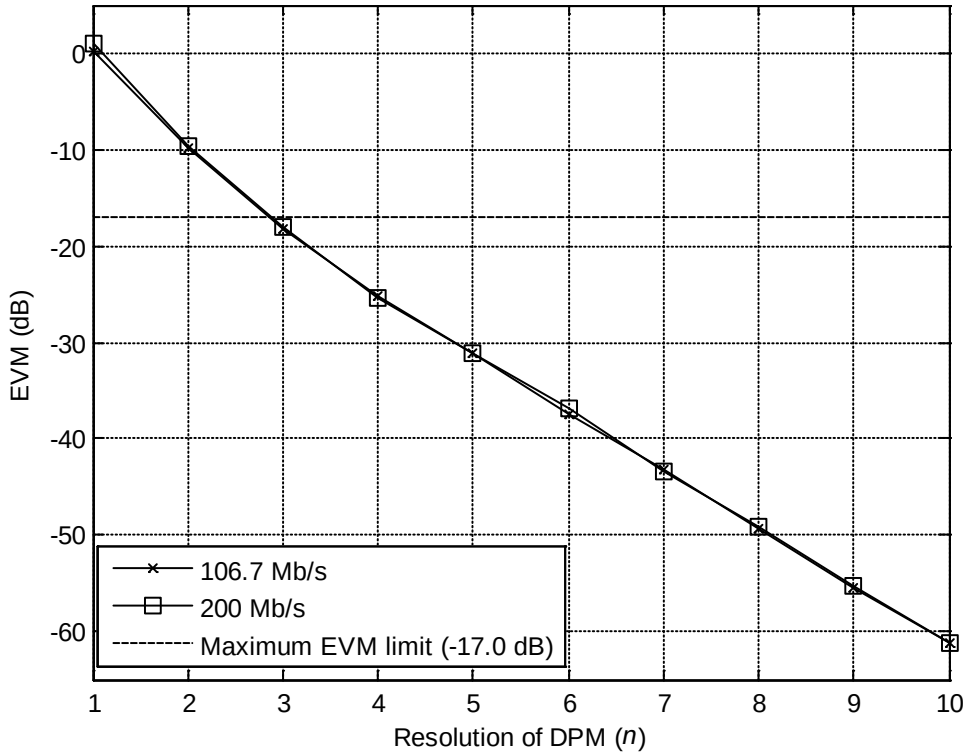

Figure 4-13: Performance in EVM with resolution *n* for 106.7 Mb/s and 200 Mb/s.

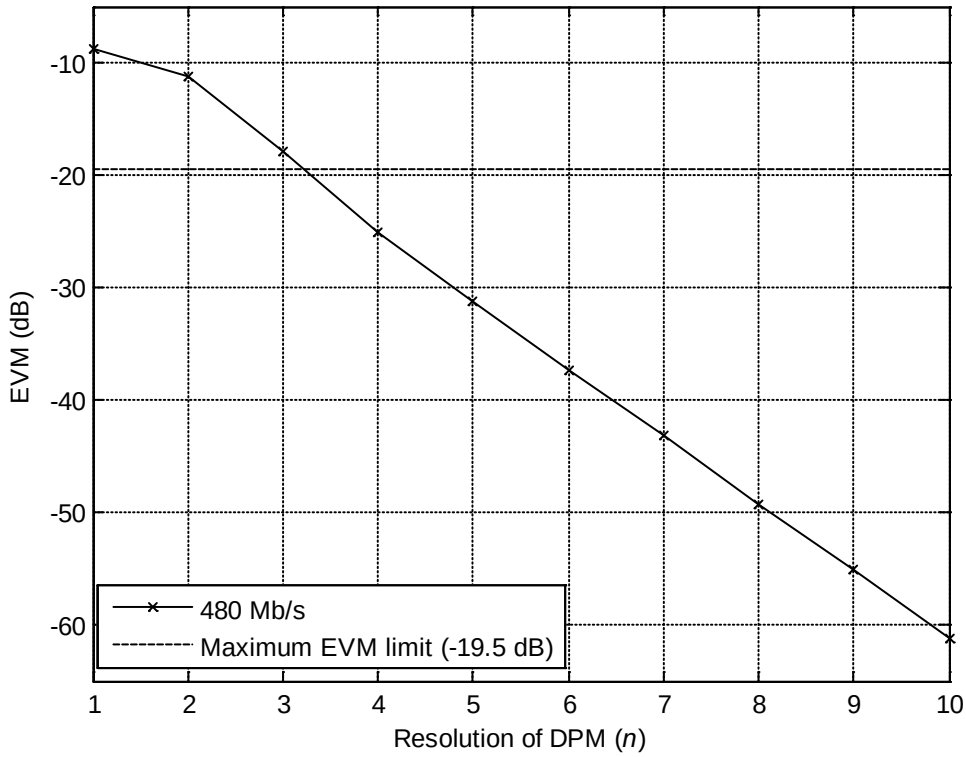

Figure 4-14: Performance in EVM with resolution *n* for 480 Mb/s.

Table 4-2: Summary of minimum resolution *n* for various data rates.

Data Rate (Mb/s)	Maximum EVM Limit (dB)	Minimum Resolution of DPM (*n*)
53.3	-17.0	1
106.7	-17.0	3
200	-17.0	3
480	-19.5	4

4.5 Digital Polar Transmitter (DPT) Simulation

The minimum resolution of DPA, m, and DPM, n, have been determined in the previous sections. There is a need to find a set of $\{m,n\}$ for the DPT which will be able to meet the EVM requirements in for different data rates, allowing only one DPT to be used. By changing the control bits for amplitude and phase, this DPT will be able to transmit different RF signals for different data rates. Simulation is performed by sweeping both the DPA resolution, m, and the DPM resolution, n, to determine the set of $\{m,n\}$ for the DPT.

4.5.1 Results

The result is simulated for the DPT to determine the minimum resolutions, $\{m,n\}$, required for satisfying the EVM limit in for various data rates. Figure 4-15, Figure 4-16, Figure 4-17 and Figure 4-18 show the simulation results for data rates of 53.3 Mb/s, 106.7 Mb/s, 200 Mb/s and 480 Mb/s respectively for the m bits resolution of DPA, and the n bits resolution of DPM. In general, results show that EVM generally improves as the resolution of the DPA, m, and the resolution of DPM, n, increase.

For data rate of 53.3 Mb/s (see Figure 4-15), it can be observed that n does not affect the EVM performance of the DPT. As explained earlier, the phase signal for data rate of 53.3 Mb/s fluctuates between only two phase values (0 and π) and hence, there is no loss of phase information during the phase mapping, resulting in no change in EVM with n. However, EVM improves as m increases.

For data rates of 106.7 Mb/s and 200 Mb/s (see Figure 4-16 and Figure 4-17 respectively), an increase in m does not have significant impact on the EVM for $n=1$ but an increase in m will improve the EVM performance at $n \geq 2$. In addition, for a fixed value of m, an increase in n will improve EVM performance.

For data rate of 480 Mb/s (see Figure 4-18), an increase in m does not have significant impact on the EVM for $n \leq 2$ but an increase in m will improve the EVM performance at $n \geq 3$. An increase in n does not have significant impact on the EVM for $m=1$ but an increase in n will improve the EVM performance for $m \geq 2$.

Table 4-3 summarizes the minimum resolutions $\{m,n\}$ required to pass the EVM requirement. The minimum resolutions $\{2,1\}$ and $\{3,3\}$ will meet the EVM requirement for data rates of 53.3 Mb/s and 106.7 Mb/s respectively. For data rates of 200 Mb/s and 480 Mb/s, minimum resolutions of $\{3,4\}$ or $\{4,3\}$ will meet the EVM requirements.

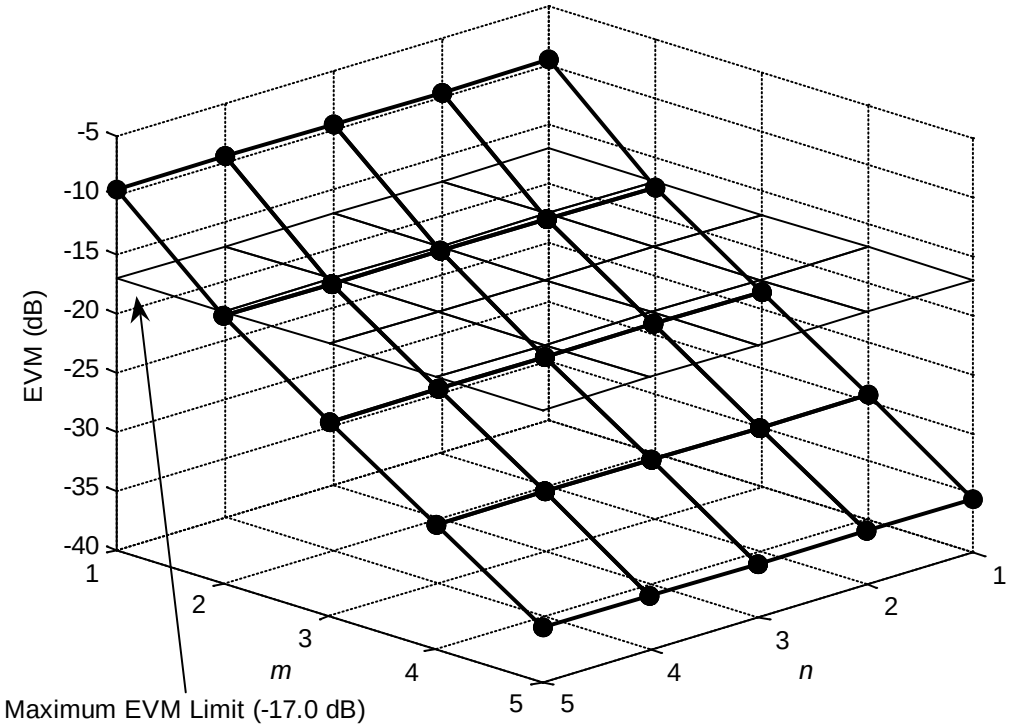

Figure 4-15: Effect of resolutions {*m*,*n*} for data rate of 53.3 Mb/s.

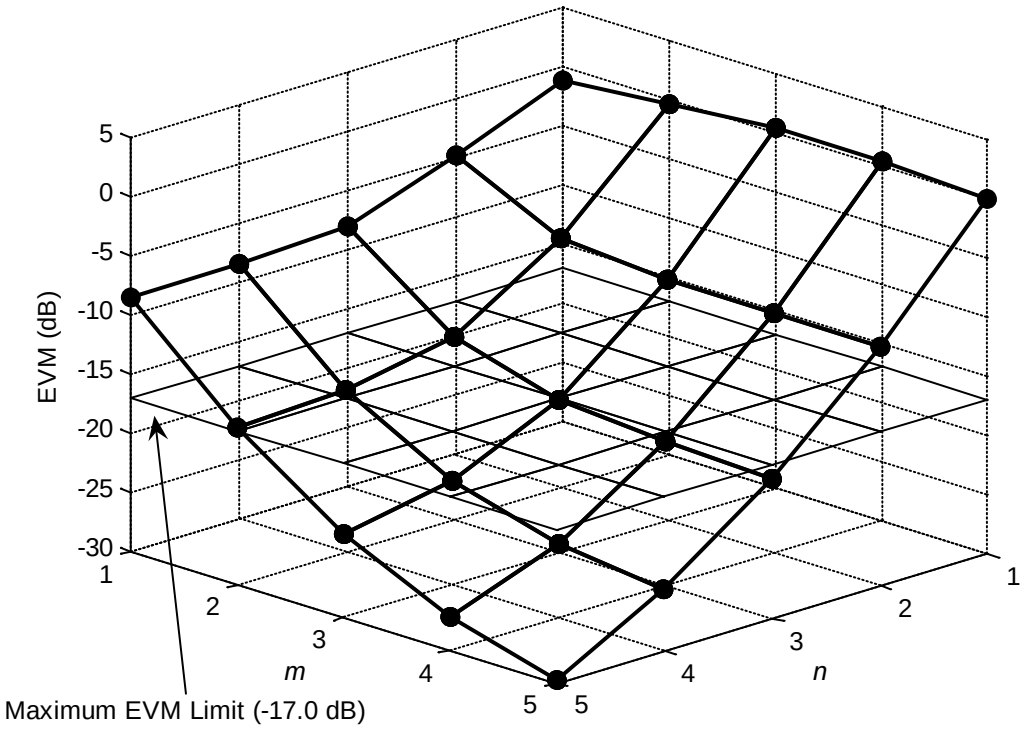

Figure 4-16: Effect of resolutions {*m*,*n*} for data rate of 106.7 Mb/s.

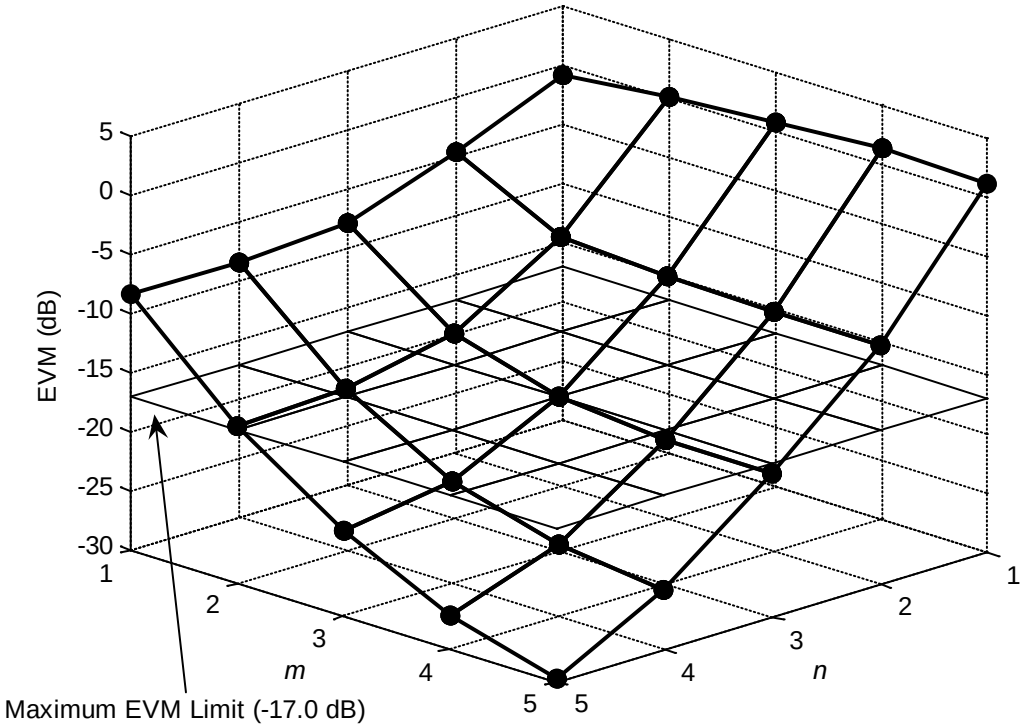

Figure 4-17: Effect of resolutions {*m*,*n*} for data rate of 200 Mb/s.

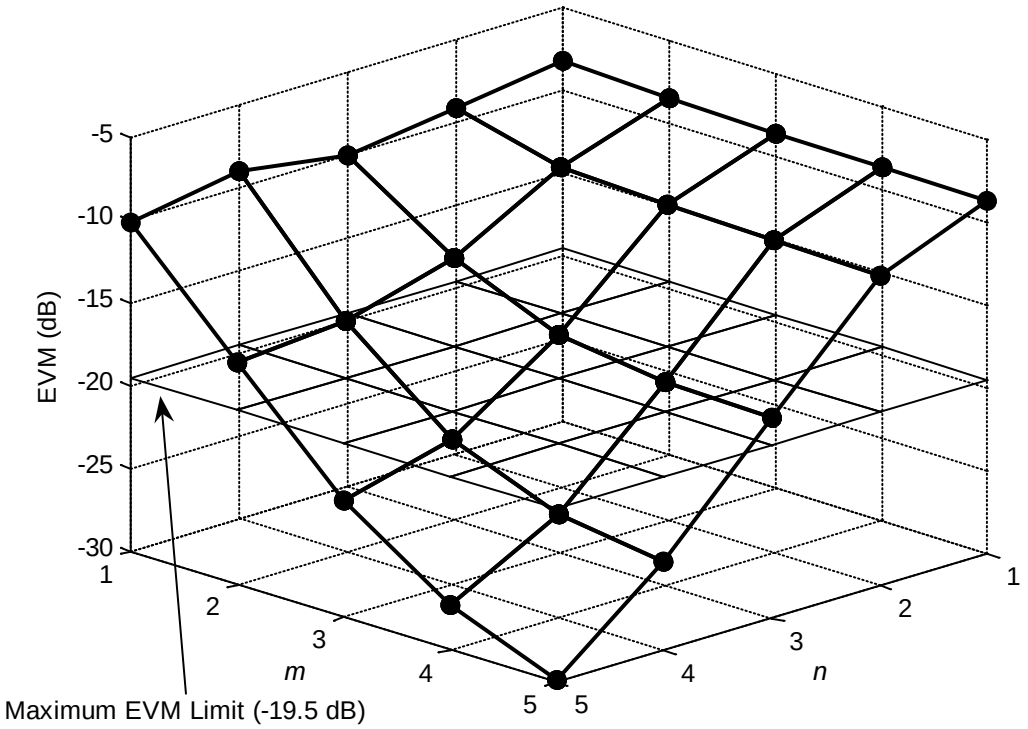

Figure 4-18: Effect of resolutions {*m*,*n*} for data rate of 480 Mb/s.

Table 4-3: Summary of resolutions {*m*,*n*} for various data rates.

Data Rate (Mb/s)	Maximum EVM Limit (dB)	{*m*,*n*}
53.3	-17.0	{2,1}
106.7	-17.0	{3,3}
200	-17.0	{3,4} or {4,3}
480	-19.5	{3,4} or {4,3}

4.6 Summary

In this chapter, a digital polar transmitter (DPT) for MB-OFDM UWB is proposed. The DPT consists digital phase modulator (DPM) which produces the digital phase-modulated RF signal and digital power amplifier (DPA) which will modulate the amplitude of the RF signal digitally. The operations of both DPM and DPA are discussed.

In addition, the minimum DPM resolution m and the minimum DPA resolution n are determined for different data rates. The minimum resolutions $\{m,n\}=\{2,1\}$ and $\{m,n\}=\{3,3\}$ will meet the EVM requirement for data rates of 53.3 Mb/s and 106.7 Mb/s respectively. For data rates of 200 Mb/s and 480 Mb/s, minimum resolutions of $\{m,n\}=\{3,4\}$ or $\{4,3\}$ will meet the EVM requirements.

CHAPTER 5

MISMATCH IN GAIN AND PHASE IN DIGITAL POLAR TRANSMITTER FOR UWB

The digital polar transmitter (DPT) for MB-OFDM UWB has been proposed in the previous chapter. However, the DPT still suffers from non-idealities in the amplitude and phase. This chapter explores the various non-idealities along the amplitude and phase in a DPT.

5.1 Digital Polar Transmitter (DPT)

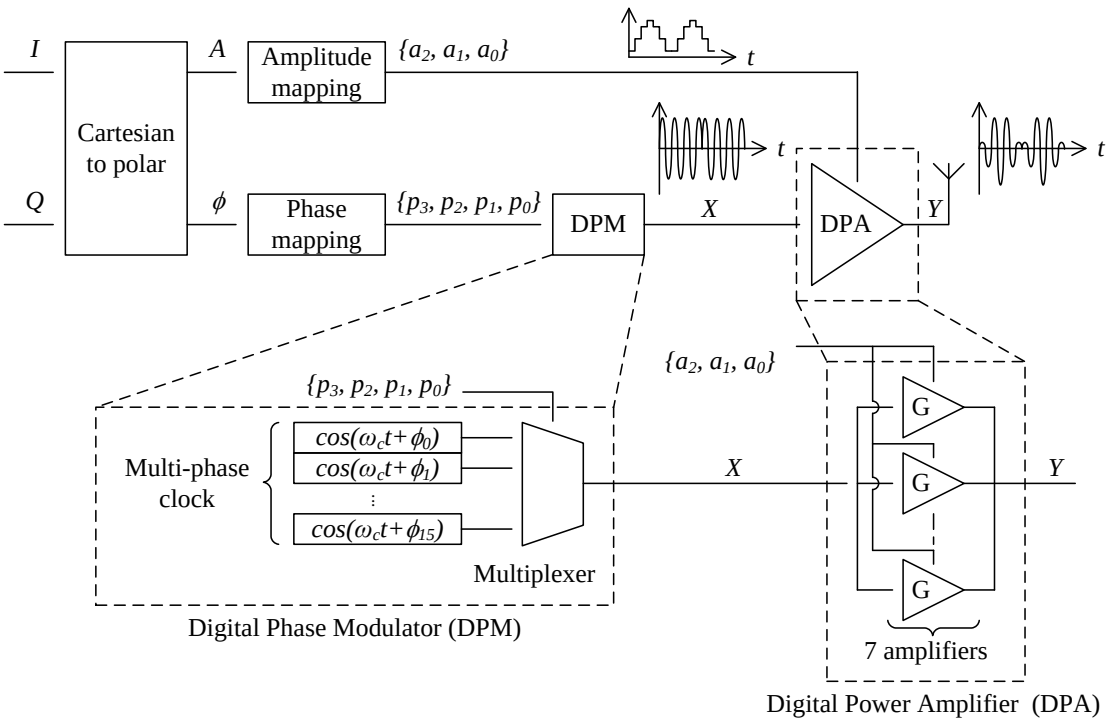

Figure 5-1: DPT with {*m*,*n*} = {*3*,*4*}.

The minimum resolution of DPA, m, and DPM, n, have been determined in Chapter 4. The DPT with $\{m,n\} = \{3,4\}$ as shown in Figure 5-1 will be able to meet the EVM requirements in for different data rates. The EVM performances for various data rates are shown in Table 5-1.

Table 5-1: Performance in EVM for DPT with {*m*,*n*} = {3,4} for various data rates.

Data Rate (Mb/s)	Maximum EVM Limit (dB)	EVM (dB)
53.3	-17.0	-23.5
106.7	-17.0	-21.2
200	-17.0	-21.3
480	-19.5	-21.2

5.2 Time Delay Mismatch

The linearity of the DPT system requires accurate recombination of the amplitude and phase information. A time delay mismatch between the amplitude and phase signals will result in the wrong restoration of the amplitude signal to the phase signal, causing linearity degradation in the DPT. To restore the correct amplitude signal onto the phase-modulated signal, the delay of the amplitude and phase signals have to be matched. The amount of time delay mismatch the DPT can tolerate will be studied.

The simulation setup in Figure 5-2 is used to evaluate the effect of the delay mismatch on the EVM performance of the DPT. The differential time delay is defined as $D_2 - D_1$. The delays are set to multiple, *n*, of the Time Step (Time Step = 1/(528 MHz $\times$ 2^3)). A differential delay of less than 0, i.e. $D_2 - D_1 < 0$, means that the amplitude signal contribute more delay than the phase signal while a differential delay of more

than 0, i.e. $D_2 - D_1 > 0$, means that the phase signal contributes more delay than the amplitude signal. Simulations are performed by sweeping the differential time delay.

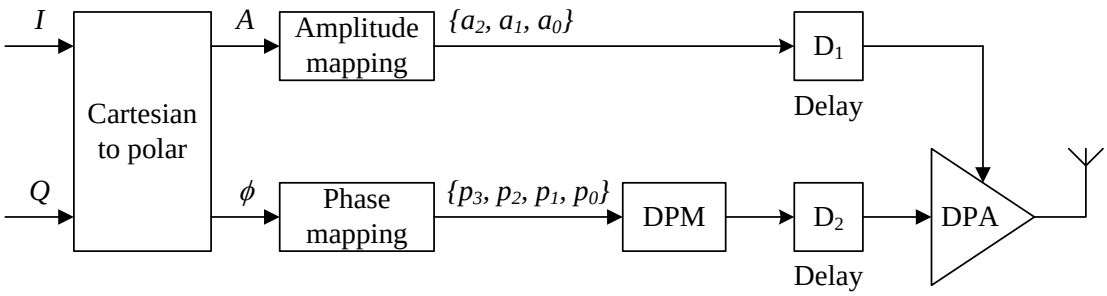

Figure 5-2: Digital polar transmitter with delays in amplitude and phase signals.

5.2.1 Results

The results are shown in Figure 5-3 and Figure 5-4. It can be observed that the trend is the same for different data rates. The results are summarized in Table 5-2. For data rate of 53.3 Mb/s, a time delay mismatch of less than 0.62 ns can be tolerated. On the other hand, the time delay mismatch requirement is more stringent for other data rates. A time delay mismatch of less than 0.36 ns is required for data rates of 106.7 Mb/s and 200 Mb/s and a time delay mismatch of less than 0.14 ns is required for data rate of 480 Mb/s.

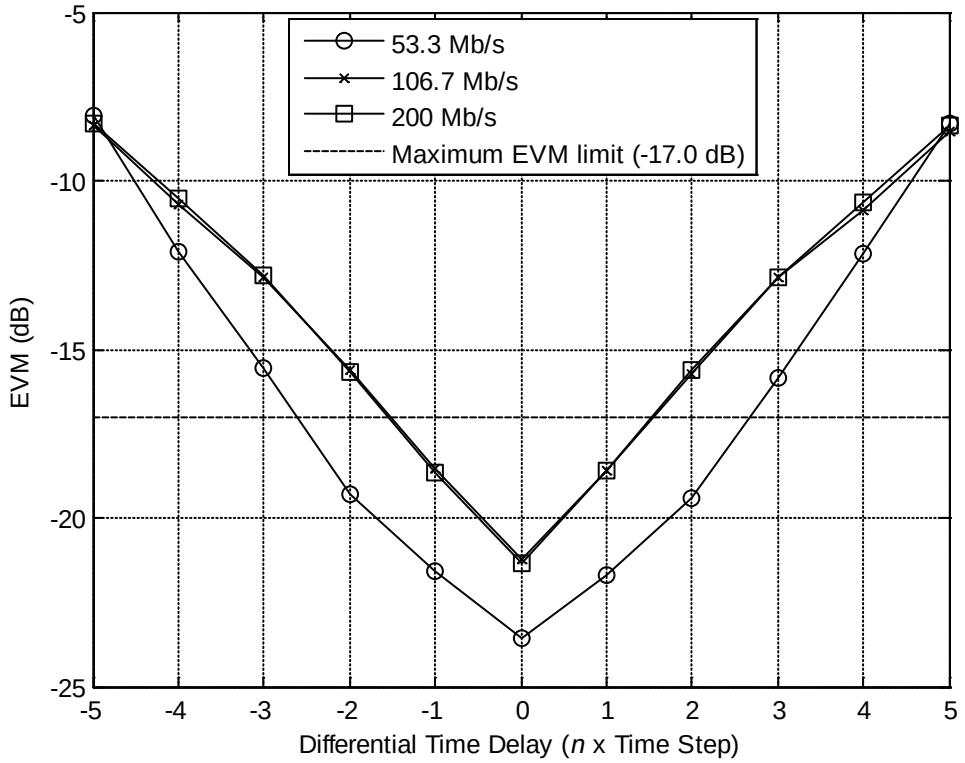

Figure 5-3: Differential delay in digital polar transmitter for 53.3 Mb/s, 106.7 Mb/s and 200 Mb/s.

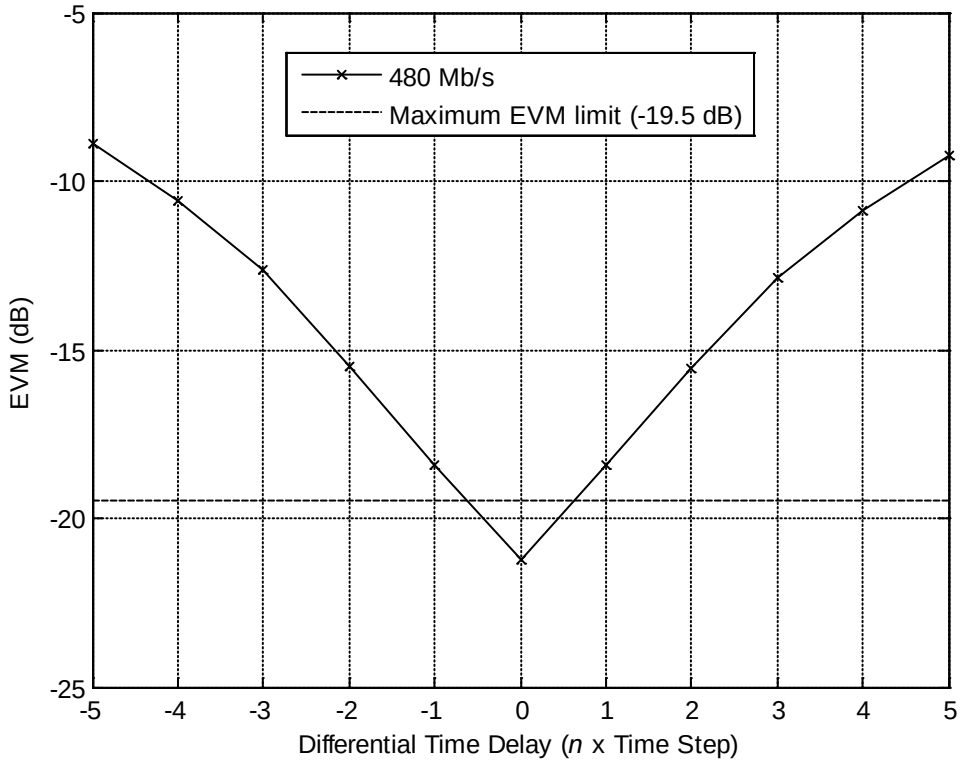

Figure 5-4: Differential delay in digital polar transmitter for 480 Mb/s.

Table 5-2: Summary of differential time delay for various data rates.

Data Rate (Mb/s)	Maximum EVM Limit (dB)	$D_2 - D_1 < 0$ (Amplitude Delay)		$D_2 - D_1 > 0$ (Phase Delay)	
		n × Time Step	ns	n × Time Step	ns
53.3	-17.0	-2.60	-0.62	2.65	0.63
106.7	-17.0	-1.50	-0.36	1.55	0.37
200	-17.0	-1.55	-0.37	1.50	0.36
480	-19.5	-0.60	-0.14	0.60	0.14

5.3 Mismatch in Gain

The 3-bit DPA consists of an array of 7 parallel amplifiers of equal amplification, G, as shown in Figure 5-5. The least significant bit (LSB), a_0, will control 1 amplifier while bit a_1 will control 2 amplifiers. The most significant bit (MSB), a_2, will control 4 amplifiers.

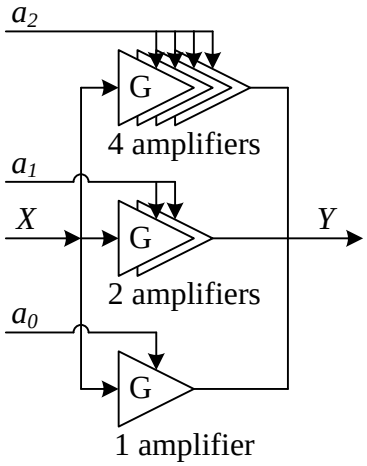

Figure 5-5: 3-bit digital power amplifier (DPA).

In practice, the gain of each amplifier in the DPA will deviate from its desired gain, G, due to manufacturing variations. To evaluate the effect of mismatch in gain,

simulations are performed in ADS Ptolemy [48] for various data rates. The gain variation is defined as $\Delta G_{a_i} / G_{a_i}$, where G_{a_i} is the gain of the amplifiers associated with amplitude control bit, a_i, and ΔG_{a_i} is the gain variation. G_{a_0} is G for LSB bit, a_0, while G_{a_2} is $4G$ for MSB bit, a_2. Simulations are performed by sweeping the gain variation. For each simulation, the gain of the amplifiers is varied for one bit while the gain for other amplifiers controlled by other bits are kept as ideal.

5.3.1 Results

The results are shown in Figure 5-6, Figure 5-7, Figure 5-8 and Figure 5-9. It can be observed that the trend is the same for different data rates. EVM deteriorates as the gain variation increases. The results are summarized in Table 5-3. For data rate of 53.3 Mb/s, as shown in Figure 5-6, gain variations of less than ±70%, ±40% and ±30% are required for amplitude control bits, a_0, a_1 and a_2, respectively in order to pass the EVM requirement. For data rates of 106.7 Mb/s and 200 Mb/s, gain variations of less than ±60%, ±30% and ±30% are required for amplitude control bits, a_0, a_1 and a_2, respectively. For data rate of 480 Mb/s, the requirement is more stringent and gain variations of less than ±30%, ±20% and ±20% are required for amplitude control bits, a_0, a_1 and a_2, respectively. Hence, some form of compensation is needed to reduce the mismatch in gain between the amplifiers to improve the EVM results.

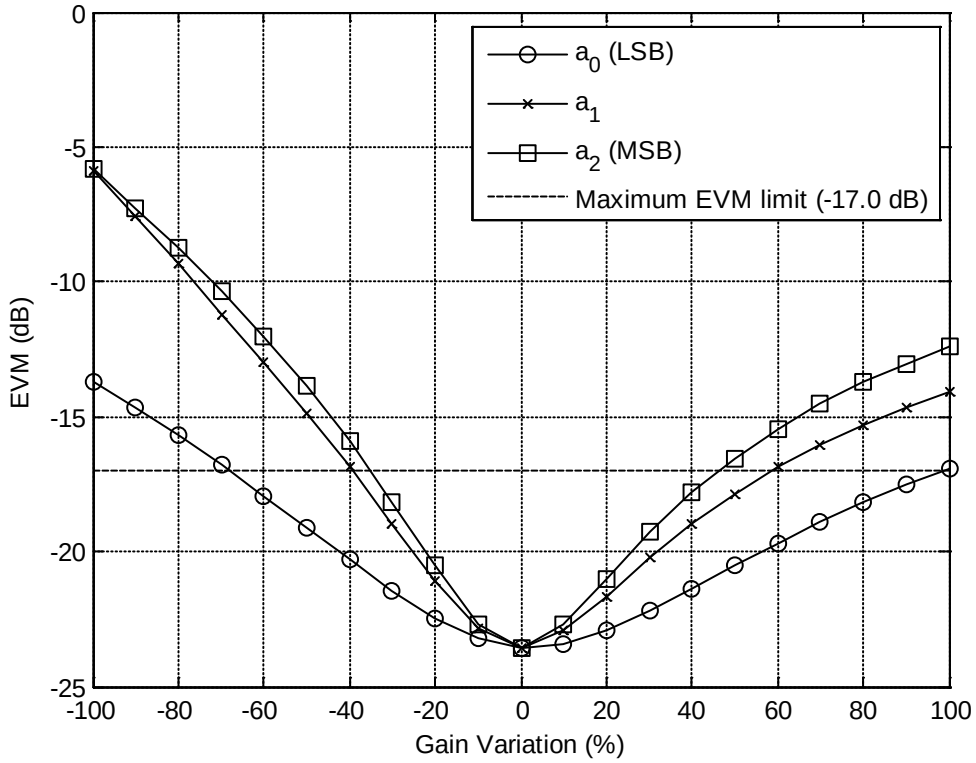

Figure 5-6: Effect of gain variation for amplifiers for 53.3 Mb/s.

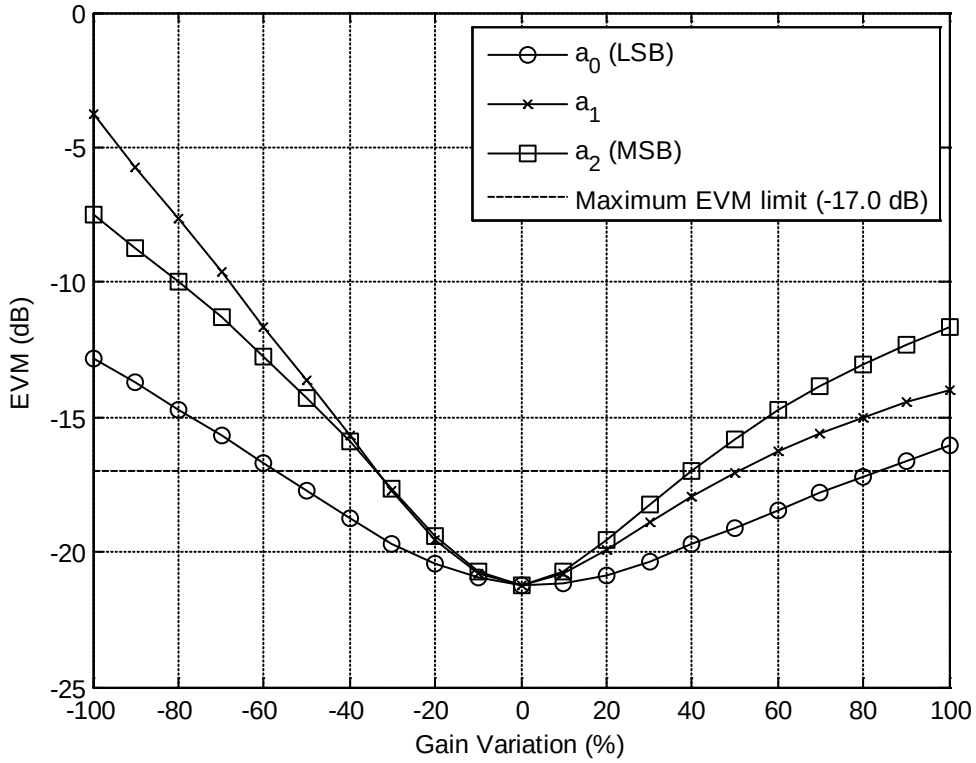

Figure 5-7: Effect of gain variation for amplifiers for 106.7 Mb/s.

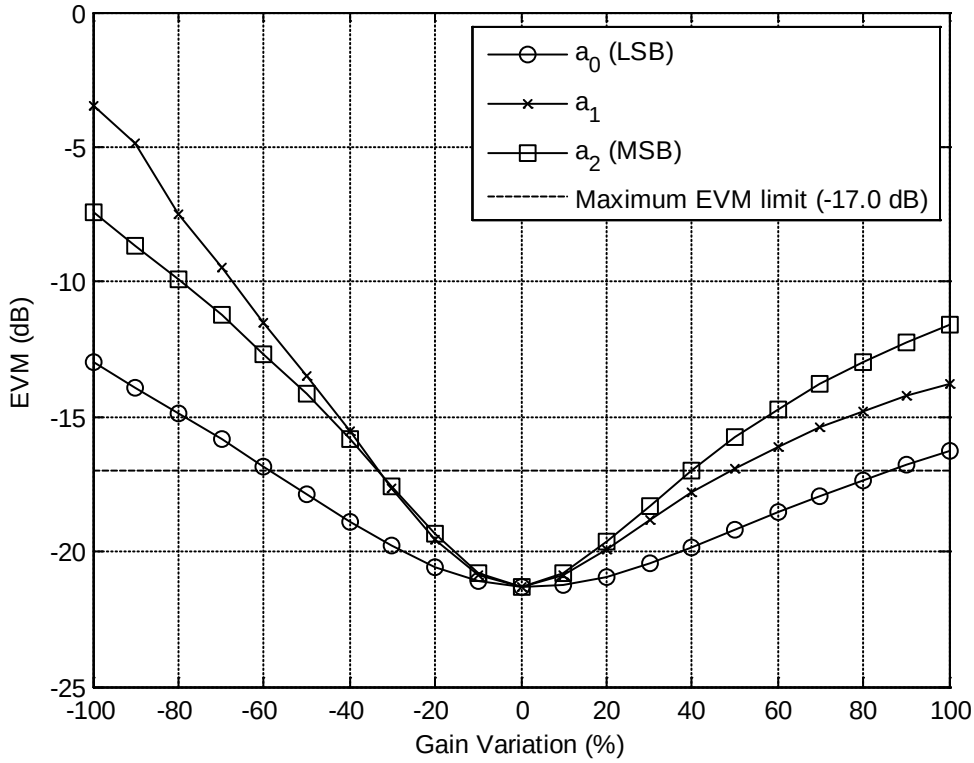

Figure 5-8: Effect of gain variation for amplifiers for 200 Mb/s.

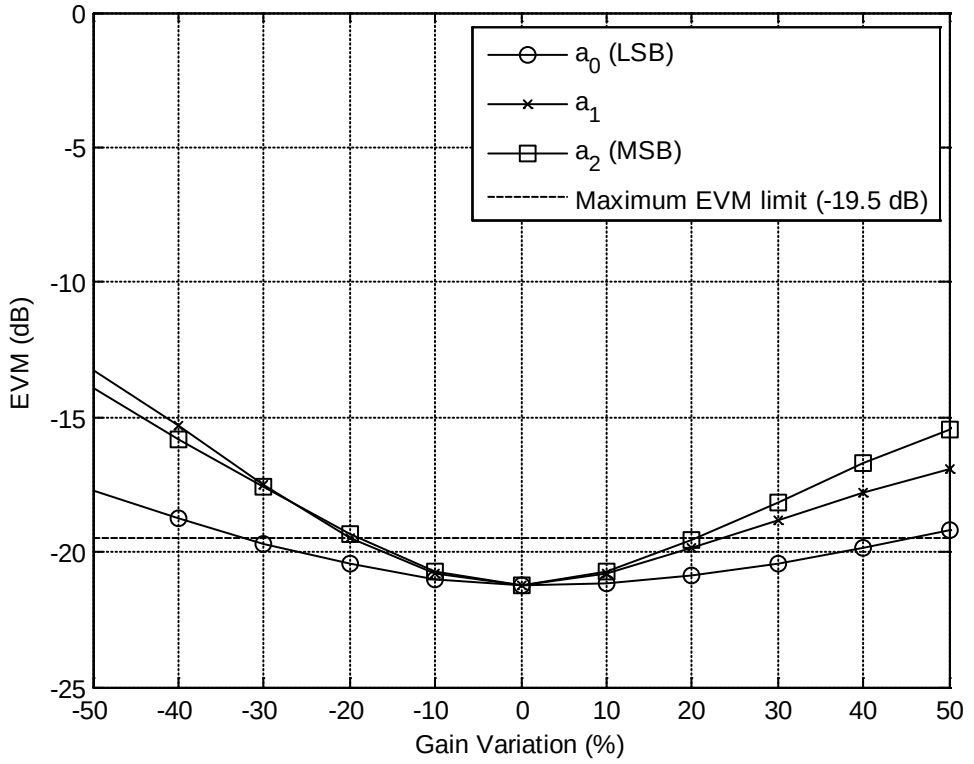

Figure 5-9: Effect of gain variation for amplifiers for 480 Mb/s.

Table 5-3: Summary of gain variation for various data rates.

Data Rate (Mb/s)	Maximum EVM Limit (dB)	Gain Variation (%)		
		a_0	a_1	a_2
53.3	-17.0	±70	±40	±30
106.7	-17.0	±60	±30	±30
200	-17.0	±60	±30	±30
480	-19.5	±30	±20	±20

5.4 Error in Phase

The 4-bit DPM, as shown in Figure 5-10, consists of a multi-phase clock generating 16 different phases, $\{\phi_{15},\ldots,\phi_1,\phi_0\}$, of the carrier frequency (ω_c) signal and a multiplexer which will select the signal with the correct phase. In practice, the phases will deviate from the ideal phases due to manufacturing variations, creating some deviations from the ideal phases. To evaluate the effect of the error in phase, simulations are performed in ADS Ptolemy [48] for various data rates.

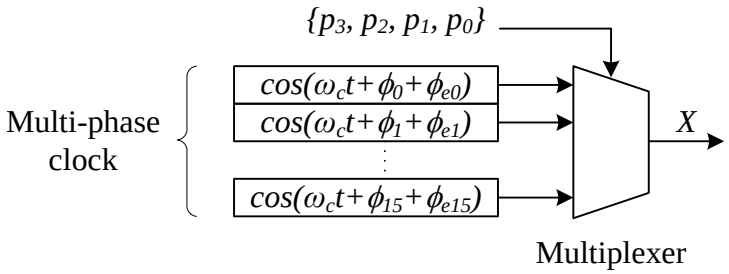

Figure 5-10: 4-bit digital phase modulator (DPM).

The phase error variation for phase, ϕ_i, is defined as ϕ_{ei}/ϕ_{LSB}, where ϕ_{ei} is the phase error and ϕ_{LSB} is the least significant bit (LSB) change of the phase control bit.

Simulations are performed by sweeping the phase error variation for each phase at a time.

5.4.1 Results

Figure 5-11, Figure 5-12, Figure 5-13 and Figure 5-14 show the probability distribution of the 16 phases, $\{\phi_{15},\ldots,\phi_1,\phi_0\}$ for a burst of UWB data for different data rates. It can be observed that the two phases, $\phi_0 = 0$ and $\phi_8 = \pi$, occur frequently in the burst of UWB data for different data rates. Hence, only simulation results for these two phases are presented.

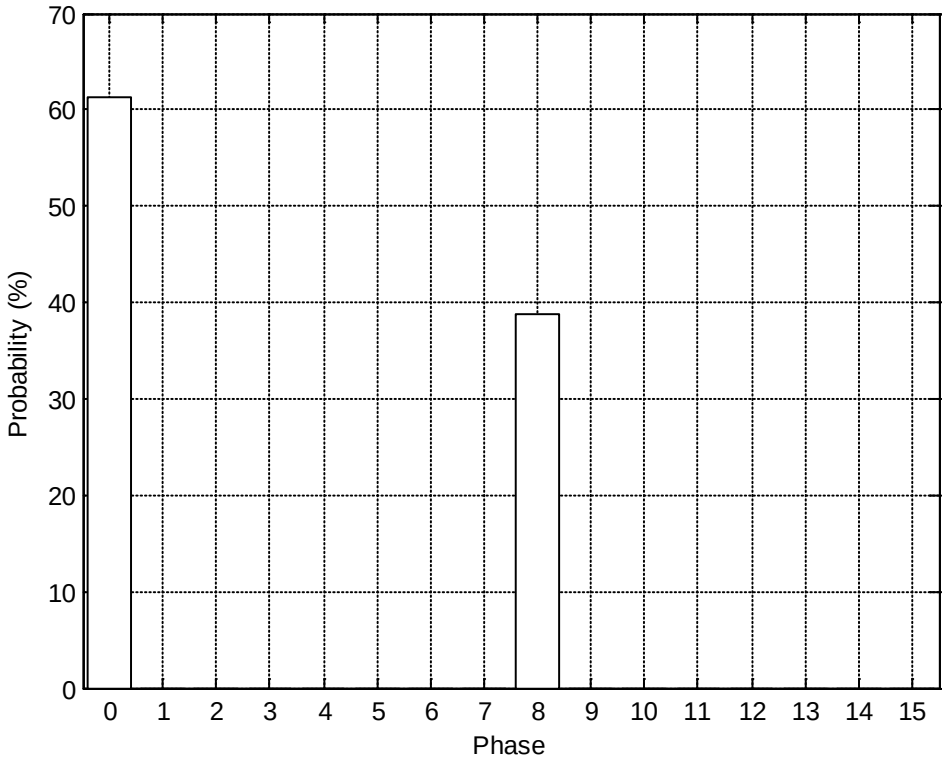

Figure 5-11: Probability distribution of phases from the DPM for 53.3 Mb/s.

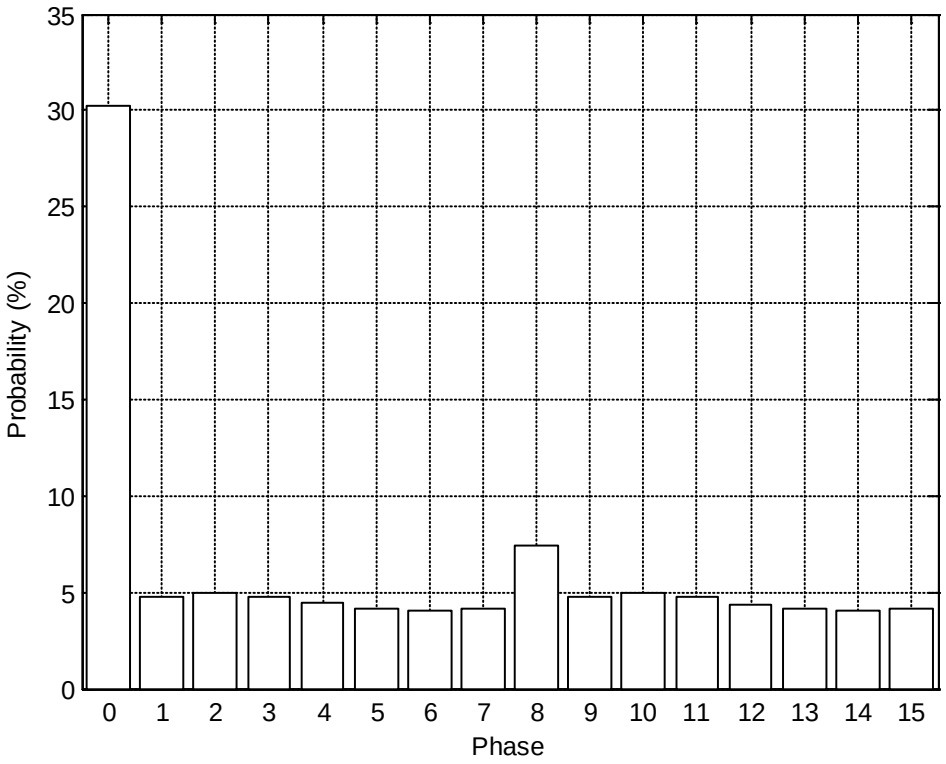

Figure 5-12: Probability distribution of phases from the DPM for 106.7 Mb/s.

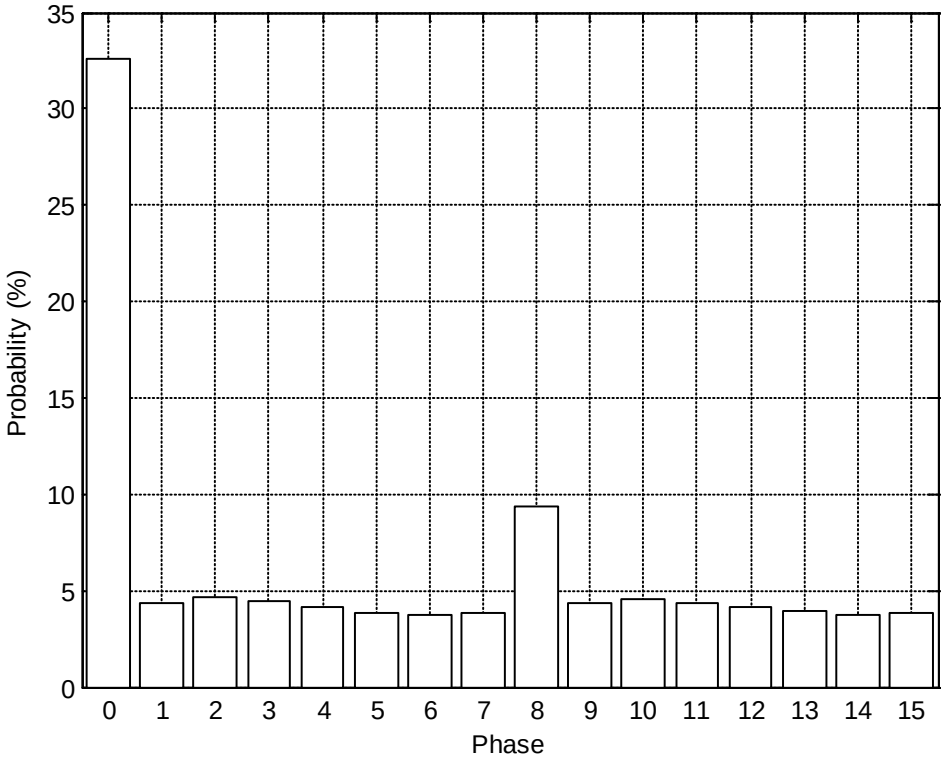

Figure 5-13: Probability distribution of phases from the DPM for 200 Mb/s.

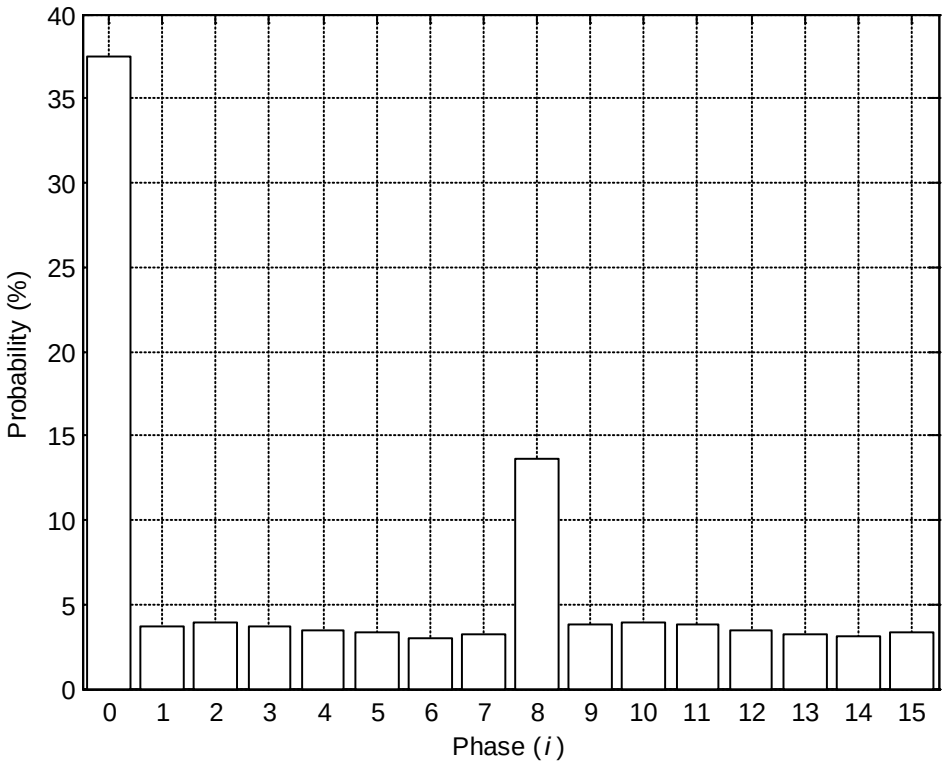

Figure 5-14: Probability distribution of phases from the DPM for 480 Mb/s.

The results for the two phases, $\phi_0 = 0$ and $\phi_8 = \pi$, at different data rates are shown in Figure 5-15, Figure 5-16, Figure 5-17 and Figure 5-18. It can be observed that the trend is the same for different data rates. EVM deteriorates as the phase error variation increases. For data rates of 53.3 Mb/s, 106.7 Mb/s and 200 Mb/s, increase in phase error variations will result in the degradation of the EVM performance. However, the DPT will still pass the EVM requirement of -17 dB in [2]. For data rate of 480 Mb/s, the requirement is more stringent and phase variations of less than ±90%, is required to pass the EVM requirement. It should be noted that the error in the phase is only evaluated for the two phases, $\phi_0 = 0$ and $\phi_8 = \pi$. Hence, the EVM results will worsen if errors in other phases are considered as well. To improve the EVM results,

the multi-phase clock needs to have some form of compensation to reduce the errors in the phases.

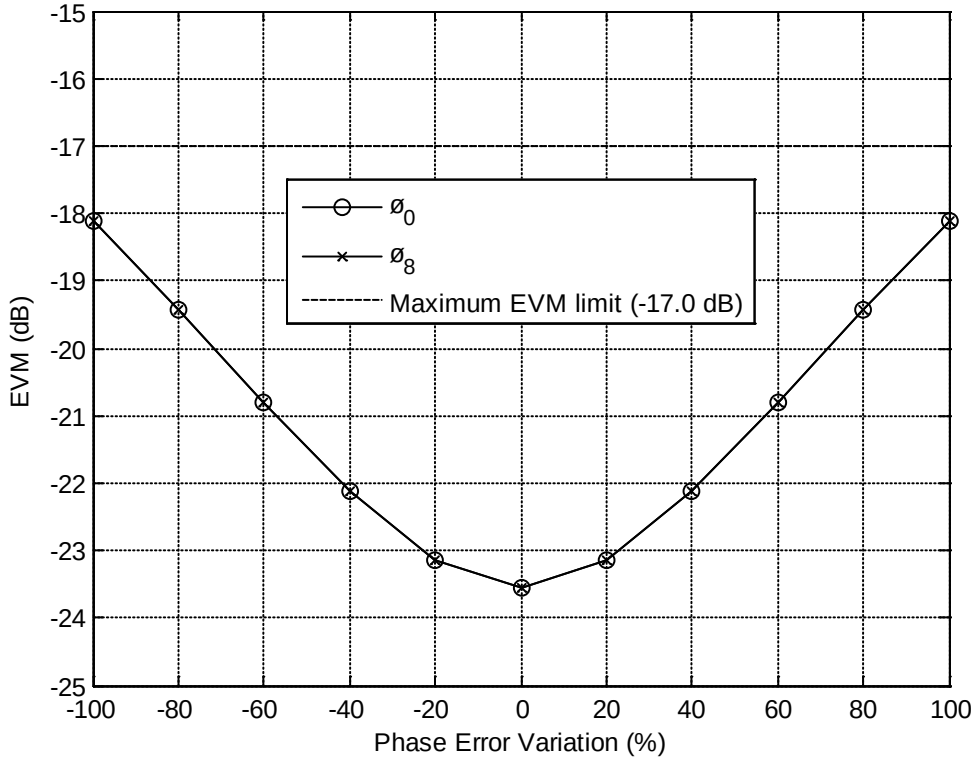

Figure 5-15: Effect of errors in phases on EVM for 53.3 Mb/s.

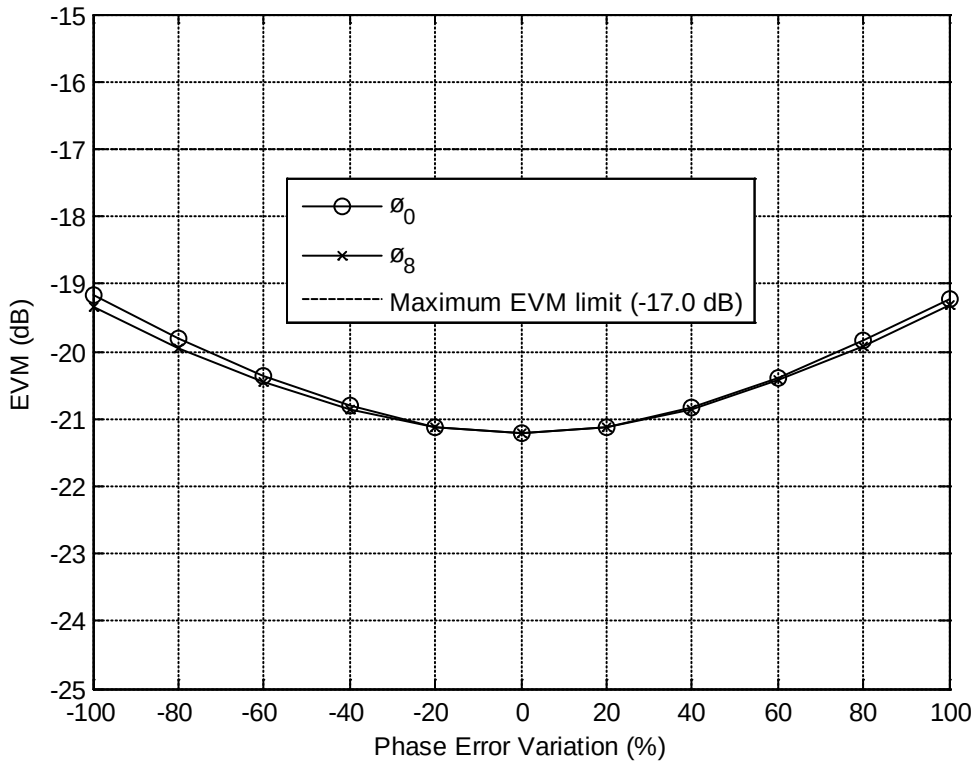

Figure 5-16: Effect of errors in phases on EVM for 106.7 Mb/s.

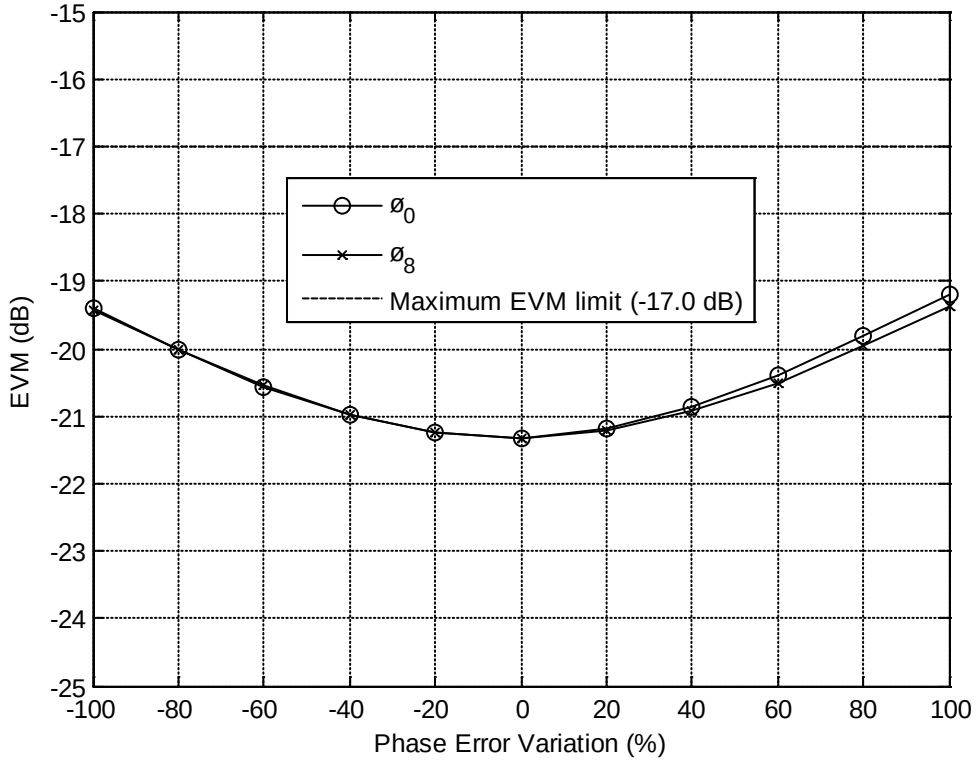

Figure 5-17: Effect of errors in phases on EVM for 200 Mb/s.

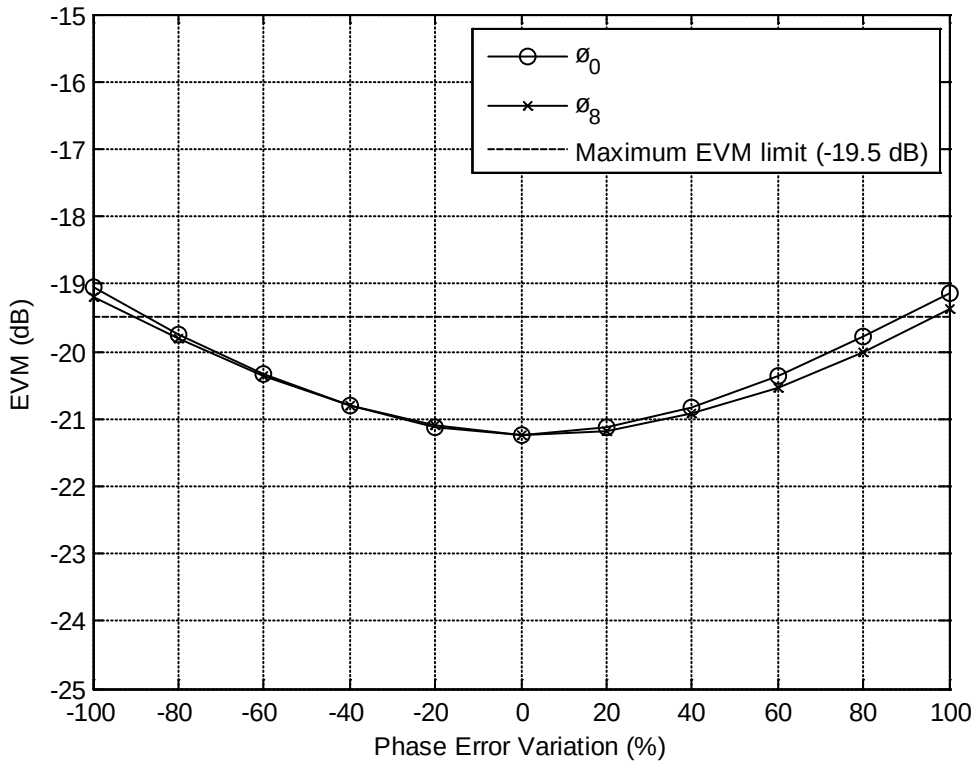

Figure 5-18: Effect of errors in phases on EVM for 480 Mb/s.

5.5 Summary

In this chapter, the non-idealities in the amplitude and phase signals, like mismatches in delay, gain and phase, in a digital polar transmitter (DPT) for MB-OFDM UWB are discussed. Simulations results show that a time delay mismatch of less than 0.62 ns can be tolerated for data rate of 53.3 Mb/s. For data rates of 106.7 Mb/s and 200 Mb/s, a time delay mismatch of less than 0.36 ns is required. A time delay mismatch of less than 0.14 ns is required for data rate of 480 Mb/s. In addition, simulation results show that EVM performance of the DPT degrades as the gain variation and phase error variation increase. To reduce these variations, compensating methods need to be employed in the circuitries for DPA and DPM.

CHAPTER 6

CONCLUSIONS

In this thesis, the system considerations for the amplitude and phase signals in the MB-OFDM UWB polar transmitter are studied. Simulation results show that the bandwidth of the phase needs to be several times wider than that of the amplitude [13]. The frequency responses of the amplitude and phase signals do not necessarily have the same bandwidth. The bandwidth of the amplitude can be relaxed in comparison to that of the phase provided that the frequency responses of the signals are linear-phase and the time delays between the amplitude and phase signals are matched [13]. In the case where frequency responses are not linear-phase, delay equalization has to be employed.

To take advantage of the advancement of deep-submicron semiconductor technology which favors more digital circuitries, a digital polar transmitter (DPT) for MB-OFDM UWB is proposed [14]. The DPT consists digital polar modulator (DPM) which produces the digital phase-modulated RF signal and digital power amplifier (DPA) which will modulate the amplitude of the RF signal digitally. The minimum DPM resolution m and the minimum DPA resolution n are determined for different data rates. A DPT with $\{m, n\} = \{3, 4\}$ will meet the EVM requirements for data rates.

In addition, the non-idealities in the amplitude and phase signals, like delay mismatch, mismatch in gain and error in phase, in the proposed DPT are discussed. Simulations results show that a time delay mismatch of less than 0.62 ns can be tolerated for data

rate of 53.3 Mb/s. For data rates of 106.7 Mb/s and 200 Mb/s, a time delay mismatch of less than 0.36 ns is required. A time delay mismatch of less than 0.14 ns is required for data rate of 480 Mb/s. Simulation results also show that EVM performance of the DPT degrades as the gain variation and phase error variation increase. To reduce these variations, compensating methods need to be employed in the circuitries for DPA and DPM.

Future work can be done to investigate the non-idealities, such as switching delays and voltage spikes when switches are turned on and off, in the amplifier control in the digital power amplifier (DPA) and the multiplexer in the digital phase modulator (DPM). These non-idealities may degrade the EVM performance and need to been studied. Furthermore, the DPA acts as a digital-to-analog converter (DAC) and studies need to be done to evaluate the need for any filtering at the output of the DPT. Finally, new compensating methods need to be used to reduce these effects in the DPT. For the DPA, the use of dynamic element matching (DEM) method introduced in [49] can reduce the gain variation in the DPA. For the DPM, the phase error variation from the multi-phase clock can be reduced by the use of delay-locked loop (DLL) to generate the multi-phase signals.

REFERENCE

[1] L. Yang and G. B. Giannakis, "Ultra-Wideband Communications: An Idea Whose Time Has Come," *IEEE Signal Processing Magazine*, vol. 21, no. 6, pp. 26-34, Nov. 2004.

[2] "Standard ECMA-368: High Rate Ultra Wideband PHY and MAC Standard", *EMCA International*, 1st Edition, Dec. 2005.

[3] "Standard ECMA-369: MAC-PHY Interface for EMCA-368", *EMCA International*, 1st Edition, Dec. 2005.

[4] Federal Communications Commission, "FCC 02-48: Report and Order on UWB", 22 Apr. 2002.

[5] L. R. Kahn, "Single-Sideband Transmission by Envelope Elimination and Restoration," in *Proc. of IRE*, vol. 40, no. 7, pp. 803-806, Jul. 1952.

[6] F. H. Raab, "Intermodulation Distortion in Kahn-technique Transmitters," IEEE Trans. Microwave Theory and Techniques, vol. 44, no. 12, pp. 2273-2278, Dec. 1996.

[7] P. Nagle, P. Burton, E. Heaney, *et al.*, "A Wide-Band Linear Amplitude Modulator for Polar Transmitters Based on the Concept of Interleaving Delta

Modulation," IEEE J. Solid-State Circuits, vol. 37, no. 12, pp. 1748-1756, Dec. 2002.

[8] A. Montalvo, "Polar Modulators for Linear Wireless Transmitters," ISSCC Tutorial, Feb. 2005.

[9] M. Talonen, S. Lindfors, "System Requirements for OFDM Polar Transmitter," in *Proc. of European Conference on Circuit Theory and Design*, vol. 3, pp. 69-72, 28 Aug.-2 Sep. 2005.

[10] R. B. Staszewski and P. T. Balsara, "All-Digital Frequency Synthesizer in Deep-Submicron CMOS," *Wiley-Interscience*, 2006.

[11] R. B. Staszewski, K. Muhammad, D. Leipold, *et al.*, "All-Digital TX Frequency Synthesizer and Discrete-Time Receiver for Bluetooth Radio in 130-nm CMOS," *IEEE J. Solid-State Circuits*, vol. 39, no. 12, pp. 2278-2291, Dec. 2004.

[12] R. B. Staszewski, J. L. Wallberg, S. Rezeq, *et al.*, "All-Digital PLL and Transmitter for Mobile Phones," *IEEE J. Solid-State Circuits*, vol. 40, no. 12, pp. 2469-2482, Dec. 2005.

[13] W.-F. Loke, M. Y.-W. Chia and P.-Y. Chee, "Design Considerations for Multi-Band OFDM Polar Transmitter of Ultra-WideBand System," *IET Electronics Letters*, vol. 43, no. 22, pp. 1183-1184, Oct. 2007.

[14] W.-F. Loke, M. Y.-W. Chia and P.-Y. Chee, "Phase Wrapping Digital Polar Transmitter for Multi-band OFDM Ultra-Wideband System," *IEEE International Microwave Symp.*, Jun. 2009, accepted.

[15] R. van Nee and R. Prasad, "OFDM for Wireless Multimedia Communications," *Artech House*, 2000.

[16] D. Porcino and W. Hirt, "Ultra-Wideband Radio Technology: Potential and Challenges Ahead," *IEEE Communications Magazine*, vol. 41, no. 7, pp. 66-74, Jul. 2003.

[17] J. G. Proakis, "Digital Communications," *McGraw-Hill*, 4th Edition, 2001.

[18] W. P. Siriwongpairat and K. J. R. Liu, "Ultra-Wideband Communications Systems: Multiband OFDM Approach," *Wiley-Interscience*, 2008.

[19] I. Oppermann, M. Hämäläinen and J. Iinatti, "UWB Theory and Applications," *John Wiley and Sons*, 2004.

[20] A. Batra, J. Balakrishnan and A. Dabak, "Multi-Band OFDM: A New Approach for UWB," *Proc. of IEEE Int. Symp. on Circuits and Systems (ISCAS)*, vol. 5, pp. 365-368, 23-26 May 2004.

[21] V. S. Somayazulu, J. R. Foerster and S. Roy, "Design Challenges for Very High Data Rate UWB Systems," *Proc. of Asilomar Conf. on Signals, Systems and Computers*, vol. 1, pp. 717-721, 3-6 Nov. 2002.

[22] J. Balakrishnan, A. Batra and A. Dabak, "A Multi-Band OFDM System for UWB Communication," *IEEE Conf. on Ultra Wideband Systems and Technologies*, pp. 354-358, 16-19 Nov. 2003.

[23] S. A. Ghorashi, B. Allen, M. Ghavami, *et al.*, "An Overview of MB-UWB OFDM," *IEE Seminar on Ultra Wideband Communications Technologies and System Design*, pp. 107-110, 8 Jul. 2004.

[24] MultiBand OFDM Alliance SIG, "Multi-Band OFDM Physical Layer Proposal for IEEE 802.15 Task Group 3a," 14 Sep. 2004.

[25] J. K. Jau, Y. A. Chen, S. C. Hsiao, *et al.*, "Highly Efficient Multimode RF Transmitter Using the Hybrid Quadrature Polar Modulation Scheme," *IEEE MTT-S Int. Microwave Symp. Dig.*, pp. 789-792, Jun. 2006.

[26] B. Razavi, "RF Microelectronics," *Prentice Hall*, 1998.

[27] T. H. Lee, "The Design of CMOS Radio-Frequency Integrated Circuits," *Cambridge University Press*, 2nd Edition, 2003.

[28] A. Loke and F. Ali, "Direct Conversion Radio for Digital Mobile Phones - Design Issues, Status, and Trends," *IEEE Trans. Microwave Theory and Techniques*, vol. 50, no. 11, Nov. 2002.

[29] D. H. Moralis and K. Feher, "The Effects of Filtering on the performance of QPSK, Offset QPSK, and MSK Signals," *IEEE Trans. Communications*, vol. 28, no. 12, pp. 1999-2009, Dec. 1980.

[30] A. Shirvani and B. A. Wooley, "Design and Control of RF Power Amplifiers," *Kluwer Academic Publishers*, 2003.

[31] M. Johansson and T. Mattsson, "Transmitter Linearization using Cartesian Feedback for Linear TDMA Modulation," *Proc. of IEEE Veh. Tech. Conf.*, pp. 439-444, May 1991.

[32] D. C. Cox, "Linear Amplification with Nonlinear Components," *IEEE Trans. Communications*, vol. 22, no. 12, pp. 1942-1945, Dec. 1974.

[33] E. McCune, "Polar Modulation and Bipolar RF Power Devices," *Proc. of Bipolar/BiCMOS Circuits and Tech. Meeting*, pp. 1-5, Oct. 2005.

[34] D. K. Su and W. J. McFarland, "An IC for Linearizing RF Power Amplifiers using Envelope Elimination and Restoration", *IEEE J. Solid-State Circuits*, vol. 33, no. 12, pp. 2252-2258, Dec. 1998.

[35] W. B. Sander, S. V. Schell and B. L. Sander, "Polar Modulator for Multi-mode Cell Phones," *Proc. of IEEE Custom Integrated Circuits Conf.*, pp. 439-445, Sep. 2003.

[36] A. W. Hietala, "A Quad-band 8PSK/GMSK Polar Transceiver," *IEEE J. Solid-State Circuits*, vol. 41, no. 5, pp. 1133-1141, May 2006.

[37] T. Sowlati, D. Rozenblit, R. Pullela, *et al.*, "Quad-Band GSM/GPRS/EDGE Polar Loop Transmitter," *IEEE J. Solid-State Circuits*, vol. 39, no. 12, pp. 2179-2189, Dec. 2004.

[38] M. Elliott, T. Montalvo, F. Murden, *et al.*, "A Polar Modulator Transmitter for EDGE," *IEEE Solid-State Circuits Conf. (ISSCC) Tech. Dig.*, vol. 1, pp. 190-192, Feb. 2004.

[39] J. Groe, "Polar Transmitters for Wireless Communications," *IEEE Communications Magazine*, vol. 45, no. 9, pp. 58-63, Sep. 2007.

[40] K. Gentile, "DDS Simplifies Polar Modulation," *EDN Magazine*, pp. 69-74, Aug. 2004.

[41] H.-Y. Ko, Y.-C. Wang and A.-Y. Wu, "Digital Signal Processing Engine Design for Polar Transmitter in Wireless Communication Systems," *Proc. of IEEE Int. Symp. Circuits and Systems (ISCAS)*, vol. 6, pp. 6026-6029, May 2005.

[42] B.-G. Goldberg, "Digital Frequency Synthesis Demystified: DDS and Fractional-N PLLs," *Newnes*, 1999.

[43] P. Nagle, P. Burton, E. Heaney, *et al.*, "A Wide-Band Linear Amplitude Modulator for Polar Transmitters Based on the Concept of Interleaving Delta Modulation," *IEEE J. Solid-State Circuits*, vol. 37, no. 12, pp. 1748-1756, Dec. 2002.

[44] C. Zhao and R. J. Baxley, "Error Vector Magnitude Analysis for OFDM Systems," *Proc. Asilomar Conf. on Signals, Systems and Computers (ACSSC)*, pp. 1830-1834, Oct. 2006.

[45] Agilent Technologies, "Ultra-Wideband Design Library," *Agilent Advanced Design System (ADS) 2005A.*

[46] Agilent Technologies, "Digital Filter Designer," *Agilent Advanced Design System (ADS) 2005A*.

[47] K.-H. Seah, M. Y.-W. Chia, C. Papavassiliou, *et al.*, "A Digital Polar Transmitter for Ultra-WideBand System using OFDM Modulation," *IET Electronics Letters*, vol. 43, no. 8, pp. 466-468, Apr. 2007.

[48] Agilent Technologies, "Ultra-Wideband Design Library," *Agilent Advanced Design System (ADS) 2006A.*

[49] K. B. Klaassen, “Digitally Controlled Absolute Voltage Division,” *IEEE Trans. Instrumentation and Measurement*, vol. 24, no. 2, pp. 106-112, Jun. 1975.

APPENDIX A

FREQUENCY RESPONSES OF FIR FILTERS

The FIR filters are used to limit the bandwidths of the amplitude and phase. Their specifications are shown in Table A-1 and their frequency responses are shown in Figures A-1 to A-9.

Table A-1: Specifications of the FIR filters used to limit the bandwidths of the amplitude and phase.

FIR Filter	Cut-off Frequency (MHz)	Order of Filter	Group Delay (ns)
1	264	397	46.94
2	528	396	46.87
3	792	396	46.82
4	1056	396	46.91
5	1320	396	46.83
6	1584	396	46.88
7	1848	396	46.92
8	1948	396	46.90
9	2064	396	46.88

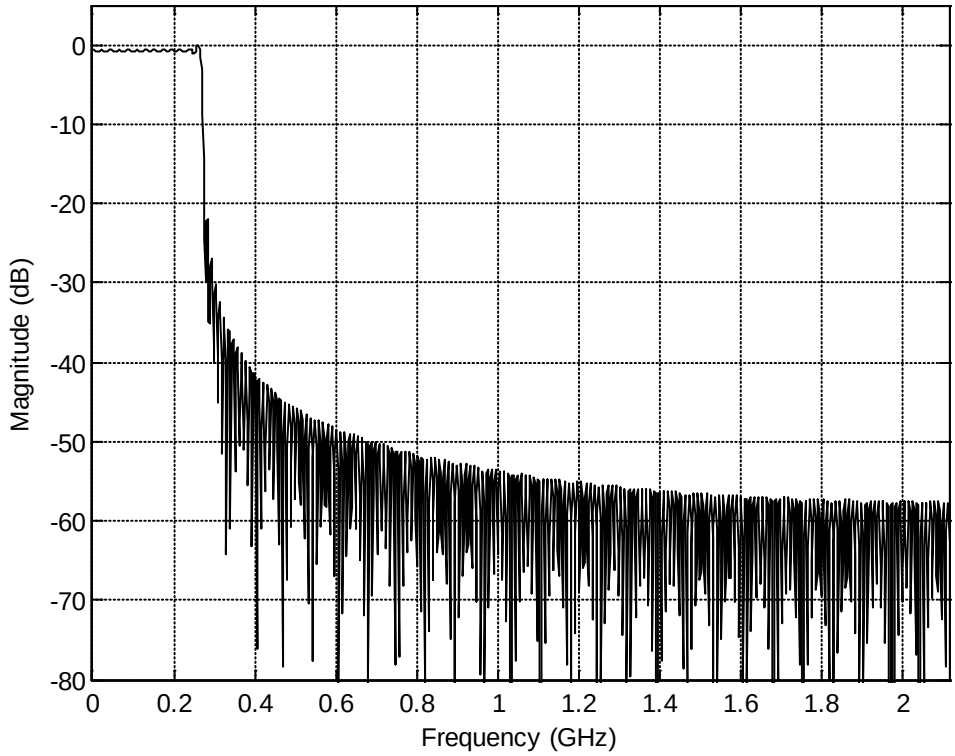

Figure A-1: Frequency response of FIR filter with cut-off frequency at 264 MHz.

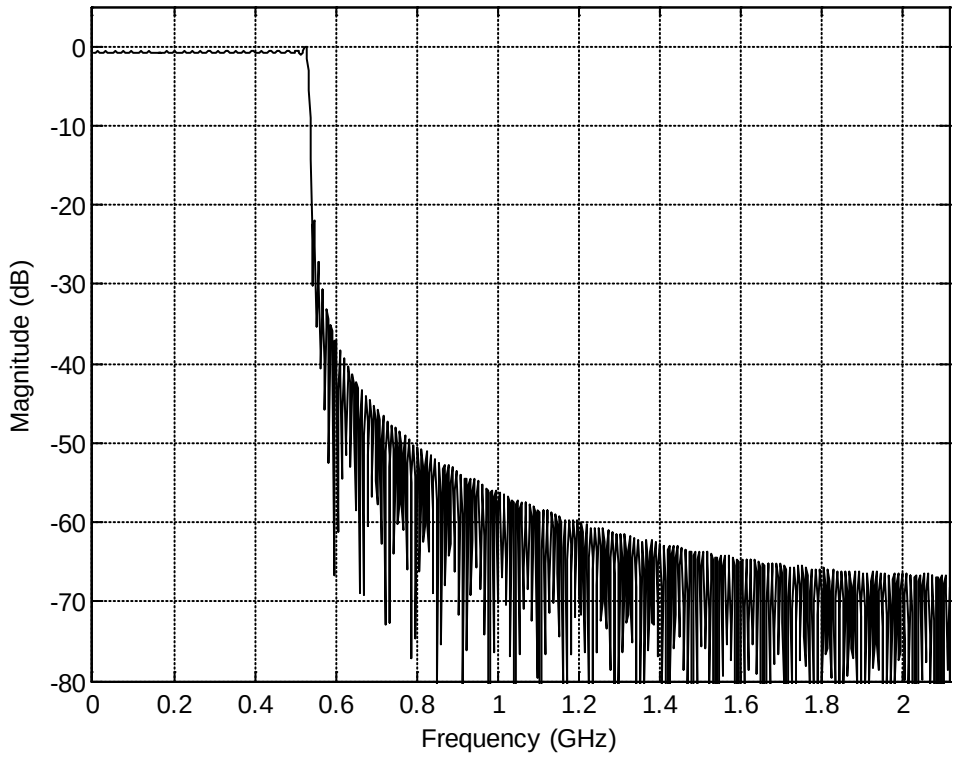

Figure A-2: Frequency response of FIR filter with cut-off frequency at 528 MHz.

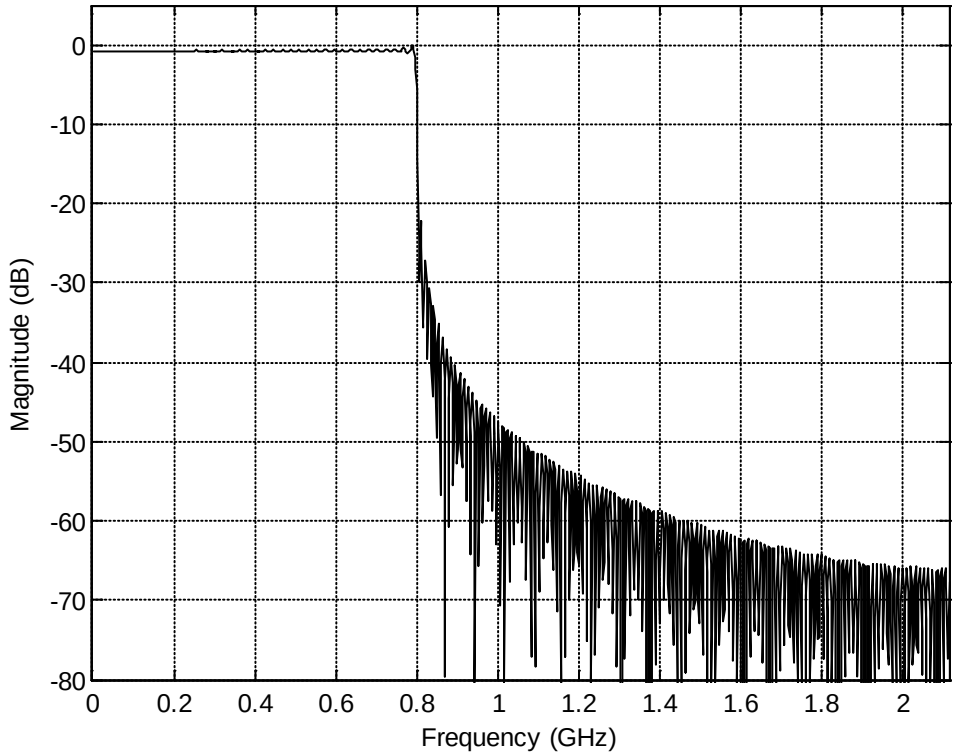

Figure A-3: Frequency response of FIR filter with cut-off frequency at 792 MHz.

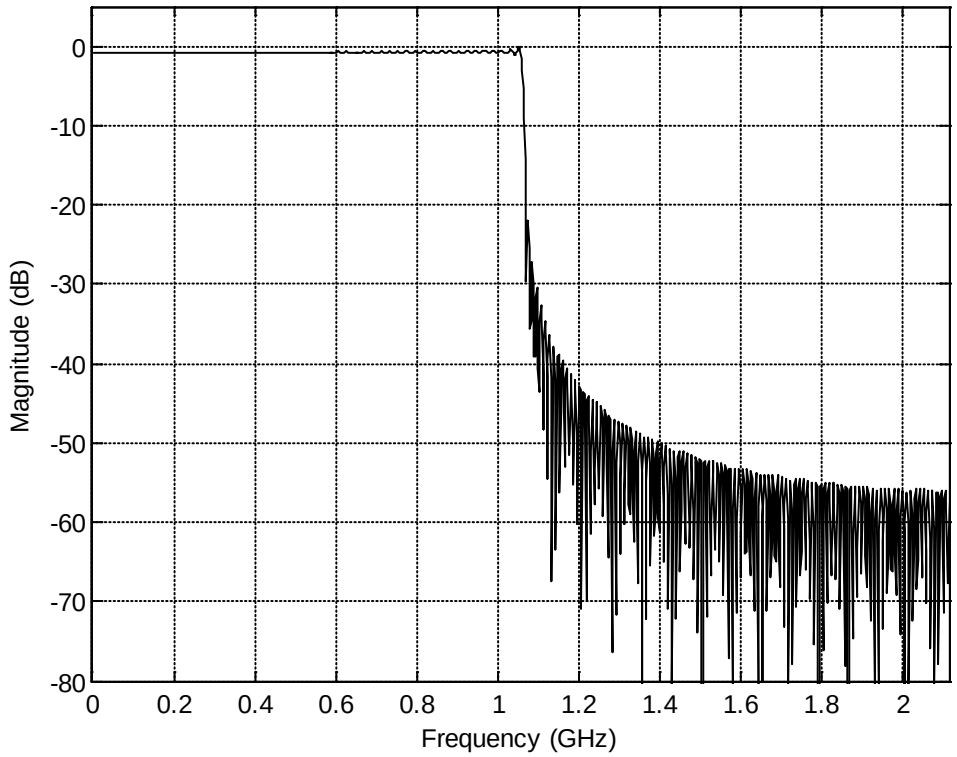

Figure A-4: Frequency response of FIR filter with cut-off frequency at 1056 MHz.

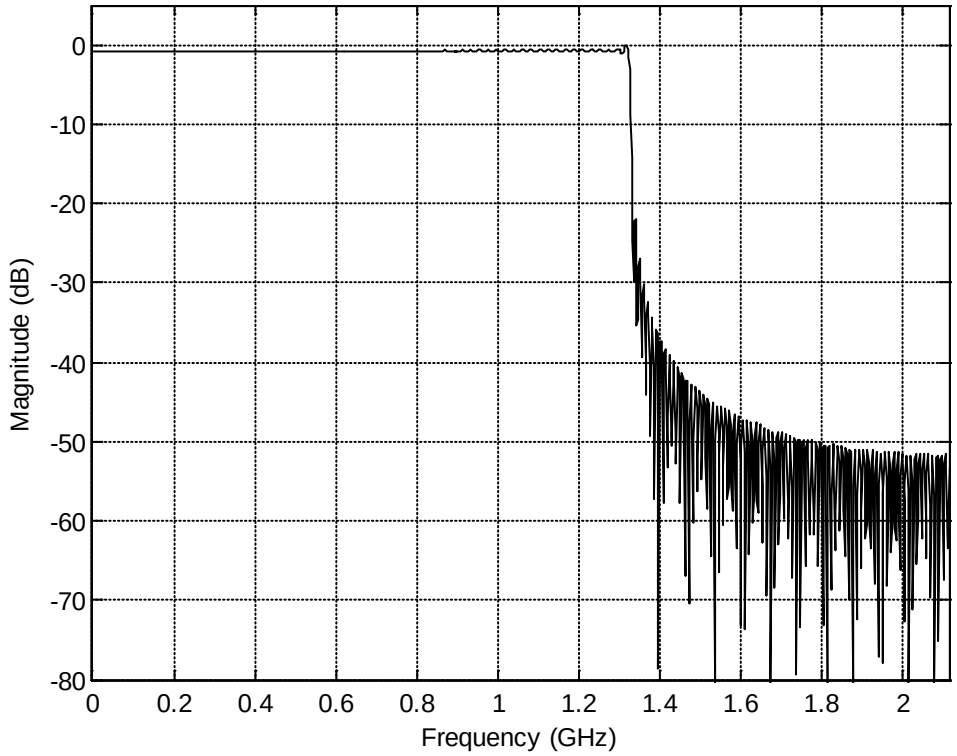

Figure A-5: Frequency response of FIR filter with cut-off frequency at 1320 MHz.

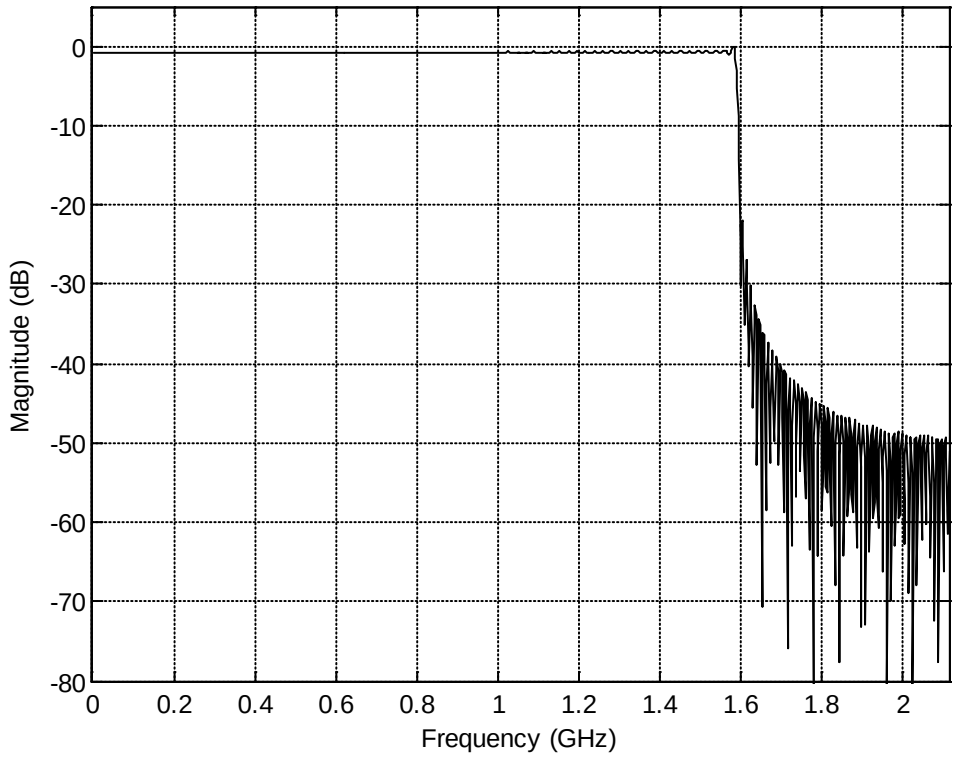

Figure A-6: Frequency response of FIR filter with cut-off frequency at 1584 MHz.

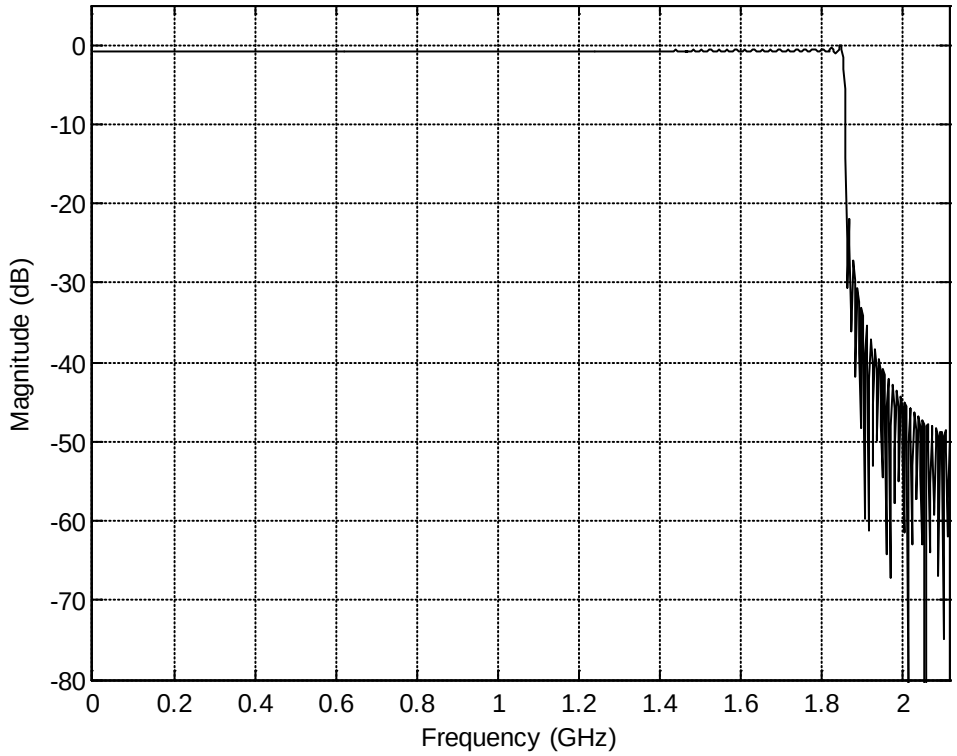

Figure A-7: Frequency response of FIR filter with cut-off frequency at 1848 MHz.

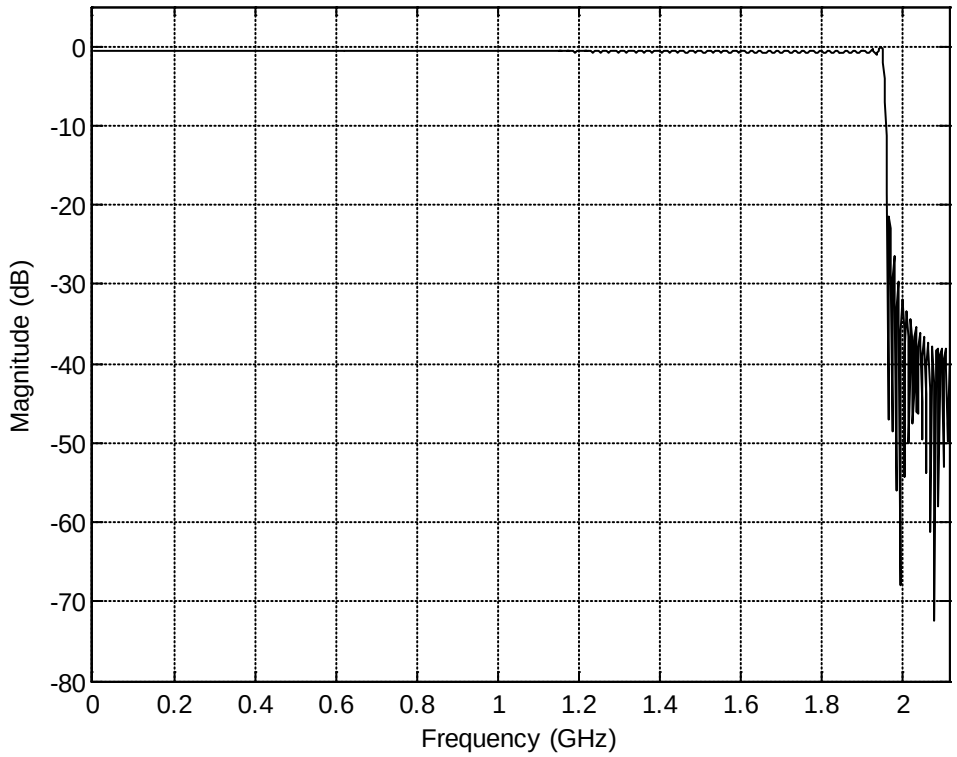

Figure A-8: Frequency response of FIR filter with cut-off frequency at 1948 MHz.

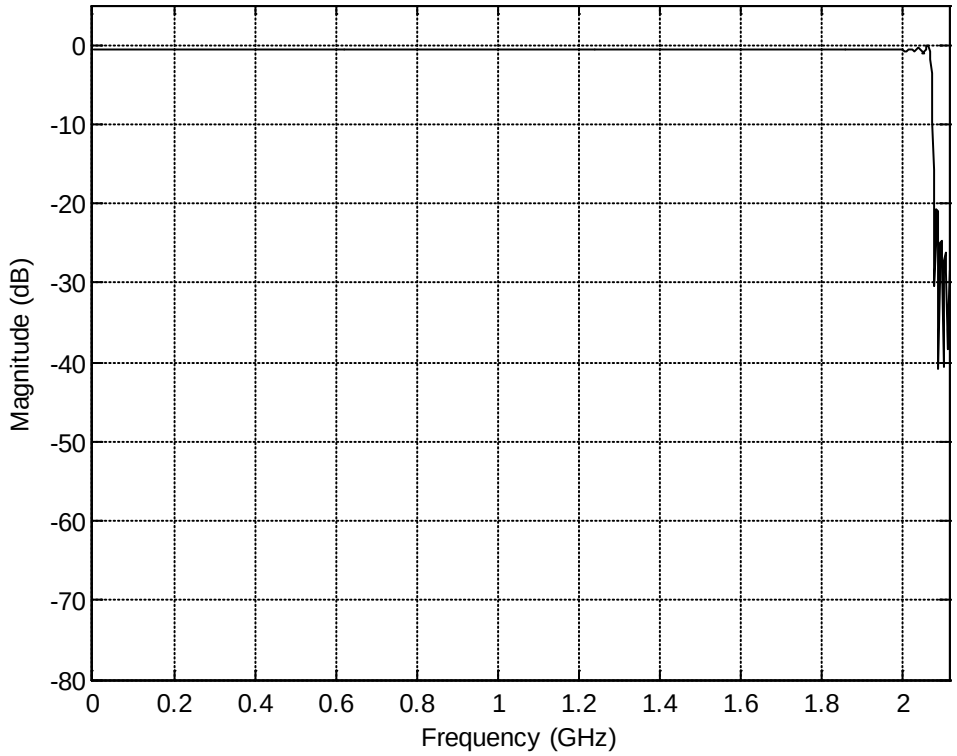

Figure A-9: Frequency response of FIR filter with cut-off frequency at 2064 MHz.